Characterization of Embryonic Stem Cell Transplantation Immunobiology using Molecular Imaging

Characterization of Embryonic Stem Cell Transplantation Immunobiology using Molecular Imaging

PROEFSCHRIFT

ter verkrijging van

de graad van Doctor aan de Universiteit Leiden,

op gezag van de Rector Magnificus Prof.mr. P. F. van der Heijden,

volgens besluit van het College voor Promoties

te verdedigen op 21 april 2009

klokke 16.15 uur

door

Rutger-Jan Swijnenburg

geboren te Amersfoort in 1978

PROMOTIECOMMISSIE

Promotores: Prof. Dr. J.F. Hamming
                 Prof. Dr. R.C. Robbins (Stanford University, USA)

Co-promotor: Dr. J.C. Wu (Stanford University, USA)

Referent: Prof. Dr. C.L. Mummery

Overige Leden: Prof. Dr. O.T. Terpstra
                 Prof. Dr. P.H. Quax

Seeing is Believing

CONTENTS

CHAPTER 1

General Introduction

STEM CELLS

Stem cells have two unique qualities. First, they are capable of self-renewal, ensuring a lifetime supply of ancestors for replacement or repair. Second, they may differentiate into intermediate and downstream types of cells specific to the organ or tissue, including progenitor cells (which can multiply but not renew) and terminally differentiated cells[1]. As such, their potential in cell replacement therapy and regenerative medicine has been widely acknowledged. There are two general types of stem cells, referred to as adult stem cells (ASCs) and embryonic stem cells (ESCs).

ASCs appear sequentially during fetal development, and are limited in their developmental potential. As a result, stem cells isolated from a fully developed animal or human are already programmed to become brain, blood, bone or other cells of the resident tissue or organ[2]. For example, the blood system has self-renewing long- and short-term hematopoietic stem cells, which give rise to a number of multipotent progenitors and nine fully differentiated cells of the myeloid and lymphoid lineages. Generally, adult stem cells are few in number, hard to isolate, and with the exception of some neural types, difficult to culture and expand.

In contrast, ESCs are generally derived by culturing a few dozen cells removed from the interior of a blastocyst (Figure 1). In mammals, this collection of cells, called the inner cell mass, eventually develops into the epiblast and hypoblast, and subsequent gastrulation forms the germ layers of the animal proper. Approximately 10% of the time, a self-renewing, pluripotent cell line will result, with potential to differentiate into all of the cell and tissue types of the adult animal, including downstream stem and progenitor cells[3]. When cultured on a supporting feeder layer of mouse embryonic fibroblast, ESCs can be expanded indefinitely *in vitro*, while maintaining a stable karyotype. When engrafted unmodified into immunocompromised mice, both mouse (m) and human (h)ESCs form teratomas comprised of tissue types from endoderm, ectoderm and mesoderm lineages.

The pluripotent and self-renewing nature of ESC makes them an ideal source from which to generate multiple tissues for regenerative therapies. The first hESC lines were generated by Thompson et al. in 1998[4]. Since then, successful *in vitro* differentiation of many cell types has been reported, including cardiomyocytes, neurons, pancreatic beta cells, hepatocytes, oligodendrocytes and erythrocytes[5]. Not surprisingly, this area of research is generating unprecedented interest from the general public not only because of the expectation of a new horizon in clinical medicine, but also through the intense debate over the ethical and safety issues, and practical hurdles to therapy. With respect to the latter, one of the most important obstacles facing *in vivo* engraftment and function of transplanted hESCs is the potential immunologic barrier. That is, since ESC-derived therapeutic cells will not be "self derived", they would be predicted to face an aggressive recipient immune system and be the focus of rejection[6]. At the same time, hESCs theoretically represent an immune-privileged cell population, as embryos consisting of 50% foreign paternal material are usually not rejected
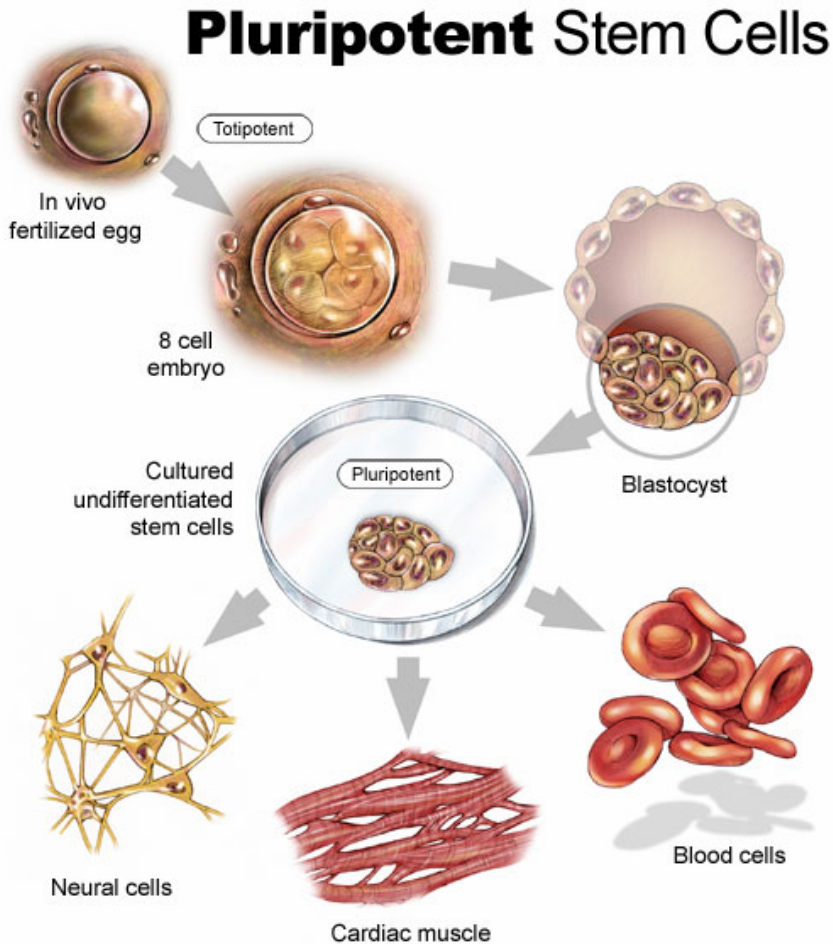
Figure 1. Derivation, culture, and differentiation of embryonic stem cells. Undifferentiated embryonic stem cells are isolated from the inner cell mass of an embryo at the blastocyst stage. The cells can be propagated indefinitely *in vitro* and differentiated towards different adult cell types, such as neurons, cardiomyocytes and erythrocytes. (Source of image: www.researchfoundation.org/whatsnew/pluripotent.htm)

by the maternal host. Futhermore, some types of adult stem cells (for example mesenchymal and amnion) have been reported to avoid immune rejection though production of immu-nosuppressive molecules, facilitating their survival following intra- and even interspecies transplantation[7]

The subject of ESC immunogenicity has been the topic of much debate[8]. The aim of the work presented in this dissertation is to clarify and characterize the immunobiology of ESC

transplantation and to provide a clear answer as to whether rejection of ESC is something that could potentially hamper successful implementation into clinical therapy.

IMMUNOBIOLOGY OF TRANSPLANTATION

Tissues, organs or cells transplanted between genetically non-identical (allogeneic) individuals will inevitably lead to rejection secondary to activation of the innate and adaptive immune systems. In general, the greater the number of genetic differences between the donor and recipient, the more rapid the rejection response. The major system characterized as responsible for tissue incompatibility is the Major Histocompatibility Complex (MHC) The MHC encodes a series of highly polymorphic groups of genes[9]. The MHC locus produces two classes of cell surface glycoproteins, referred to as class I and class II MHC molecules. In humans, the MHC is called human leukocyte antigen (HLA). HLA class I and class II molecules play a central role in allogeneic (allo)antigen recognition by T lymphocytes. They are essentially cell-surface receptors embedded in the plasma membrane which display antigen, in the form of a peptide inserted into the peptide binding groove of each molecule, for presentation to T cells. Most human cells express HLA class I molecules but the expression of HLA class II molecules is restricted to antigen-presenting cells (APCs), such as dendritic cells[10].

Alloantigens can be recognized by the immune system by two distinct pathways known as the direct and indirect pathways of allorecognition. For direct recognition of donor alloantigens, donor cells act as the antigen-presenting cells and present the mismatched MHC molecules as intact molecules to the recipient immune system for recognition by recipient T cells. For indirect recognition of donor alloantigens the donor molecules are processed into small peptides and presented by recipient-derived APCs to recipient T cells following migration to the regional lymph nodes[11].

T lymphocytes, or T cells, possess surface-bound receptors for antigen called the T cell receptor (TcR). CD4^{+} T cells in general recognize exogenous antigen on the surface of an APC in conjunction with MHC class II molecules. The other major T cell subset, CD8^{+} T cells, in general recognizes endogenous antigens displayed by a transformed or infected host cell in complex with MHC class I molecules[10]. Upon activation, T cells will undergo clonal proliferation. Furthermore, activated T-cells can provide a co-stimulatory signal to B-cells. Upon activation, B cells terminally differentiate into plasma cells, which produce a secreted form of the B-cell receptor (BcR) called antibody. Massive attack of the transplanted graft by both activated T-cells and B-cell derived antibody ultimately leads to rejection[10].

IMMUNOBIOLOGY OF EMBRYONIC STEM CELL TRANSPLANTATION

It has been shown that, in their undifferentiated state, hESCs express low levels of MHC-I[12, 13]. MHC-I expression increased two to four-fold when the cells were induced to spontaneously differentiate to EBs, and an eight to ten-fold when induced to differentiate into teratomas [12]. Futhermore, MHC-I expression was strongly upregulated after treatment of the cells with interferon-γ, a potent MHC expression inducing cytokine known to be released during the course of an immune response. MHC-II antigens were not expressed on hESCs or hESC derivatives [12].

Although the presence of MHC-antigens on ESC suggest susceptibility of the cells to immune attack, recent reports have shown that both mESCs and hESCs seem to have the capability to evade immune recognition in allogeneic as well as in xenogeneic hosts. mESCs have been shown to survive in immunocompetent mice [14], as well as in rats [15] and sheep [16] for many weeks after transplantation. In addition, not only have hESCs been reported to inhibit allogeneic T-cell proliferation *in vitro*, but also to evade immune recognition in xenogeneic immunocompetent mice [17]. In contrast, a recent report found that one month after transplantation, hESC were totally eliminated in a similar model [18].

IN VIVO VISUALIZATION OF TRANSPLANTED STEM CELL FATE: THE ROLE OF MOLECULAR IMAGING

Specific studies evaluating immunogenicity of hESCs *in vivo* are few and have yielded mixed conclusions regarding hESC's potential to induce immune response and/or survive in allogeneic and/or xenogeneic hosts[17-19]. In these studies, results were based on histological techniques to evaluate hESC survival. These techniques provide only a "snapshot" representation rather than a comprehensive picture of cell survival over time. To allow non-invasive cell tracking, our group has developed and validated reporter gene-based molecular imaging techniques.

Molecular imaging can be defined as the characterization, visual representation, and quantification of biologic processes at the cellular and molecular level within intact living organisms. All molecular imaging techniques have two requisites: 1) a molecular probe that provides a quantifiable signal based on the presence of a gene, RNA, biochemical process, receptor, or cell; and 2) a method to monitor the molecular probe[20]. The earliest molecular imaging approaches relied on radiolabeled tracers as probes that could be repeatedly monitored for short periods of time, clinically known as nuclear imaging. A recent advance in the field of molecular imaging has come in the form of reporter gene imaging. The concept behind reporter gene imaging is outlined in Figure 2.
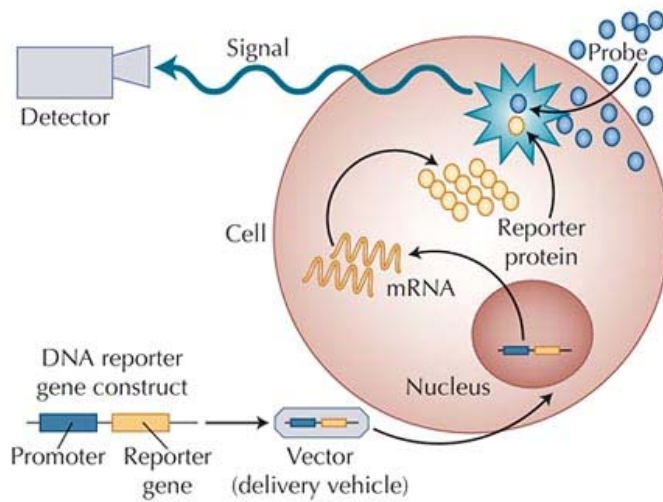
Figure 2. Concept of reporter gene imaging. The DNA promoter construct contains a promoter region that drives the reporter gene. The construct is deliverd into the cell nucleus via a viral or nonviral vector. The reporter gene is then transcribed to mRNA and subsequently translated to reporter gene protein within the cell. The molecular probe diffuses into the cytosol to interact with the reporter protein resulting in the generation of a signal (thick arrow), registered by the detector. (Reproduced with permission from Sheik et al.[20])

In particular, firefly luciferase (Fluc) reporter gene-based optical bioluminescence imaging (BLI) has proven to be a reliable technique for assessing engraftment and survival of stem cells following transplantation[21]. In BLI, the reporter gene produces a Fluc enzyme, which oxidizes the reporter probe (D-luciferin) to produce light as a signal. Ultrasensitive charged coupled device (CCD) cameras can then sense the photons as they pass from within the stem cell, though tissue and out of the subject. An important advantage in using BLI is that the expression of the Fluc reporter gene, is expressed only by living cells, making it a highly accurate tool for following transplant rejection of organs or cells in the living subject[22].

CHARATERIZATION OF EMBRYONIC STEM CELL TRANSPLANTATION IMMUNOBIOLOGY USING MOLECULAR IMAGING: SCOPE OF THE THESIS

The scope of the current thesis is to gain insight into immunological aspects of transplantation of embryonic stem cells or their differentiated progeny by using molecular imaging techniques to follow cell fate.

The first part of this thesis describes *in vivo* bioluminescent imaging (BLI) as a novel tool to visualize and quantify survival and rejection of transplanted cells and/or organs. **Chapter 2** describes a 'proof of concept' study of the use of non-invasive BLI to visualize cardiac allograft rejection following transplantation. By performing heterotopic transplantation of Fluc/eGPF transgenic L2G mouse donor hearts into allogeneic wild-type recipients, cardiac allograft

rejection can be quantified non-invasively and longitudinally. In addition, by using a transgenic mouse line in which a CD5 promoter drives the expression of luciferase gene as cardiac donors, new insights are gained concerning the pace and distribution of CD5+ passenger leukocytes leaving the donor heart and traveling throughout the recipient body. In **Chapter 3**, non-invasive BLI is utilized to track mononuclear bone marrow cells (BMCs) isolated from L2G mice following injection into the infarcted myocardium of syngeneic FVB recipients. In this study, the viability and effects of transplanted BMCs on cardiac function in the acute and sub-acute inflammatory phases of MI is investigated. In addition, the phenotype of BMCs transplanted into acute inflammatory myocardium is analyzed.

The second part of the thesis focused on immunological aspects of ESC transplantation. In the first two chapters, a comprehensive introduction into the potentials and pitfalls of hESC transplantation is given. **Chapter 4** describes the potential of hESC to differentiate into multiple somatic cell types that can potentially cure patients in the future. Furthermore, it introduces molecular imaging techniques and explains its value for non-invasive tracking of hESCs following transplantation. **Chapter 5** focuses specifically on a promising derivative of ESC: the ESC-derived cardiomyocyte. It describes progress in hESC-to-cardiomyocyte differentiation and potential role in cardiac regenerative therapy and summarizes the hurdles that still need to be overcome before ESC-derived cardiomyocyte transplantation can be translated into the clinics. Finally, it lays out how molecular imaging can contribute to progress in this field.

Chapter 6 describes the first study ever to address immunological aspects of embryonic stem cell transplantation *in vivo*. It shows that allogeneic mESCs are eventually rejected when transplanted into infarcted mouse myocardium. *In vivo* differentiated mESCs elicit an accelerated immune response as compared to undifferentiated mESCs. In order to visualize and quantify ESC immunogenicity, molecular imaging of transplanted ESC was introduced in **Chapter 7**, a manuscript that was kindly previewed by Fedak[23]. In this study, *in vivo* BLI is used to non-invasively track the fate of transplanted mESCs stably transduced with a double fusion reporter gene consisting of firefly luciferase (Fluc) and enhanced green fluorescent protein (eGFP). Following syngeneic intramuscular transplantation, the mESCs survive and differentiate into teratomas. In contrast, allogeneic mESC transplants are infiltrated by a variety of inflammatory cells, leading to rejection within 28 days. Acceleration of rejection is observed when mESCs are allotransplanted following prior sensitization of the host. Finally, the study demonstrates that mESC-derivatives are more rapidly rejected as compared to undifferentiated mESCs. These data show that mESCs do not retain immune-privileged properties *in vivo* and are subject to immunological rejection as assessed by novel molecular imaging approaches.

In **Chapter 8**, a manuscript that was previewed by Chidgey et al in *Cell Stem Cell*[6], the step towards hESCs is made and the immunogenicity of human ESC is addressed in a xenogeneic mouse model. By using BLI of Fluc/eGFP transduced hESC, it is shown that post-transplant

survival is significantly limited in immunocompetent as opposed to immunodeficient mice. Repeated transplantation of hESCs into immunocompetent hosts results in accelerated hESC death, suggesting an adaptive donor-specific immune response. The specific role of T-lymphocyte subsets in mediation of the murine anti-hES cell immune response is further delineated. In addition, the efficacy of various combinations of clinically available immuno-suppressive regimens for enhancing survival of transplanted hES cells *in vivo is* compared.

Finally, **Chapter 9** includes a summary of this thesis as well as a discussion on future prospects of ESC transplantation and ways to overcome the immunological challenges. **Chapter 10** provides a summary in Dutch.

REFERENCES:

1. Scott CT, Reijo Pera RA. The road to pluripotence: the research response to the embryonic stem cell debate. *Human molecular genetics.* 2008;17:R3-9.
2. Wagers AJ, Weissman IL. Plasticity of adult stem cells. *Cell.* 2004;116:639-648.
3. Turksen K, Troy TC. Human embryonic stem cells: isolation, maintenance, and differentiation. *Methods in molecular biology (Clifton, N.J.* 2006;331:1-12.
4. Thomson JA, Itskovitz-Eldor J, Shapiro SS, Waknitz MA, Swiergiel JJ, Marshall VS, Jones JM. Embryonic stem cell lines derived from human blastocysts. *Science (New York, N.Y.* 1998;282:1145-1147.
5. Murry CE, Keller G. Differentiation of embryonic stem cells to clinically relevant populations: lessons from embryonic development. *Cell.* 2008;132:661-680.
6. Chidgey AP, Boyd RL. Immune privilege for stem cells: not as simple as it looked. *Cell stem cell.* 2008;3:357-358.
7. Uccelli A, Moretta L, Pistoia V. Mesenchymal stem cells in health and disease. *Nature reviews.* 2008.
8. Yuan X, Zhang H, Wei YJ, Hu SS. Embryonic stem cell transplantation for the treatment of myocardial infarction: immune privilege or rejection. *Transplant immunology.* 2007;18:88-93.
9. Game DS, Lechler RI. Pathways of allorecognition: implications for transplantation tolerance. *Transplant immunology.* 2002;10:101-108.
10. Boyd AS, Higashi Y, Wood KJ. Transplanting stem cells: potential targets for immune attack. Modulating the immune response against embryonic stem cell transplantation. *Advanced drug delivery reviews.* 2005;57:1944-1969.
11. Grinnemo KH, Sylven C, Hovatta O, Dellgren G, Corbascio M. Immunogenicity of human embryonic stem cells. *Cell Tissue Res.* 2008;331:67-78.
12. Drukker M, Katz G, Urbach A, Schuldiner M, Markel G, Itskovitz-Eldor J, Reubinoff B, Mandelboim O, Benvenisty N. Characterization of the expression of MHC proteins in human embryonic stem cells. *Proc Natl Acad Sci U S A.* 2002;99:9864-9869.
13. Draper JS, Pigott C, Thomson JA, Andrews PW. Surface antigens of human embryonic stem cells: changes upon differentiation in culture. *J Anat.* 2002;200:249-258.
14. Koch CA, Geraldes P, Platt JL. Immunosuppression by embryonic stem cells. *Stem cells (Dayton, Ohio).* 2008;26:89-98.
15. Min JY, Yang Y, Sullivan MF, Ke Q, Converso KL, Chen Y, Morgan JP, Xiao YF. Long-term improvement of cardiac function in rats after infarction by transplantation of embryonic stem cells. *The Journal of thoracic and cardiovascular surgery.* 2003;125:361-369.
16. Menard C, Hagege AA, Agbulut O, Barro M, Morichetti MC, Brasselet C, Bel A, Messas E, Bissery A, Bruneval P, Desnos M, Puceat M, Menasche P. Transplantation of cardiac-committed mouse embryonic stem cells to infarcted sheep myocardium: a preclinical study. *Lancet.* 2005;366:1005-1012.
17. Li L, Baroja ML, Majumdar A, Chadwick K, Rouleau A, Gallacher L, Ferber I, Lebkowski J, Martin T, Madrenas J, Bhatia M. Human embryonic stem cells possess immune-privileged properties. *Stem cells (Dayton, Ohio).* 2004;22:448-456.
18. Drukker M, Katchman H, Katz G, Even-Tov Friedman S, Shezen E, Hornstein E, Mandelboim O, Reisner Y, Benvenisty N. Human embryonic stem cells and their differentiated derivatives are less susceptible to immune rejection than adult cells. *Stem Cells.* 2006;24:221-229.
19. Grinnemo KH, Sylven C, Hovatta O, Dellgren G, Corbascio M. Immunogenicity of human embryonic stem cells. *Cell Tissue Res.* 2007.

20. Sheikh AY, Wu JC. Molecular imaging of cardiac stem cell transplantation. *Current cardiology reports.* 2006;8:147-154.

21. Cao YA, Wagers AJ, Beilhack A, Dusich J, Bachmann MH, Negrin RS, Weissman IL, Contag CH. Shifting foci of hematopoiesis during reconstitution from single stem cells. *Proceedings of the National Academy of Sciences of the United States of America.* 2004;101:221-226.

22. Cao YA, Bachmann MH, Beilhack A, Yang Y, Tanaka M, Swijnenburg RJ, Reeves R, Taylor-Edwards C, Schulz S, Doyle TC, Fathman CG, Robbins RC, Herzenberg LA, Negrin RS, Contag CH. Molecular imaging using labeled donor tissues reveals patterns of engraftment, rejection, and survival in transplantation. *Transplantation.* 2005;80:134-139.

23. Fedak PW. Cardiac regeneration with embryonic stem cells: historic recapitulation of heart transplantation. *Stem cells and development.* 2008;17:1021-1022.

PART I:

**Non-invasive Visualization
of Organs and Cells
after Transplantation**

CHAPTER 2

In vivo Visualization of Cardiac Allograft Rejection and Trafficking Passenger Leukocytes Using Bioluminescence Imaging

Masashi Tanaka, Rutger-Jan Swijnenburg, Feny Gunawan, Yu-An Cao, Yang Yang, Anthony D. Caffarelli, Jorg L. de Bruin, Cristopher H. Contag, and Robert C. Robbins

ABSTRACT

Background: We investigated the feasibility of bioluminescence imaging (BLI) for the *in vivo* assessment of cardiac allograft viability and visualization of passenger leukocytes during the course of acute rejection.

Methods and Results: Hearts of FVB (H-2^q) luciferase-GFP transgenic mice (β-actin promoter) or FVB luciferase transgenic mice (CD5 promoter) were heterotopically transplanted into either BALB/c (H-2^d) or FVB recipients. Light intensity emitting from the recipient animals was measured daily by *in vivo* BLI until 12 days post-transplant. Graft beating score (0 to 4) was assessed by daily abdominal palpation until 12 days post-transplant. Inflammatory cell infiltration (CD45 stain) and structural changes of GFP$^+$ cardiomyocytes were followed by immunohistochemistry. All cardiac allografts were acutely rejected by 12 days post-transplant. The intensity of emitting light from cardiac allografts declined 4 days post-transplant and correlated with graft beating scores ($R^2 = 0.91$, $p = 0.02$). Immunohistochemistry confirmed these results by showing an increase of CD45$^+$ inflammatory cell infiltration and destruction of GFP$^+$ cardiomyocytes in the cardiac allografts during acute rejection. *In vivo* BLI visualized migration and proliferation of CD5$^+$ passenger leukocytes in both syngeneic and allogeneic recipients. In the allograft recipients, light signal from CD5$^+$ passenger leukocytes peaked at 6 hours and diminished by 12 hours; whereas in the syngeneic recipients, the signal remained high until 10 days post-transplant.

Conclusion: BLI is a useful modality for the quantitative assessment of *in vivo* cardiac graft viability and tracking of passenger leukocytes *in vivo* during the course of acute rejection.

INTRODUCTION

Allogeneic heart transplantation has become a commonly used therapy for end-stage heart disease. Early graft loss due to acute rejection, even though reduced by current immuno-suppressive strategies, remains a significant problem in clinical heart transplantation.[1] In addition, many cardiac allograft recipients experience episodes of acute rejection, and these episodes are a critical risk factor for the subsequent development of graft coronary artery disease which predisposes to late graft loss.[2] Acute rejection is an immune response mediated by the coordinated infiltration and effector functions of host alloantigen-specific T cells in the allograft.[3] In addition, donor-derived passenger leukocyte migration contributes to acute rejection.[4]

Cell migration is a crucial element during the development of the immune system and mediates the immune response during acute cardiac rejection. There is extensive and continual redistribution of cells to different anatomic sites throughout the body. These trafficking patterns control immune function and host responses to transplanted heart. The ability to monitor the fate and function of migrating cells, therefore, is imperative to both understanding the role of lymphocytes in acute cardiac rejection and to devising rational therapeutic strategies. Determining the fate of immune cells and understanding the functional changes associated with migration and proliferation requires effective means of obtaining *in vivo* measurements in the context of intact organ systems.

We have developed *in vivo* bioluminescence imaging (BLI) based on the observations that light passes through mammalian tissues, and that luciferase can serve as internal biological sources of light in the living body.[5] This method is a rapid and noninvasive functional imaging method that employs light-emitting reporters and external photon detection to follow biological processes in living animals in real time. Using this approach we have elucidated the spatiotemporal trafficking patterns of malignant cells, lymphocytes, and other mature immune cells within living animal models of human biology and disease.[5-8] In addition, to enable the *in vivo* study of biological processes that involve movement of cells within the three-dimensional organism, e.g., developmental cell migration, immune cell trafficking, engraftment of bone marrow and other tissues, we have previously generated a transgenic donor mouse line in which a CMV-β-actin promoter drives the expression of two reporters, luciferase and green fluorescent protein (GFP). Furthermore, we have also developed a trans-genic mouse line in which a CD5 promoter drives the expression of luciferase gene.

Using these transgenic mice and *in vivo* BLI technology, we tested the hypothesis that *in vivo* BLI can be used for the *in vivo* assessment of allograft viability and *in vivo* visualization of donor-derived CD5+ cells during the course of acute rejection.

MATERIALS AND METHODS

Animals.

Previously, we made a transgenic mouse line (FVB-L2G85) by pronuclear injection of a gene construct expressing two reporters, firefly luciferase and GFP, under the control of the widely expressed β-actin promoter (Y.-A.C., unpublished data). The overexpression of luciferase and GFP in heart was confirmed by bioluminescent and fluorescent microscopy (Figure 1A and B).
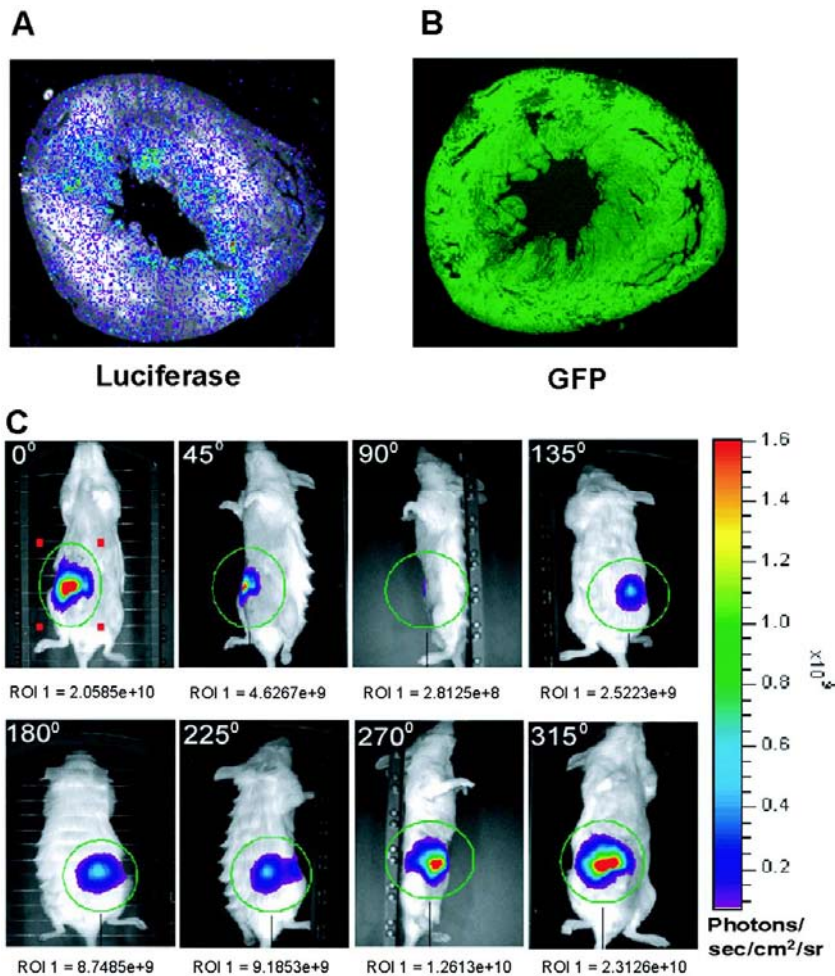
Figure 1. Bioluminescent and fluorescent microscopic analysis of heart sections from luciferase and green fluorescent protein (GFP) double transgenic mouse and *in vivo* 3-D bioluminescent imaging of the luciferase-GFP transgenic heart recipient mouse. Ex vivo bioluminescent imaging of donor heart section from luciferase-GFP transgenic mouse (A). Fluorescent microscopic analysis of section of the heart from luciferase-GFP transgenic mouse (B). *In vivo* 3-D bioluminescent imaging of the recipient mouse in which luciferase-GFP transgenic donor heart was heterotopically transplanted (C).

We have also developed a transgenic mouse line in which a CD5 promoter drives the expression of luciferase gene.[9] Female BALB/c and FVB mice (4 to 6 weeks old) were obtained from The Jackson Laboratory and used as recipient. All procedures were approved by the Animal Care and Use Committee of Stanford University.

Mouse heterotopic heart transplantation.

Hearts of transgenic FVB-L2G85 mice (H-2^q) were heterotopically transplanted into wild-type BALB/c (H-2^d) or syngeneic FVB recipient abdomen as an acute rejection model. Heterotopic cardiac transplantation was performed according to the method of Corry *et al*[10] with some modifications. Anesthesia was induced with 3% inhaled isoflurane (Halocarbon Laboratories, River Edge, NJ). During surgery, the animals were maintained on 2.5% inhaled isoflurane. The total ischemic time of cardiac allograft was 40 minutes.

Graft Survival and Allograft Functional Analyses.

Graft viability was assessed by direct abdominal palpation of the heterotopically transplanted heart as previously described.[11] Cardiac graft function was expressed as the beating score, assessed by the Stanford cardiac surgery lab graft scoring system (0: no contraction, 1: contraction barely palpable, 2: obvious decrease in contraction strength, but still contracting in a coordinated manner; rhythm disturbance, 3: strong, coordinated beat but noticeable decrease in strength or rate; distention/stiffness, 4: strong contraction of both ventricles, regular rate, no enlargement or stiffness).

In vivo bioluminescent imaging.

Mice were anesthetized with 2% inhaled isoflurane and luciferin was administered at a dose of 150 mg/kg i.p. At the time of imaging, animals were placed in a light-tight chamber and using an *in vivo* imaging system employing a cooled charge couple device (CCD) camera (IVIS 100, Xenogen Corp., Alameda, CA), photons transmitted through the tissue emitted from intracellular luciferase were collected for 10 seconds to 10 minutes (as indicated in the figure legends) depending on the intensity of the bioluminescence emissions.

Because bioluminescence is dependent upon tissue penetration, the intensity from the cardiac grafts may vary depending upon the location of the grafts in the abdomen (i.e. cardiac grafts can change position and bowel may cover the grafts); therefore, we chose the 3D imaging system, which allowed us to obtain signal intensity from 8 different directions (Figure 1C). Thus allowing us to calculate the summation of light intensities obtained from 8 different direction scans, which then was used to represent cardiac allograft viability.

Using applications in LivingImage software (Xenogen Corp) an overlay on Igor image analysis software (Wavemetrics, OR), gray scale reference images were collected under low light, and the intensity of the bioluminescent signals from the animal was measured in complete darkness (blue least intense and red most). The 2 images were then superimposed and

annotated using Canvas (Deneba, Miami, FL). To quantify allograft viability, the light emitting from the allograft was outlined as the region of interest (ROI) and ROI photon intensity was measured using LivingImage software. *In vivo* photon intensity measures were correlated to ex vivo tissue sections by dissecting the tissues, incubating fresh tissues in D-luciferin, and imaging these tissues without the overlying tissues.

Tissue collection and immunofluorescent histology.

To evaluate inflammatory cell infiltration, cardiomyocyte destruction and proliferation of donor derived fibroblasts, cardiac grafts were perfused with saline and rapidly excised at different days after transplantation. They were fixed in 2% paraformaldehyde for 2 hours and cryoprotected in 30% sucrose overnight. Then, tissue was frozen in optimal cutting temperature compound (OCT Compound, Sakura Finetek USA, Inc. Torrance, CA) and sectioned at 5 μm on a cryostat. Sections were blocked and incubated with either rat anti-CD45, rat anti-CD5 or mouse anti-Vimentin (all BD Pharmingen) primary antibodies for 1 hour at room temperature. After washing in PBS, sections were incubated with either goat anti-rat Alexa Fluor 594 (red), goat anti-rat Alexa Fluor 488 (green) or goat anti-mouse Texas Red (all Molecular probes, Eugene, OR) secondary antibodies for 30 minutes at room temperature. Sections were then washed in PBS, counterstained with 4,6-diamidino-2-phenylindole (DAPI, Molecular probes) and examined with a Leica DMRB fluorescent microscope (Leica Microsystems, Frankfurt, Germany).

Statistics.

Values are expressed as mean ± SE. Differences in cardiac graft beating score and light intensity of cardiac grafts were analyzed by a 2-way repeated-measures ANOVA. Correlation between cardiac graft beating score and light intensity emitted from cardiac grafts were analyzed by regression analysis (StatView 5.0; SAS Institute, Cary, NC). Significance was accepted at $p < 0.05$.

RESULTS

In vivo visualization of acute cardiac rejection and quantitative analyses of cardiac allograft viability using bioluminescence imaging.

Bioluminescent and fluorescent microscopic analysis of the heart from luciferase-GFP transgenic mice confirmed expression of both luciferase and GFP (Figure 1A and B). There was no bioluminescent signal from the non-transgenic littermates (Data not shown). Using the heart of luciferase-GFP transgenic mice as donor organ, we investigated the feasibility of BLI for quantitative assessment of cardiac allograft viability in the course of acute rejection. As the luciferase-GFP transgenic mice have FVB background, we used BALB/c mice as recipients to
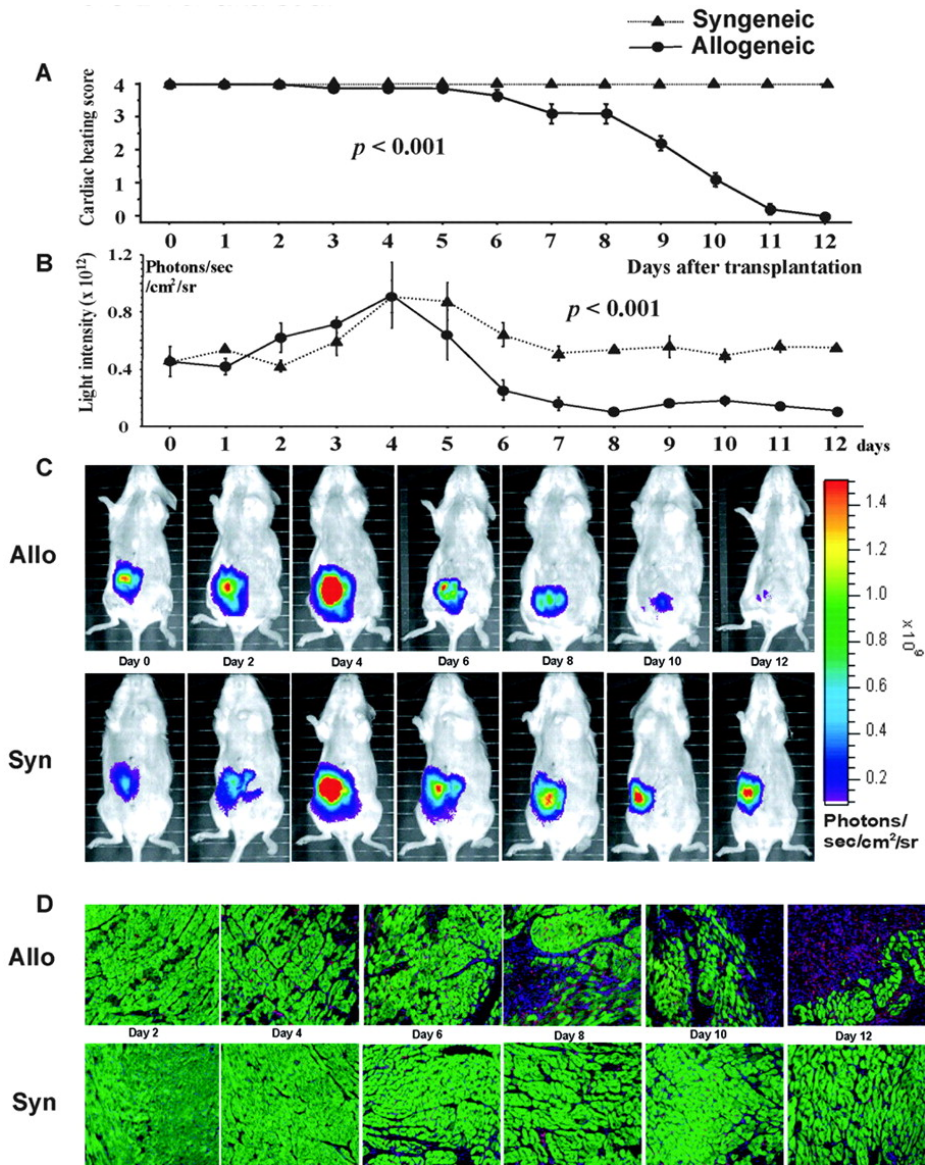
Figure 2. *In vivo* visualization of acute cardiac rejection and quantitative analyses of cardiac allograft viability using bioluminescence imaging. Cardiac graft beating score of the study group (A). Light intensity of the study group (B). *In vivo* 3-D bioluminescent imaging of the study group (C). Representative sections of immunohistochmically stained cardiac grafts of the study group. Red = inflammatory cells (CD45 stain), green = cardiomyocyte (GFP), blue = nuclei (DAPI stain) (magnification x400). Note that the light intensity of the luciferase-green fluorescent protein (GFP) transgenic donor heart recipient mice correlates with cardiac graft function and histology in the course of acute cardiac rejection. Allo = allogeneic = FVB luciferase-GFP transgenic donor heart were heterotopically transplanted into BALB/c recipient (n = 5). Syn = syngeneic = FVB luciferase-GFP transgenic donor heart were heterotopically transplanted into FVB recipient (n = 5).

induce acute rejection. In the course of acute rejection, we measured cardiac graft viability *in vivo* using 3D BLI as described earlier.

All FVB cardiac allografts transplanted into BALB/c recipients were acutely rejected by 12 days following transplantation. In contrast, all FVB cardiac isografts transplanted into FVB recipients survived until 12 days after transplantation. Cardiac allograft beating score assessed by daily abdominal palpation showed significant difference between isografts and allograft ($p < 0.001$, Figure 2A). The intensity of emitting light from cardiac allografts declined 4 days post-transplant and correlated with graft beating scores ($R^2 = 0.91$, $p = 0.02$, Figure 2B and C). To confirm correlation between cardiac graft viability and light intensity, cardiac allo- and isografts were procured at day 2, 4, 6, 8, 10, and 12 days after transplantation and stained with an antibody against CD45, a marker expressed on all inflammatory cells. Immunohistochemistry showed an increase of inflammatory cell infiltration and destruction of GFP+ cardiomyocytes in the cardiac allografts in the course of acute rejection (Figure 2D). In contrast, only mild inflammatory cell infiltration as well as preserved GFP+ cardiomyocyte structure were observed in cardiac isografts by 12 days after transplantation (Figure 2D). Taken together, changes of photon signal intensity of cardiac graft correlate with cardiac graft viability and histological findings in the course of acute cardiac rejection. Therefore, our data suggest that *in vivo* BLI may be a useful tool for the quantitative assessment of cardiac graft viability *in vivo*.

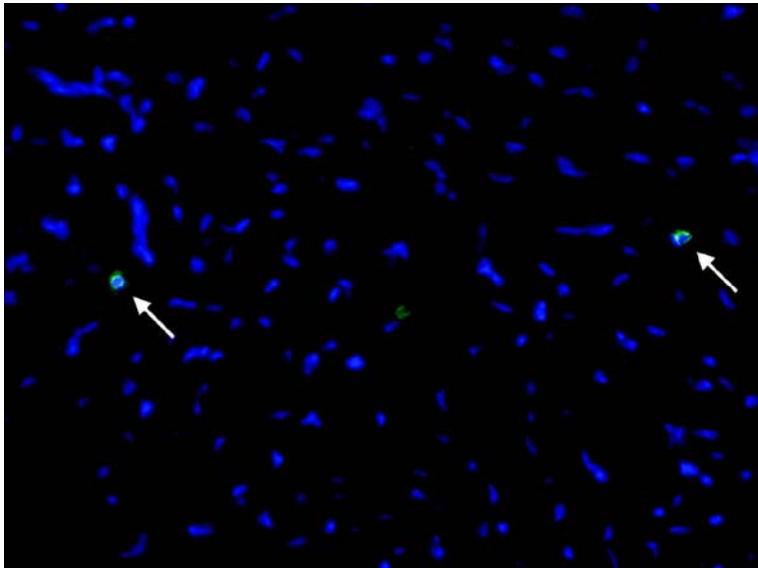**Figure 3. Donor-derived CD5+ passenger leukocytes in CD5 promoter luciferase transgenic donor heart.** Representative sections of CD5 promoter luciferase transgenic donor heart stained with anti-mouse CD5 recognized by FITC conjugated secondary antibody (green). Sections were counterstained with 4,6-diamidino-2-phenylindole (DAPI, blue). Arrowheads show representative CD5+ donor-derived passenger leukocytes in donor heart (X400).

In vivo visualization of donor-derived passenger CD5^{+} cell response in the cardiac allograft recipients in the course of acute rejection.

Solid organ grafts contain bone marrow-derived hematopoietic cells, passenger leukocytes, of donor origin. These donor-derived hematopoietic cells are transferred to the recipient at the time of transplantation.[4] We next investigated the possibility of BLI to visualize passenger leukocytes and track their destination *in vivo* using CD5 promoter luciferase transgenic mice as a donor of syngeneic and allogeneic cardiac transplantation. As shown in figure 3, the presence of CD5^{+} donor-derived passenger leukocytes in donor heart was confirmed by immunohistochemistry. However, *In vivo* BLI of donor heart did not show emitting light from CD5^{+} donor-derived passenger leukocytes probably because of the small number of CD5^{+} donor-derived passenger leukocytes in donor hearts. Interestingly, *in vivo* BLI successfully visualized migration and proliferation of CD5^{+} donor-derived passenger leukocytes shortly after transplantation (30 minutes) in both syngeneic and allogeneic recipients, indicating these cells proliferated immediately (Figure 4). In the cardiac allograft recipients, biolumi-
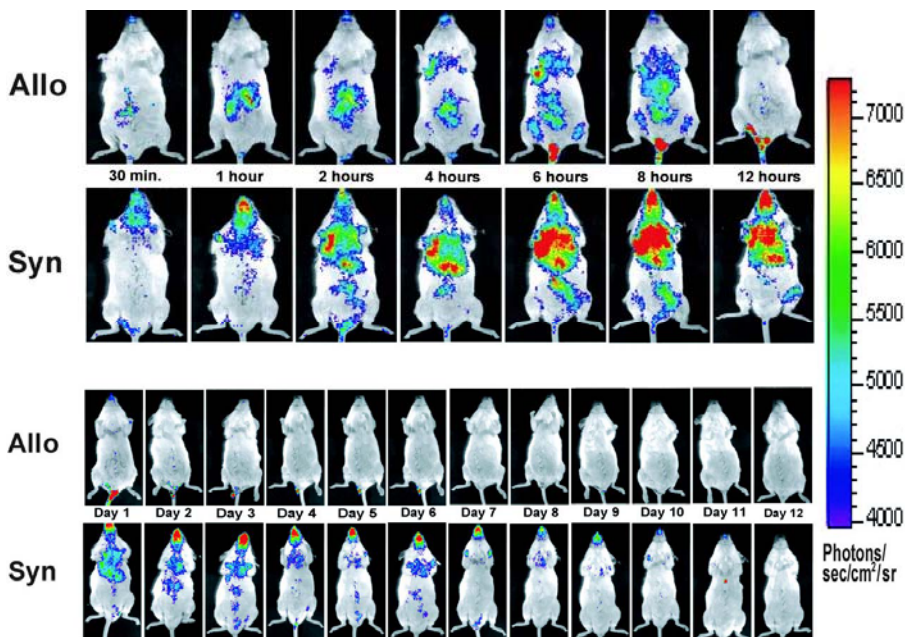
Figure 4. *In vivo* **visualized donor-derived CD5^{+} passenger leukocytes showed donor-derived CD5^{+} passenger leukocytes proliferate immediately after transplantation and diminished at 24 hours after transplantation in the course of acute rejection.** *In vivo* bioluminescent imaging of the recipient mice in which CD5 promoter luciferase transgenic donor hearts were heterotopically transplanted. Note that the light intensity of allograft recipient increased 30 minutes after transplantation, and peaked at 6 hours, and decreased at 12 hours, and diminished at 1 day after transplantation. In contrast, the light intensity of isografts recipient increased at 30 minutes after transplantation and peaked at 1 and 2 days, stayed by 10 days after transplantation. Allo = allogeneic = FVB CD5 promoter luciferase transgenic donor heart were heterotopically transplanted into BALB/c recipient (n = 5). Syn = syngeneic = FVB CD5 promoter luciferase transgenic donor heart were heterotopically transplanted into FVB recipient (n = 3).

nescence signal from CD5^{+} donor-derived passenger leukocytes increased with time. The signal peaked at 6 and 8 hours after transplantation, rapidly decreased at 12 hours, and had diminished at 1 day after transplantation (Figure 4). In contrast, *in vivo* BLI of the syngeneic recipients showed that signal intensity from CD5^{+} donor-derived passenger leukocytes increased at 30 minutes after transplantation, peaked at 1 and 2 days and was measurable until 10 days after transplantation (Figure 4). CD5^{+} donor-derived passenger leukocytes migrated from the cardiac allograft in the abdomen through the recipient body and were observed at anatomic sites corresponding to the location of regional abdominal lymph nodes (1 hour) liver (2 hours) thoracic lymph nodes (4 hours) and inguinal lymph nodes (6 hours). In comparison, in the syngeneic recipients, CD5^{+} donor-derived passenger leukocytes were found in the neck (30 minutes), chest and liver (2 hours). Confirmation of tissue origin was obtained by *ex vivo* imaging of dissected tissue incubated with D-luciferin (Data not shown). Since all FVB cardiac allografts transplanted into BALB/c recipients were acutely rejected at 12 days following transplantation, our data suggest that the contribution of the donor-derived CD5^{+} passenger leukocytes to acute rejection is limited to the early phase of acute rejection.

DISCUSSION

This study was designed to show the feasibility of using *in vivo* BLI to visualize the changes of cardiac allograft viability and donor-derived passenger CD5^{+} cells in response to cardiac allografting during the course of acute rejection. Using *in vivo* BLI, we have successfully shown that light intensity emitted from cardiac allografts decreases after 4 days in the course of acute rejection. In addition, the light intensity emitted from donor-derived passenger CD5^{+} cells diminished within 1 day after allo-transplantation. *In vivo* BLI of different promoter luciferase transgenic donor heart recipients allowed us to quantify the kinetics of the viability of the cardiac allografts and the location of the donor-derived passenger CD5^{+} cells longitudinally.

Graft beating score is non-quantitative as well as a subjective classification system. It is useful to determine cardiac graft survival as used elsewhere, however, it is not suitable to assess cardiac graft viability because this method assess only whether the cardiac allograft is beating or not. *In vivo* BLI of the cardiac graft provides detailed information of cardiac allograft viability in the course of acute rejection by calculating emitting light from each cardiac cells within the cardiac graft with 3D imaging. Therefore, this modality may be useful tool to assess cardiac graft viability in the clinical heart transplantation.

We observed a temporal increase of light intensity 3 to 5 days after transplantation. We attempted to prove donor-derived cells proliferation including passenger leukocytes and fibroblast by staining with anti-CD45 antibody and anti-vimentin antibody. However, we did not see any GFP and CD45 double positive cells at day 3 to 5, and we did not see an increase of GFP or vimentin positive cells from day 0 to day 6. This temporal increase of light intensity

may be due to increase of luciferase gene expression by ischemia-reperfused injured myocardium. We have observed a similar phenomenon in other animal models of BLI exposed to stress (unpublished data).

By using this *in vivo* imaging approach, we found that donor-derived passenger CD5^{+} cells in cardiac allograft proliferated immediately after transplantation and diminish by 24 hours after transplantation in the course of acute rejection. In addition, these cells migrated to liver and thoracic lymph nodes, but not migrate to spleen. In contrast, donor-derived passenger CD5^{+} cells in syngeneic graft stay by around 10 days after transplantation and diminished maybe because of their life-time (around 7 days). This study is the first study to visualize donor-derived passenger leukocytes in the recipient. Traditionally, the evaluation of donor-derived passenger leukocyte migration from the transplanted organ to the other organs and destruction of cardiomyocyte structure by acute rejection have been performed post mortem on histological specimens or other biological experiments. Therefore, it has always been controversial what is the *in vivo* sequence of these events. BLI is useful modality for immune cell trafficking *in vivo* and reducing the number of animals per experiment since changes in a given population can be studied over time.

We observed CD5^{+} donor-derived passenger leukocytes also proliferated immediately after transplantation in syngenic recipients. This data suggests that alloantigen-dependent response is not necessary to drive CD5^{+} donor-derived passenger leukocytes' proliferation. One can suggest that alloantigen-independent response, such as ischemia-reperfusion of CD5^{+} donor-derived passenger leukocytes might cause their proliferation in recipient after transplantation.

Donor-derived passenger leukocytes that are transplanted with the graft have the capacity to present donor alloantigens as intact molecules to the responding T cells by means of the so-called direct pathway of allorecognition.[12] CD5 is expressed at relatively high levels on all T lineage cells, at low levels on B-1a cells, and is below detectable levels on B-2 cells.[9] Therefore, the light signal we observed in this CD5 promoter luciferase mice donor study is emitted from donor-derived passenger T cells. In the present study, we demonstrated donor-derived passenger T cells diminished within 24 hours post-transplant in cardiac allograft recipient. Further studies using luciferase gene driven by other cell surface markers such as CD4 (T helper cell), CD8 (cytotoxic T cell), CD11c (dendritic cell), CD11b (macrophage), and B220 (B cell) for the *in vivo* visualization of immune response will increase our basic understanding of not only the passenger leukocyte function and destination in allograft recipient, but also the mechanisms of immune response in solid organ and cellular transplantation.

We have assessed CD5^{+} cell location in the cardiac transplant recipient mice in the course of acute rejection using BLI. We did not assess functional and immunological change of these cells. Nevertheless, this is the first study to visualize CD5^{+} cells *in vivo* in the course of acute rejection.

The results of this study provide the foundation for refinement of bioluminescence imaging in a non-human primate study. Clinically this novel method of noninvasive diagnosis of cardiac allograft rejection could potentially eliminate the need for routine surveillance endomyocardial biopsy. Application of *in vivo* BLI to the study of cardiovascular disease as well as transplant immunobiology will greatly accelerate and refine preclinical analyses, and lead to the development of tools with clinical utility. A number of advances have already been described and suggest that there is considerable growth yet to be realized in the nascent field of molecular imaging.

REFERENCES

1. Taylor DO, Edwards LB, Mohacsi PJ, Boucek MM, Trulock EP, Keck BM, Hertz MI. The registry of the International Society for Heart and Lung Transplantation: twentieth official adult heart transplant report--2003. *J Heart Lung Transplant.* Jun 2003;22(6):616-624.

2. Vassalli G, Gallino A, Weis M, von Scheidt W, Kappenberger L, von Segesser LK, Goy JJ. Alloimmunity and nonimmunologic risk factors in cardiac allograft vasculopathy. *Eur Heart J.* Jul 2003;24(13):1180-1188.

3. Miura M, Morita K, Kobayashi H, Hamilton TA, Burdick MD, Strieter RM, Fairchild RL. Monokine induced by IFN-gamma is a dominant factor directing T cells into murine cardiac allografts during acute rejection. *J Immunol.* Sep 15 2001;167(6):3494-3504.

4. Wood KJ. Passenger leukocytes and microchimerism: what role in tolerance induction? *Transplantation.* May 15 2003;75(9 Suppl):17S-20S.

5. Contag PR, Olomu IN, Stevenson DK, Contag CH. Bioluminescent indicators in living mammals. *Nat Med.* Feb 1998;4(2):245-247.

6. Sweeney TJ, Mailander V, Tucker AA, Olomu AB, Zhang W, Cao Y, Negrin RS, Contag CH. Visualizing the kinetics of tumor-cell clearance in living animals. *Proc Natl Acad Sci U S A.* Oct 12 1999;96(21):12044-12049.

7. Edinger M, Cao YA, Verneris MR, Bachmann MH, Contag CH, Negrin RS. Revealing lymphoma growth and the efficacy of immune cell therapies using in vivo bioluminescence imaging. *Blood.* Jan 15 2003;101(2):640-648.

8. Edinger M, Sweeney TJ, Tucker AA, Olomu AB, Negrin RS, Contag CH. Noninvasive assessment of tumor cell proliferation in animal models. *Neoplasia.* Oct 1999;1(4):303-310.

9. Yang Y, Contag CH, Felsher D, Shachaf CM, Cao Y, Herzenberg LA, Tung JW. The E47 transcription factor negatively regulates CD5 expression during thymocyte development. *Proc Natl Acad Sci U S A.* Mar 16 2004;101(11):3898-3902.

10. Corry RJ, Winn HJ, Russell PS. Primarily vascularized allografts of hearts in mice. The role of H-2D, H-2K, and non-H-2 antigens in rejection. *Transplantation.* Oct 1973;16(4):343-350.

11. Tanaka M, Terry RD, Mokhtari GK, Inagaki K, Koyanagi T, Kofidis T, Mochly-Rosen D, Robbins RC. Suppression of graft coronary artery disease by a brief treatment with a selective epsilonPKC activator and a deltaPKC inhibitor in murine cardiac allografts. *Circulation.* Sep 14 2004;110(11 Suppl 1):II194-199.

12. Jones ND, Van Maurik A, Hara M, Gilot BJ, Morris PJ, Wood KJ. T-cell activation, proliferation, and memory after cardiac transplantation in vivo. *Ann Surg.* Apr 1999;229(4):570-578.

CHAPTER 3

Timing of Bone Marrow Cell Delivery Has Minimal Effects on Cell Viability and Cardiac Recovery Following Myocardial Infarction

Rutger-Jan Swijnenburg, Johannes A. Govaert, Koen E.A. van der Bogt, William Stein, Mei Huang, Jeremy I. Pearl, Grant Hoyt, Hannes Vogel, Christopher Contag, Robert C. Robbins, and Joseph C. Wu

ABSTRACT

Background: Despite ongoing clinical trials, the optimal time for delivery of bone marrow mononuclear cells (BMCs) following myocardial infarction (MI) is unclear. We compared the viability and effects of transplanted BMCs on cardiac function in the acute and sub-acute inflammatory phases of MI.

Methods and Results: The time-course of acute inflammatory cell infiltration was quantified by FACS analysis of enzymatically digested hearts of FVB mice (n=12) following LAD ligation. Mac-1$^+$Gr-1^{high} neutrophil infiltration peaked at day 4. BMCs were harvested from transgenic FVB mice expressing firefly luciferase (Fluc) and green fluorescent protein (GFP). Afterwards, 2.5×10^6 BMCs were injected into the left ventricle of wild-type FVB mice either immediately (Acute BMC) or 7 days (Sub-acute BMC) after MI, or after a sham procedure (n=8 per group). *In vivo* bioluminescence imaging (BLI) showed an early signal increase in the Acute BMC group at day 7, followed by a trend towards improved BMC survival in the Sub-acute BMC group that persisted until the BLI signal reached background levels after 42 days. Compared to controls (MI + saline injection), echocardiography showed a significant preservation of fractional shortening at 4 weeks (Acute BMC vs saline; $P<0.01$) and 6 weeks (both BMC groups vs saline; $P<0.05$), but no significant differences between the two BMC groups. FACS analysis of BMC injected hearts at day 7 revealed that GFP$^+$ BMCs expressed hematopoietic (CD45, Mac-1, Gr-1) markers, minimal progenitor (Sca-1, c-kit), and no endothelial (CD133, Flk-1) or cardiac (Trop-T) cell markers.

Conclusion: Timing of BMC delivery has minimal effects on intramyocardial retention and preservation of cardiac function. In general, there is poor long-term engraftment and BMCs tend to adopt inflammatory cell phenotypes.

INTRODUCTION

Ischemic heart disease is the principal cause of heart failure and its prevalence continues to increase[1]. Due to the low regenerative capacity of the human heart, myocardial infarction (MI) leads to an irreversible loss of cardiomyocytes and ventricular remodeling. In recent years, treatment with autologous bone marrow-derived stem cells has been suggested to reduce myocardial damage in patients with MI[2]. Although different bone marrow cell sub-populations have been proposed to aid to cardiac repair, unfractionated autologous bone marrow mononuclear cells (BMCs) were used as donor cells in the majority of clinical trials, mainly because of the ability to safely and quickly isolate these cells. The mononuclear part of the bone marrow includes a heterogeneous mixture of cells with varying percentages of hematopoietic stem cells, endothelial progenitor cells, mesenchymal stem cells, and side population cells, as well as adult myeloid and lymphoid cells[3].

The potential mechanism(s) by which transplanted BMCs can improve cardiac function remains a subject of debate. Beyond these mechanical considerations, several basic technical issues remain to be clarified, such as the optimal cell type, route of delivery, and timing of cell transplantation. Following acute MI, a robust inflammatory response occurs that is necessary for healing and scar formation and contributes to cardiac remodeling[4]. The benefits of BMC transplantation in the acute phase after MI may thus be jeopardized by the local inflammation that renders the myocardium a hostile environment for the injected cells. On the other hand, experimental studies have demonstrated that BMC transplantation can lead to a reduction of cardiomyocyte apoptosis[5], suggesting that early timing of cell delivery might be the most efficient. Clearly, the optimal time point for cell delivery after myocardial infarction remains unknown.

To date, very few studies have addressed the timing of BMC transplantation, and those studies have relied on post-mortem analysis such as real-time PCR[6] and immunohistochemistry[7]. These methods are highly dependent on the chosen time points of animal sacrifice and provide only a limited "snapshot" representation rather than a complete picture of cell survival over time. To overcome these issues, our group has been developing and validating imaging techniques for tracking transplanted stem cells *in vivo*[8]. In this study, we investigated the viability and effects of transplanted BMCs on cardiac function in the acute and sub-acute inflammatory phases of MI using molecular imaging techniques. In addition, we analyzed the phenotype of BMCs transplanted into acute inflammatory myocardium.

MATERIALS AND METHODS

Transgenic L2G animals expressing Fluc-GFP.

The donor group consisted of male L2G85 mice (8 weeks old), which were bred on FVB background and ubiquitously expressed green fluorescent protein (GFP) and firefly luciferase (Fluc) reporter genes driven by a β-actin promoter as previously described[9]. Recipient animals consisted of syngeneic, female FVB/NJ mice (8 weeks old, Jackson Laboratories, Bar Harbor, ME, USA). Animal care was provided in accordance with the Stanford University School of Medicine guidelines and policies for the use of laboratory animals.

Preparation of bone marrow mononuclear cells (BMCs).

BMCs were harvested from the long bones of male L2G85 transgenic mice and isolated by centrifugation in a density cell separation medium (Ficoll-Hypaque; GE Healthcare, Piscataway, NJ) prior to intramyocardial injection.

BMC proliferation assay.

Proliferation was determined by the 3-(4,5-Dimethylthiazol-2-yl)-2,5-diphenyltetrazolium bromide (MTT) assay. 5×10^5 BMCs were plated in 100 µl IMDM (10% FBS) into a 96-well plate in triplicates and were incubated under normoxic ($95\%O_2/5\%CO_2$) and hypoxic ($1\%O_2/5\%CO_2/94\%N_2$) conditions for 32 hours. 20 µl of MTT was added to each well, followed by incubation for an additional 4 hours. Absorbance was determined with a multi-well absorbance reader (Genios, Tecan Systems Inc., San Jose, CA) at 490 nm using Magellon v6.2 software.

Surgical model for acute and subacute myocardial infarction.

Female FVB mice (8 weeks old) were intubated with a 20-gauge angiocath (Ethicon Endo-Surgery, Inc. Cincinnati, OH) and placed under general anesthesia with isoflurane (2%). Myocardial infarction (MI) was created by ligation of the mid-left anterior descending (LAD) artery with 8-0 ethilon suture through a left anterolateral thoracotomy as described[10]. In the acute MI model, both the infarct and peri-infarct regions were injected with 25 µL containing 2.5×10^6 cells or saline immediately following MI using a Hamilton syringe with a 30-gauge needle. In the subacute model, BMCs were injected after re-thoracotomy on day 7 following MI. All surgical procedures were performed in a blinded fashion by one micro-surgeon (G.H.) with many years of experience on this model.

Flow cytometric analysis of cell and/or myocardial tissue.

Freshly isolated BMCs were washed and incubated with conjugated primary antibody for 45 min at 4˚C. For tissue analysis, hearts were surgically explanted, minced and digested for 2 hours in Collagenase D (2 mg/mL; Worthington Biochemical) at room temperature in RPMI

1640 media (Sigma Chemical Co.) with 10% fetal calf serum (FCS; Life Technologies). Myocardial cell suspensions were run through a 70-m cell strainer, washed in FACS buffer (PBS 2% FCS) and incubated with conjugated primary antibody for 45 min at 4°C. For Troponin T staining, a 30-min incubation in cell permeabilization buffer was performed prior to antibody incubation. Finally, cells were washed, incubated with 7-amino-actinomycin D (7-AAD) cell viability solution (eBiosciences), and analyzed on a FACSCalibur system (BD Biosciences). The following antibodies were used in this study: APC-conjugated CD45 (clone: 30-F11), Gr-1 (RB6-8C5) and C-kit (2B8); Phycoerythin (PE)-conjugated Mac-1 (M1/70), Flk-1 (Avas 12α1) (BD Biosciences), Sca-1 (D7) and CD133 (13A4) (eBioscience); purified goat-anti Troponin T-C (C-19) (Santa Cruz Biotechnology) followed by Alexa Fluor 647 Chicken Anti-Goat IgG (Molecular probes)

In vivo optical bioluminescence imaging (BLI).

BLI was performed using the IVIS 200 (Xenogen, Alameda, CA, USA) system. Recipient mice were anesthetized with isoflurane and placed in the imaging chamber. After acquisition of a baseline image, mice were intraperitoneally injected with D-Luciferin (400 mg/kg body weight). Mice were imaged on days 2, 4, 7, and weekly until sacrifice at week 6. BLI signal was quantified in units of maximum photons per second per centimeter square per steridian (photons/s/cm^2/sr) and presented as $\text{Log}^{[\text{photons/s/cm2/sr}]}$.

Echocardiography to assess left ventricular fractional shortening (LVFS).

Echocardiography was performed using the General Electric Vivid 7 Dimension imaging system equipped with a 13-MHz linear probe (General Electric, Milwaukee). Animals were induced with isoflurane, received continuous inhaled anesthetic (1.5%–2%) for the duration of the imaging session, and were imaged in the supine position. Echocardiography was performed by an independent operator (J.A.G.) blinded to the study conditions. M-mode short axis views of the left ventricle were obtained and archived. Analysis of the M-mode images was performed using GE built-in analysis software. Left ventricular end diastolic diameter (EDD) and end-systolic diameter (ESD) were measured and used to calculate fractional shortening (FS) by the following formula: FS = (EDD – ESD)/EDD.

Ex vivo TaqMan PCR.

In our protocol, the transplanted cells were derived from male mice and were transplanted into female recipients, which facilitates quantification of male cells in the explanted female hearts by tracking the *Sry* locus found on the Y chromosome. Animals were sacrificed and hearts (n=3 per group) were explanted, minced, and homogenized in 2 mL DNAzol (Invitrogen, Carlsbad, CA, USA). The DNA was isolated according to the manufacturer's protocol. The DNA was quantified on a ND-1000 spectrophotometer (NanoDrop Technologies, Wilmington, DE, USA) and 500 ng DNA was processed for TaqMan PCR using primers specific for the *Sry*

locus. RT-PCR reactions were conducted in iCylcer IQ Real-Time Detection Systems (Bio-Rad, Hercules, CA, USA). Detection levels were compared to a standard curve to assess the number of viable cells per sample. All samples were conducted in triplets.

Tissue collection, immunofluorescent, and histological analysis.

Explanted hearts were fixed in 2% paraformaldehyde for 2 hours at room temperature and cryoprotected in 30% sucrose overnight at 4°C. Tissue was frozen in optimum cutting temperature compound (OCT compound, Sakura Finetek) and sectioned at 5 μm on a cryostat. Serial sections were blocked and incubated with rat anti-CD45 (clone 30-F11) (BD Biosciences) for 1 hour at room temperature, followed by goat anti-rat Alexa 594 (Molecular Probes) for 30 min. Sections were counterstained with 4,6-diamidino-2-phenylindole (DAPI, Molecular Probes) and analyzed with a Leica DMRB fluorescent microscope (Leica Microsystems, Frankfurt, Germany). Hematoxylin and Eosin (H&E) staining (Sigma) was performed according to established protocols.

Statistical analysis.

Data are presented as mean ± SEM. Comparisons between groups were done by independent sample t-tests or analysis of variance (ANOVA) with LSD post hoc tests, where appropriate. Differences were considered significant for *P*-values <0.05. Statistical analysis was performed using SPSS statistical software for Windows (SPSS)

RESULTS

Quantification of acute myocardial inflammation following myocardial infarction in mice.

Acute MI triggers an acute inflammatory phase, dominated by infiltrating neutrophils that produce reactive oxygen species and proteases that cause cardiomyocyte injury. This is followed by a proliferative phase, in which infiltrating macrophages produce cytokines and growth factors that stimulate fibroblast proliferation and neovascularization[11]. After inducing MI in our mice, conventional histology showed a robust and progressive infiltration of inflammatory cells into the infarcted area over time, followed by scar formation and subsequent remodeling of the left ventricle (Fig 1A). To determine the transition of the inflammatory into proliferative phase, we performed a quantitative analysis of intra-myocardial infiltrating cell subsets using flow cytometry of enzymatically digested hearts. MI was created by LAD ligation in FVB mice (n=12), which were sacrificed on days 2, 4, 7, and 14 following MI (n=3 per group). Progressive infiltration of CD45+ infiltrating leukocytes was found to peak on day 4 and day 7 following MI (Fig 1B and D). More specifically, early infiltration of Mac-1+Gr-1high neutrophils was found to peak on day 4 (Fig 1C and E), whereas Mac-1+Gr-1low macrophages

A

Day 2   Day 4   Day 7   Day 14

B

Side scatter

L

CD45

C

Gr-1

N

M

Mac-1

D

All Leukocytes   Neutrophils   Macrophages

% CD45+

% Mac-1+Gr-1high

% Mac-1+Gr-1low

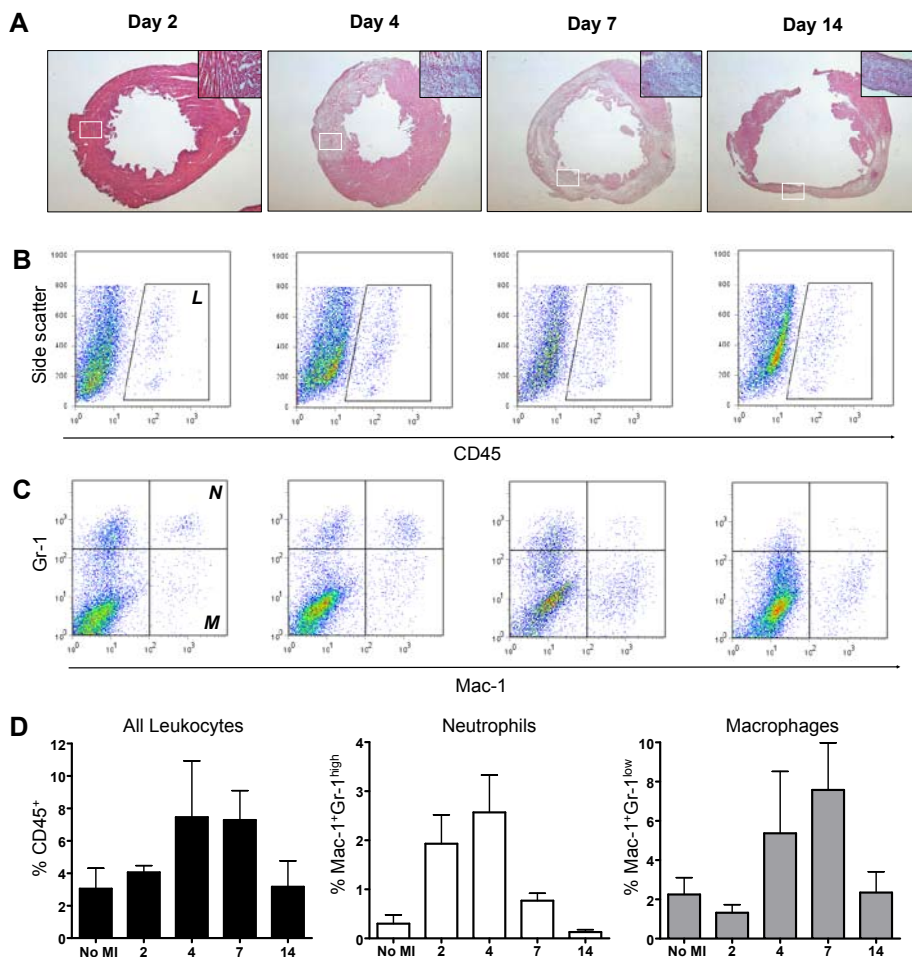No MI   2   4   7   14   No MI   2   4   7   14   No MI   2   4   7   14

Figure 1. Quantification of myocardial inflammation following LAD ligation in FVB mice. (a) H&E staining performed on sections of the left ventricle at different time-points following LAD ligation shows increasing infiltration of mononuclear cells over time leading to ventricular remodeling. **(b)** Corresponding panels of flow cytometric analysis show that intramyocardial infiltration of CD45+ leukocytes reaches a maximum at 4 to 7 days following LAD ligation. **(c)** More specifically, infiltration of Mac-1+Gr-1high neutrophils (*N*) peaks on day 4, whereas Mac-1+Gr-1low macrophages (*M*) peak on day 7 following LAD ligation. **(d)** Graphical representation of infiltration of inflammatory cell subsets.

infiltrated the heart most predominantly on day 7 (Fig 1C and F). These findings demonstrate that in our murine model, transition of the aforementioned phases occurs between days 4 and 7 following MI.

Characterization of Fluc+GFP+ BMC.

We have previously validated *in vivo* BLI as a reliable tool to monitor BMC engraftment into ischemic myocardium[12]. BLI measurements correlate highly with post-mortem methods of donor cell detection[12, 13]. BMC harvested from transgenic L2G85 mice (FVB background)

exhibit a robust correlation between Fluc expression and BMC number (Fig 2A), as well as a strong expression of GFP (Fig 2B). FACS analysis confirmed the presence of stem/progenitor cells as well as adult hematopoietic cells within the BMC population (Fig 2C). The proliferation capacity of BMC was tested *in vitro*. Under hypoxic conditions, the cells showed robust proliferation when compared to BMCs kept under normoxic conditions (Fig 2D).

Effects of timing of BMC delivery following MI on cell viability.

To determine whether the survival of transplanted BMCs depends on the timing of delivery, FVB mice (n=24) were randomized into the following groups: (1) LAD ligation + immediate BMC injection (Acute BMC); (2) LAD ligation + BMC injection at 7 days post-MI (Sub-acute BMC); and (3) Sham surgery + BMC injection (BMC control). *In vivo* BLI showed an early signal
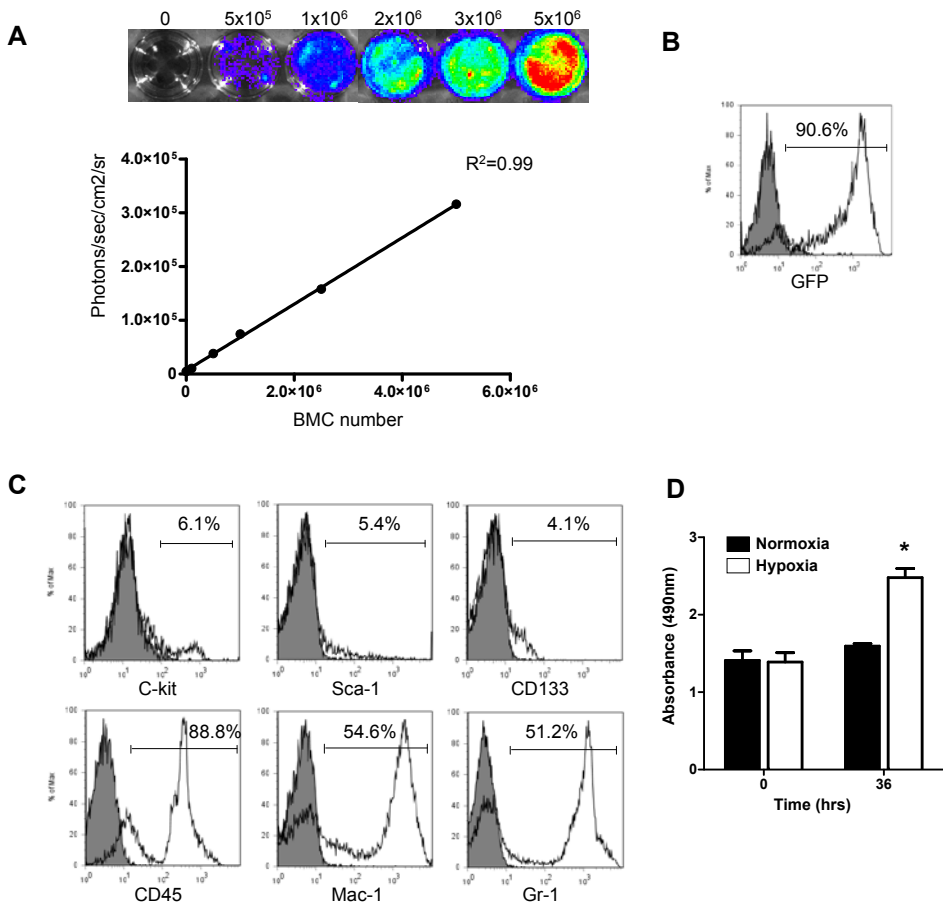
Figure 2. Characterization of firefly luciferase (Fluc) and green fluorescent protein (GFP)-positive BMCs. (a) *Ex vivo* BLI shows a robust correlation between cell number and reporter gene activity. **(b)** There is robust expression of GFP by BMCs. **(c)** Further characterization of the BMC subsets shows low numbers of stem/progenitor cells (Sca-1, c-kit, CD133) and high numbers of adult hematopoietic cells (CD45, Mac-1, Gr-1). **(d)** Viability and proliferation capacity of transgenic BMCs were confirmed *in vitro*. After 36 hours under hypoxic conditions, BMCs proliferated significantly more compared to BMCs that were maintained under normoxic conditions (*$P<0.01$).

increase in the Acute BMC group on day 7 (Acute BMC: 4.50±0.05 vs Sub-acute BMC: 4.34±0.05 Log$^{[photons/s/cm2/sr]}$; $P<0.05$), similar to validated findings in our previous study[12]. This suggests a significantly higher proliferation of donor BMCs delivered into acute MI milieu as compared to BMCs delivered in a sub-acute MI milieu. BLI further showed a trend (though not statistically
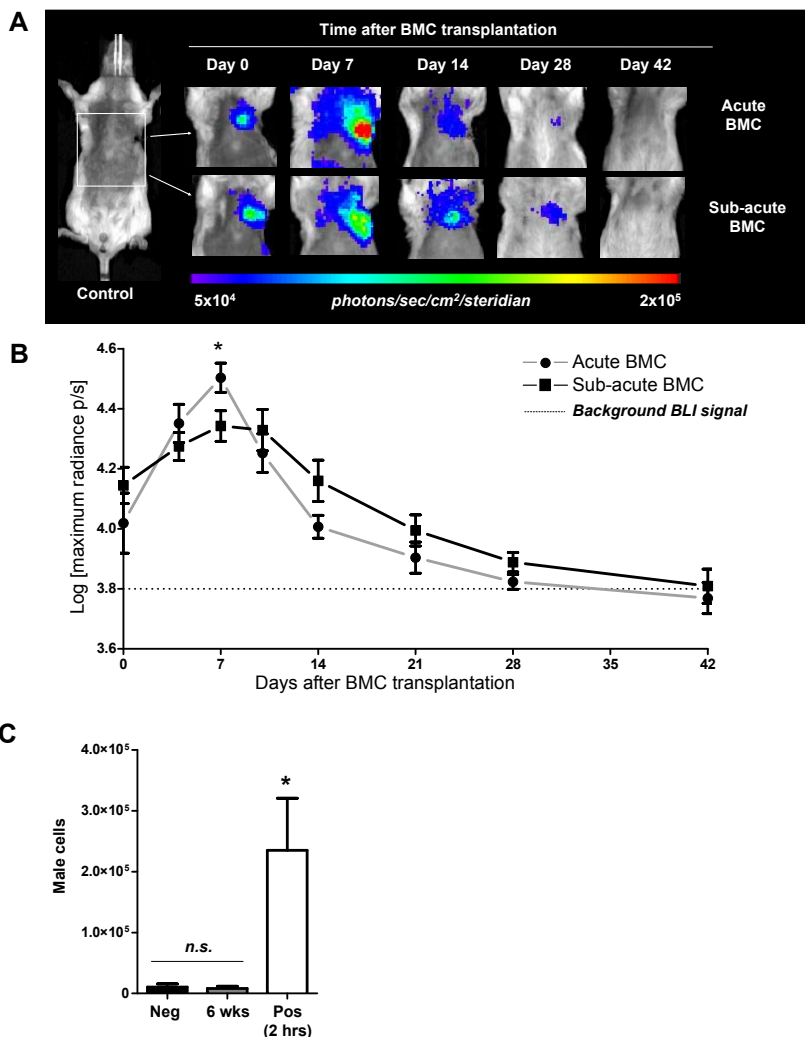
Figure 3. Longitudinal *in vivo* tracking of transplanted BMCs. (a) Representative BLI images of BMC transplanted animals either acutely (Acute BMC, upper panels) or 7 days after MI (Sub-acute BMC, lower panels) show proliferation of the cells early after transplantation. Thereafter, in both groups the BLI signal decreases gradually over time to reach background levels at day 42. Color scale bar values are in photons/s/cm^2/sr. **(b)** Graphical representation of longitudinal BLI shows a significantly increased signal intensity in the Acute BMC group at day 7 (*$P<0.05$), followed by a trend towards improved BMC survival in the Sub-acute BMC that persisted until BLI signal reached background levels at day 42 day. **(c)** *Ex vivo* quantitative TaqMan PCR found no significant differences when comparing negative control (Neg) and 6-week BMC-injected hearts. Significantly more male BMCs were found in the 2 hour positive control (Pos) hearts (n=3 per group, *n.s.* = not significant, *$P<0.001$).

significant) towards improved BMC survival in the Sub-acute BMC group that persisted until the BLI signal reached background levels in both groups at 42 days. No significant difference was in BLI signal was found between Sub-acute BMC and control BMC animals (not shown). These results suggest that, independent of timing of delivery, intramyocardial retention of BMC is limited to 6 weeks following transplant.

Ex vivo quantification of BMC survival.

To confirm BLI findings and to rule out the possibility that BMC death might have been caused by recipient immune response towards the reporter gene, we performed LAD ligation on an additional set of female FVB mice, which were randomized to receive 2.5×10^6 non-labeled (wild-type) BMCs from male FVB donors (n=6) or saline (Negative control, n=3). BMC-injected animals were sacrificed at 2 hours (Positive control) and 6 weeks (n=3 per group). Their hearts were processed for quantitative TaqMan PCR analysis. Consistent with BLI data, there were no significant differences between 6-week BMC-injected hearts and saline-injected hearts, demonstrating that no male donor BMCs could be detected intramyocardially at the 6 week time-point. In comparison, significantly higher BMC numbers were found in 2 hour BMC hearts (Fig 3C).

Effects of timing of BMC delivery on preservation of cardiac function.

Preservation of cardiac performance was analyzed by echocardiography performed pre-op-eratively (base-line) and every 2 weeks following MI in the Acute and Subacute BMC animals, and compared to a control group receiving LAD ligation + saline injection (FVB, n=8). A representative M-mode tracing used for analysis is shown in Figure 4A. A significant preservation of fractional shortening was seen in BMC groups at 4 weeks (Acute BMC: 33.2±1.7% vs saline:
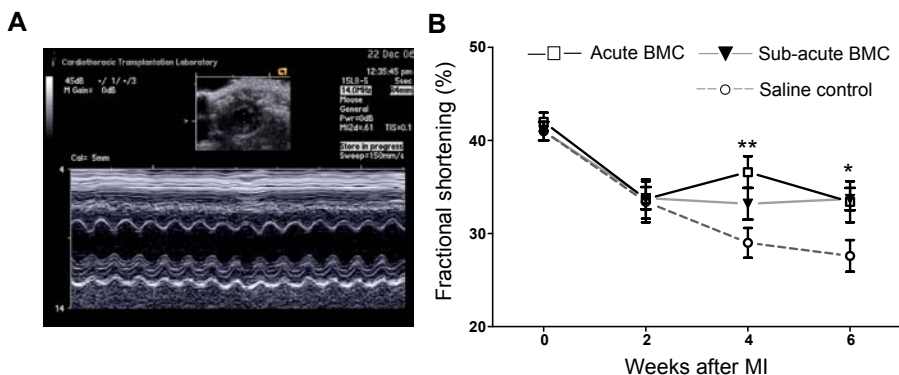
Figure 4. Echocardiographic assessment of cardiac function. **(a)** Representative M-mode echocardiogram at the level of the papillary muscle from which left ventricular diameters were measured. **(b)** Echocardiography revealed a significant preservation of left ventricular fractional shortening at 4 weeks in the Acute BMC group and 6 weeks in both BMC groups compared to saline control animals. No significant difference in cardiac performance was found between Acute and Sub-acute BMC animals. (*$P < 0.05$, **$P < 0.01$)

29.0±1.6%; *P*<0.01) and 6 weeks (Acute BMC: 33.7±1.2%; Sub-acute BMC: 33.4±2.2% vs saline: 27.6±1.7%; *P*<0.05 for both BMC groups vs. saline) following MI. However, no significant differences in cardiac contractility were found between both BMC groups during the 6-week study period (Fig 4B).

BMCs delivered into acute inflammatory environment adopt adult hematopoietic phenotypes.

In the first week following injection, BLI imaging showed a significantly higher proliferation rate of donor BMCs that were delivered into acute inflammatory myocardium, as compared to BMCs delivered into sub-acute inflammation (Fig 3A and B). Since BMCs represent a heterogeneous cell population, we aimed to investigate the phenotype of transplanted BMC at 7 days following injection into acute myocardial inflammation. LAD ligation + acute BMC (n=4) or saline (n=3) injection was performed in an additional set of FVB mice, which were sacrificed for heart procurement at 7 days post-transplant. Conventional H&E staining of sections of the left ventricle showed robust mononuclear cell infiltration and early signs of scar formation consistent with MI (Fig 5A). Immunofluorescent staining on a corresponding section revealed the presence of intramyocardial mononuclear cells, which appeared to be mostly of GFP+ donor origin (Fig 5B). Interestingly, staining with the pan-leukocyte marker
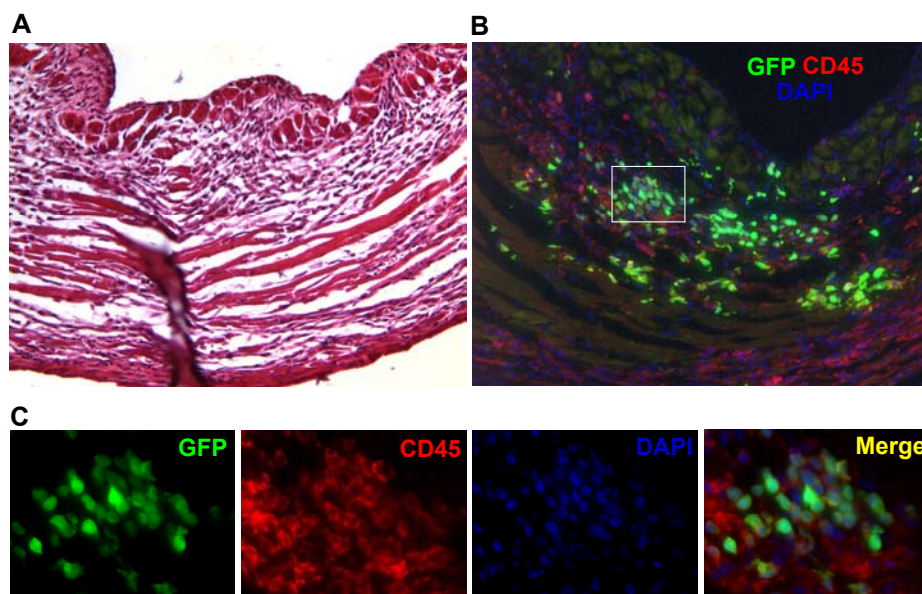
Figure 5. Immunohistochemical analysis of BMC transplanted hearts. (a) H&E staining of the left ventricular wall shows mononuclear cell infiltrates and scar formation consistent with myocardial infarction. **(b)** Immunofluorescent staining on a corresponding section reveals an abundant presence of GFP+ BMCs (green) within the infarcted myocardium, which is rich in CD45+ inflammatory cells (red). Counterstaining was performed with 4,6-diamidino-2-phenylindole (DAPI, blue). **(c)** High power views of the selected area (Fig 2B white square) reveal that the vast majority of donor BMCs express CD45 and retain round shapes with large nuclei, representing an inflammatory phenotype.

CD45 revealed that the vast majority of GFP+ donor cells co-expressed CD45 (Fig 5B and C). Next, we performed a systematic flow cytometric analysis on explanted hearts following enzymatic digestion (n=3 per group). Figure 6A shows representative flow cytometry panels confirming that GFP+ donor BMCs (right panel, arrow) co-expressed CD45, compared to saline-injected control hearts (left panel). Serial analysis showed that donor BMCs expressed CD45, Mac-1 and Gr-1, and minimal numbers of Sca-1 and c-kit, and remained negative for CD133, Flk-1 and/or Troponin (Trop)-T (Fig 6B). These results suggest that at 7 days following acute delivery, donor BMCs were mostly of adult hematopoietic phenotypes, and showed no signs of both endothelial (progenitor) cell (CD133 and Flk-1) and/or cardiomyocyte (Trop-T) differentiation.
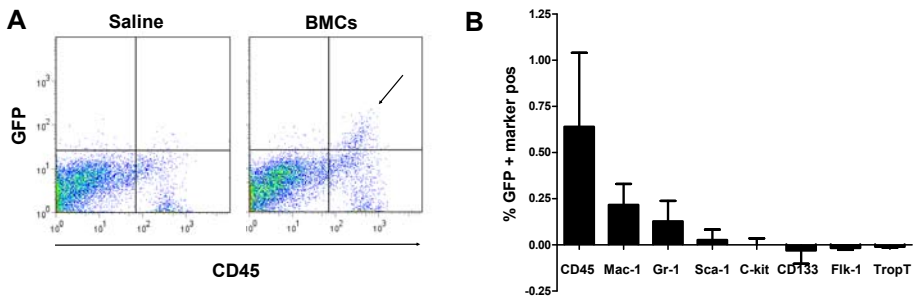
Figure 6. *Ex vivo* phenotyping of donor BMCs confirms inflammatory phenotype. (a) Representative flow cytometry panels of saline (left) and BMC (right) injected hearts at 7 days after acute BMC delivery. At this time-point GFP+ BMCs (arrow) co-express CD45, confirming their inflammatory phenotype. **(b) S**erial flow cytometric analysis reveals that GFP+ BMCs predominantly express inflammatory cell markers (CD45, Mac-1, Gr-1), rather then stem cell (Sca-1, c-kit), endothelial progenitor cell (CD133, Flk-1) or cardiomyocyte (TropT) markers. Data are presented as percentage of GFP/marker+ cells reduced by background staining.

DISCUSSION

Despite ongoing clinical trials, the optimal time-point of BMC delivery following acute MI remains a point of debate. A review of current literature reveals few studies that have systematically addressed the issue of timing of BMC transplantation[14]. This study was designed to determine the effects of timing of BMC delivery following acute MI in a standardized mouse LAD ligation model. Specifically, we have demonstrated that: (1) BMC transplantation in either acute or sub-acute myocardial infarction has a mildly positive effect on cardiac preservation, confirming earlier findings in animals models[15] and clinical trials[2]; (2) retention of BMC engraftment and preservation of cardiac function are not critically dependent on the timing of delivery; and (3) injection of BMCs into the acute inflammatory environment of myocardial infarction leads to early proliferation of donor cells that adopt adult hematopoietic phenotypes.

Earlier studies from our laboratory using *in vivo* BLI of transplanted BMCs revealed that the cells can effectively home in on and engraft into infarcted myocardium[12, 13]. Although the present study confirms the therapeutic effect of BMC transplantation in the setting of acute MI, it also clearly shows that delivery of the cells in the time-window following the hostile acute inflammatory phase–7 days after MI–does not result in extended long-term survival of donor BMCs. In addition, no significant differences were found in the preservation of cardiac function between BMCs injected groups during a 6-week period of observation.

To our knowledge, timing of BMC delivery has thus far not been investigated in experimental models. However, other cell populations, such as BM-derived mesenchymal stem cells[7] and fetal cardiomyocytes[16], showed therapeutic improvements in rat models when delivered in a the time-window of 1 to 2 weeks following MI. Most likely, the different observations made in our study are the results of the different cell populations used for transplantation. To represent the present clinical situation, we specifically used unfractioned BMCs. In addition to survival data, we show that the portion of BMCs responsible for cardiac preservation seem to be adult hematopoietic cells, rather than BM-derived endothelial, endothelial progenitor, or cardiac cells, at least following acute delivery at the time-point tested. These findings strengthen the hypothesis that preservation of cardiac performance by BMC transplantation might be attributable to modulation of the natural process of myocardial inflammation and infarct healing[17].

Investigations aimed to reveal the mechanism(s) by which stem cells might preserve cardiac function have been plenty. Early reports pointed toward the myocardial regeneration by repopulation of BM-derived endothelial cells and/or cardiomyocytes[18]; however, subsequent studies failed to support those observations[19]. Other proposed mechanisms include donor-host cell fusion and neovascularization by either vasculogenesis and/or secretion of paracrine factors leading to angiogenesis and arteriogenesis[20]. Recently, studies have focused on additional mechanisms of action of transplanted BMCs, which could be by a direct paracrine effect on the inflammatory cascade. Burchfield et al. recently reported evidence that BMCs mediate cardiac protection by release of the immunomodulatory cytokine IL-10, leading to decreased intramyocardial accumulation of T-lymphocytes, which translated into reduced LV remodeling[21]. Similarly, Ciulla et al. found transplanted BMCs to reduce serum levels of pro-inflammatory cytokines, which are known to contribute to myocardial apoptosis, necrosis, and scar formation[22]. These findings, combined with the results presented in the present study, suggest that BM progenitors could ameliorate LV remodeling following MI by continuing to differentiate along the hematopoietic lineage.

The clinical relevance of this study is significant. A recent meta-analysis of randomized clinical trials of BMC transplantation in patients suffering from acute MI found *no* significant difference in global LV function when the cells were delivered in either the <5-day or 5- to –30-day time windows[2]. The present study provides the experimental proof for these clinical findings. Specifically, we show that long-term survival and modest therapeutic efficacy

of BMCs seem to be relatively *independent* of timing of cell delivery. Clinically significant improvements of cardiac function in patients suffering from acute MI may thus be achieved by *repeated* cellular transplants, both in the acute and sub-acute phases of myocardial inflammation.

FUNDING SOURCES

REFERENCES

1. Rosamond W, Flegal K, Furie K, Go A, Greenlund K, Haase N, Hailpern SM, Ho M, Howard V, Kissela B, Kittner S, Lloyd-Jones D, McDermott M, Meigs J, Moy C, Nichol G, O'Donnell C, Roger V, Sorlie P, Steinberger J, Thom T, Wilson M, Hong Y. Heart disease and stroke statistics--2008 update: a report from the American Heart Association Statistics Committee and Stroke Statistics Subcommittee. *Circulation.* 2008;117:e25-146.

2. Abdel-Latif A, Bolli R, Tleyjeh IM, Montori VM, Perin EC, Hornung CA, Zuba-Surma EK, Al-Mallah M, Dawn B. Adult bone marrow-derived cells for cardiac repair: a systematic review and meta-analysis. *Archives of internal medicine.* 2007;167:989-997.

3. Dimmeler S, Burchfield J, Zeiher AM. Cell-based therapy of myocardial infarction. *Arteriosclerosis, thrombosis, and vascular biology.* 2008;28:208-216.

4. Nian M, Lee P, Khaper N, Liu P. Inflammatory cytokines and postmyocardial infarction remodeling. *Circulation research.* 2004;94:1543-1553.

5. Uemura R, Xu M, Ahmad N, Ashraf M. Bone marrow stem cells prevent left ventricular remodeling of ischemic heart through paracrine signaling. *Circulation research.* 2006;98:1414-1421.

6. Muller-Ehmsen J, Krausgrill B, Burst V, Schenk K, Neisen UC, Fries JW, Fleischmann BK, Hescheler J, Schwinger RH. Effective engraftment but poor mid-term persistence of mononuclear and mesenchymal bone marrow cells in acute and chronic rat myocardial infarction. *Journal of molecular and cellular cardiology.* 2006;41:876-884.

7. Hu X, Wang J, Chen J, Luo R, He A, Xie X, Li J. Optimal temporal delivery of bone marrow mesenchymal stem cells in rats with myocardial infarction. *Eur J Cardiothorac Surg.* 2007;31:438-443.

8. Zhang SJ, Wu JC. Comparison of imaging techniques for tracking cardiac stem cell therapy. *J Nucl Med.* 2007;48:1916-1919.

9. Cao YA, Wagers AJ, Beilhack A, Dusich J, Bachmann MH, Negrin RS, Weissman IL, Contag CH. Shifting foci of hematopoiesis during reconstitution from single stem cells. *Proc Natl Acad Sci U S A.* 2004;101:221-226.

10. Swijnenburg RJ, Tanaka M, Vogel H, Baker J, Kofidis T, Gunawan F, Lebl DR, Caffarelli AD, de Bruin JL, Fedoseyeva EV, Robbins RC. Embryonic stem cell immunogenicity increases upon differentiation after transplantation into ischemic myocardium. *Circulation.* 2005;112:I166-172.

11. Frangogiannis NG, Smith CW, Entman ML. The inflammatory response in myocardial infarction. *Cardiovasc Res.* 2002;53:31-47.

12. van der Bogt KE, Sheikh AY, Schrepfer S, Hoyt G, Cao F, Ransohoff KJ, Swijnenburg RJ, Pearl J, Lee A, Fischbein M, Contag CH, Robbins RC, Wu JC. Comparison of different adult stem cell types for treatment of myocardial ischemia. *Circulation.* 2008;118:S121-129.

13. Sheikh AY, Lin SA, Cao F, Cao Y, van der Bogt KE, Chu P, Chang CP, Contag CH, Robbins RC, Wu JC. Molecular imaging of bone marrow mononuclear cell homing and engraftment in ischemic myocardium. *Stem cells.* 2007;25:2677-2684.

14. Bartunek J, Wijns W, Heyndrickx GR, Vanderheyden M. Timing of intracoronary bone-marrow-derived stem cell transplantation after ST-elevation myocardial infarction. *Nature clinical practice.* 2006;3 Suppl 1:S52-56.

15. Kamihata H, Matsubara H, Nishiue T, Fujiyama S, Tsutsumi Y, Ozono R, Masaki H, Mori Y, Iba O, Tateishi E, Kosaki A, Shintani S, Murohara T, Imaizumi T, Iwasaka T. Implantation of bone marrow mononuclear cells into ischemic myocardium enhances collateral perfusion and regional function via side supply of angioblasts, angiogenic ligands, and cytokines. *Circulation.* 2001;104:1046-1052.

16. Li RK, Mickle DA, Weisel RD, Rao V, Jia ZQ. Optimal time for cardiomyocyte transplantation to maximize myocardial function after left ventricular injury. *The Annals of thoracic surgery.* 2001;72:1957-1963.
17. Mathur A, Martin JF. Stem cells and repair of the heart. *Lancet.* 2004;364:183-192.
18. Orlic D, Kajstura J, Chimenti S, Jakoniuk I, Anderson SM, Li B, Pickel J, McKay R, Nadal-Ginard B, Bodine DM, Leri A, Anversa P. Bone marrow cells regenerate infarcted myocardium. *Nature.* 2001;410:701-705.
19. Balsam LB, Wagers AJ, Christensen JL, Kofidis T, Weissman IL, Robbins RC. Haematopoietic stem cells adopt mature haematopoietic fates in ischaemic myocardium. *Nature.* 2004;428:668-673.
20. Beeres SL, Atsma DE, van Ramshorst J, Schalij MJ, Bax JJ. Cell therapy for ischaemic heart disease. *Heart.* 2008;94:1214-1226.
21. Burchfield JS, Iwasaki M, Koyanagi M, Urbich C, Rosenthal N, Zeiher AM, Dimmeler S. Interleukin-10 from transplanted bone marrow mononuclear cells contributes to cardiac protection after myocardial infarction. *Circulation research.* 2008;103:203-211.
22. Ciulla MM, Montelatici E, Ferrero S, Braidotti P, Paliotti R, Annoni G, De Camilli E, Busca G, Chiappa L, Rebulla P, Magrini F, Lazzari L. Potential advantages of cell administration on the inflammatory response compared to standard ACE inhibitor treatment in experimental myocardial infarction. *Journal of translational medicine.* 2008;6:30.

PART II:

Characterization of Embryonic Stem Cell Transplantation Immunobiology using molecular imaging

CHAPTER 4

Molecular Imaging of Human Embryonic Stem Cells: Keeping an Eye on Differentiation, Tumorigenicity, and Immunogenicity

Koen E.A. van der Bogt, Rutger-Jan Swijnenburg, Feng Cao, and Joseph C. Wu

ABSTRACT

Human embryonic stem cells (hESCs) are capable of differentiation into every cell type of the human being. They are under extensive investigation for their regenerative potential in a variety of debilitating diseases. However, the field of hESC research is still in its infancy, as there are several critical issues that need to be resolved before clinical translation. Two major concerns are the ability of undifferentiated hESCs to form teratomas and the possibility of a provoked immune reaction after transplantation of hESCs into a new host. Therefore, it is imperative to develop non-invasive imaging modalities that allow for longitudinal, repetitive, and quantitative assessment of transplanted cell survival, proliferation, and migration in vivo. Reporter gene-based molecular imaging offers these characteristics and has great potential in the field of stem cell therapy. Moreover, it has recently been shown that reporter gene imaging can be combined with therapeutic strategies. Here, we provide an outline of the current status of hESC research and discuss the concerns of tumorigenicity and immunogenicity. Furthermore, we describe how molecular imaging can be utilized to follow and resolve these issues.

INTRODUCTION

Adult stem cells have great promise as potential treatments for a variety of intractable diseases. However, these cells are generally limited in their plasticity. Therefore, it would be ideal to obtain or create a cell line that is truly able to differentiate into every cell of the body. The first such cell line was derived in the 1960's and originated from teratomas that developed spontaneously in male mice of the 129 strain. These "embryonal carcinoma" (EC) cells were capable of teratoma formation after transplantation of single cells into a new host,[1] confirming their ability to differentiate into progeny of all three germ layers (ectoderm, mesoderm and endoderm)--a phenomenon known as 'pluripotency'.[2] Further research led to the first isolation of murine embryonic stem cells (mESCs) in 1981 from the epiblast of blastocyst-stage mouse embryos,[3, 4] followed by the establishment of the first human embryonic stem cell (hESC)-line in 1998.[2] To date, there are more than 300 hESC lines, but only 22 hESC lines are commercially available and registered in the "NIH Human Embryonic Stem Cell Registry".[5]

Although most studies using hESCs in disease models show auspicious results, there are several concerns about hESC transplantation. First, the pluripotent character of hESCs is somewhat a double-edged sword. They are an attractive candidate for cell based therapies, but their pluripotency can also lead to risk of teratoma formation after transplantation. Second, since it is presently impossible to transplant hESCs syngeneically, the possibility that hESCs might provoke an immune reaction following allogeneic transplantation must be considered. This review will discuss these issues and how molecular imaging can help resolve them.

DERIVATION, MAINTENANCE, AND DIFFERENTIATION

Traditionally, hESCs are isolated from the inner cell mass of the human blastocyst, or as recently shown, can be derived from single blastomeres.[6] The isolated cells can be expanded *in vitro*, with an average doubling time of 30-35 h.[7] However, strict homeostatic culture conditions and the addition of inhibiting compounds are necessary to keep the hESCs in an undifferentiated state, a condition required for maintaining a normal karyotype and an unlimited capacity for self-renewal. This is possible by growing hESCs on a cellular feeder layer. Inactivated murine embryonic fibroblasts prove to be an effective feeder layer for the undifferentiated growth of hESCs because they secrete differentiation-inhibiting factors.[8] Due to the risk of cross-species retroviral infection, however, this is an unattractive option in the long term. Recently, several reports have described the culture of hESCs in animal-free conditions, using human feeder cells consisting of foreskin,[9] pure human fibroblast populations,[10] or uterine endometrial cells and serum-free medium.[11] Generally, these undifferentiated hESCs express transcription fac-

tors OCT-3/4, Sox-2, and NANOG; surface markers CD9, CD133, and SSEA-3/4; proteoglycans TRA-1-60/81 and TRA-2-54; and enzyme alkaline phosphatases and telomerase.[12, 13]

Following withdrawal of inhibitory factors, hESCs will aggregate into three-dimensional clusters of cells in an early stage of differentiation, thereby losing pluripotency. These clusters, named Embryoid Bodies (EBs),[14] form the first step of further differentiation into any type of progeny. Within the EBs, a microenvironment exists in which various signals will promote differentiation into all three germ layers. Although differentiation generally occurs spontaneously, much effort currently focuses on stimulating directed differentiation to achieve sufficiently large populations for clinical use. The generation of pure, differentiated cultures is indispensable for developing cell based therapies, and will help us better understand cellular developmental processes and test pharmacological strategies.

Differentiation into Mesoderm Lineages

While reports have been published of hESCs differentiating into various mesodermal lineages, including kidney, muscle, bone and blood cells,[15] it is cardiomyogenesis that has received the most attention. Cardiomyogenesis typically manifests as a beating area within the EBs around 5 days after EB-formation, the surface of which increases gradually with time.[16] Kehat and colleagues were the first to show that hESC-derived cardiomyocytes within these beating EBs actually resemble the structural and functional properties of early stage human cardiomyocytes.[16] Since then, several other methods have been tested to improve the efficiency of *in vitro* differentiation of hESCs into cardiomyocytes with moderate success.[17-19]

Differentiation into Ectoderm Lineages

Using different growth factors and stimulating environments, hESCs can also be driven to differentiate into brain, skin, and adrenal derivates.[15] The potential of hESC-derived cultures for the treatment of neurodegenerative disorders is under intensive investigation. While many groups have described neuronal differentiation within the EB,[20-22] factor-induced neuronal differentiation seems to be limited to the addition of retinoic acid (RA) and nerve growth factor (betaNGF),[21] or the use of serum-free, conditioned medium.[23] The coculture of hESCs with murine skull bone marrow-derived stromal cells also seems to induce neuronal differentiation.[24]

Differentiation into Endoderm Lineages

From the beginning, hESCs were shown to be capable of differentiating *in vitro* into liver and pancreatic cells when exposed to a variety of growth factors.[15] The creation of insulin-secreting pancreatic cell populations has generated much interest, as this might ultimately provide a cell-based therapy for patients with type I diabetes.[25] However, the identification of insulin-producing cells has proven to be difficult and susceptible to artifacts.[26] Thus, the *in vitro* pancreatic differentiation from hESCs remains a challenging multi-step culturing procedure at present.[27]

In summary, although much is being done to improve the efficacy of *in vitro* differentiation systems, little is known about the cellular interactions that occur during natural differentiation. Most of the *in vitro* differentiation methods are to some extent dependent on EB formation. The process of *in vitro* EB formation mimics the natural transcriptional pathways occurring in the developing embryo, leading not only to the differentiation into the desired cell type, but also to the production of undesired cells. The most dangerous example of the latter is undifferentiated hESCs that retain the ability to form teratomas. Until we understand the precise pathways of pluripotent differentiation, the acquisition of desired, transplantable cell types can only rely on stimulating known pathways and the pre-transplantation selection of the desired cell type.

Teratoma formation

At present no selection method exists that can yield a 100% pure population, which is a major obstacle for clinical translation. When transplanted in immunodeficient mice, hESCs form teratomas consisting of human tissues from all germ layers.[2, 28] The formation and composition of teratomas seem to be influenced by several factors, including graft site,[29] transplanted cell number, and developmental phase of the host,[24] as described next.

One factor influencing hESC-based teratoma formation is the site of transplantation, which affects both growth and composition of the tumor. As recently shown by Cooke and colleagues, teratomas rising from hESCs will grow faster and contain more undifferentiated cells when transplanted in the *liver* of nude mice, as compared to *subcutaneous* transplantation.[29] It is of major interest why hESCs differentiate at the subcutaneous site but remain undifferentiated in the liver. The authors hypothesize that this was due to the well vascularized, growth factor-rich, immune-privileged porous structure in the liver.[29] These findings are not only a stimulant for further research on graft site and teratoma formation, but also indicate the importance of *in vivo* experiments, as there may be factors present in the liver that could help maintain hESCs in an undifferentiated state *in vitro*.

Another factor influencing teratoma formation is the number of undifferentiated hESCs that are viable after transplantation. As discussed earlier, transplantation of pure undifferentiated hESC inevitably leads to teratoma formation.[2, 28] Interestingly, transplantation of selected hESC-derived cells in a more developed phase will not automatically lead to teratomas, even when this population is not 100% pure.[30] However, there are no extant studies that assess the minimal cell number needed for teratoma formation, or stated otherwise, the maximum percentage of contamination with undifferentiated hESC. Our laboratory is actively investigating these issues.

Recently, Muotri and colleagues have studied undifferentiated hESC after *in utero* transplantation into the lateral brain ventricle of day-14 mouse embryos.[24] The results showed that hESCs integrated into the brain, giving rise to neuronal and glial lineages, but not to teratomas. These findings suggest that hESCs are susceptible to environmental cues that can

modulate its differentiation and tumorigenic potential, as was suggested in earlier studies with hESCs in chick embryos.[31]

Taken together, these observations and questions are not only a stimulant for further research on teratoma biology, but also indicate the importance of developing novel imaging techniques to track their growth *in vivo* longitudinally, repetitively, and quantitatively.

Immunogenicity

Another hurdle facing clinical transplantation of hESCs is the potential immunologic barrier. The immune response generated after transplantation is directed towards alloantigens, which are antigens presented on the cell surface that are considered non-self by the recipient immune system.[32] The major system of alloantigens responsible for cell incompatibility is the major histocompatibility complex (MHC). In humans, MHC-I molecules are expressed on the surface of virtually all nucleated cells and present antigens to CD8+ cytotoxic T cells, while MHC-II molecules are normally more restricted to antigen presenting cells such as dendritic cells and macrophages, and are selectively recognized by CD4+ helper T cells.[33]

It has been shown that hESCs express low levels of MHC-I in their undifferentiated state.[34, 35] In one study, the MHC-I expression increased two to four-fold when the cells were induced to spontaneously differentiate to EB, and an eight to ten-fold when induced to differentiate into teratomas.[34] In contrast, a different group observed MHC-I downregulation after differentiation induced with retinoic acid or on Matrigel or in extended cultures.[35] In both studies, MHC-I expression was strongly upregulated after treatment of the cells with interferon-γ, a potent MHC expression-inducing cytokine known to be released during the course of an immune response. MHC-II antigens were not expressed on hESCs or hESC derivatives.[34] The latter finding confirms that, in contrast to tissue allografts, hESC transplants are devoid of highly immunogenic mature dendritic cells, or any other type of specialized antigen presenting cells. Thus, the transplanted cells may not express MHC-II molecules required for effective priming of alloreactive CD4+ T cells through direct recognition.

Previously, our group tested allogeneic undifferentiated mESCs for their ability to trigger alloimmune response in a murine model of myocardial infarction.[36] We found progressive intragraft infiltration of inflammatory cells mediating both adaptive (T cells, B cells, and dendritic cells) and innate (macrophages and granulocytes) immunity. Cellular infiltration progressed from mild infiltration at two weeks to vigorous infiltration at four weeks, leading to rejection of the mESC allograft. Moreover, we found an accelerated immune response against mESCs that had differentiated *in vivo* for 2 weeks, suggesting that mESC immunogenicity increases upon their differentiation.[36]

Although it was previously reported that hESCs failed to elicit immune responses during the first 48 hours after intramuscular injection of immunocompetent mice,[37] a recent report using a similar model found hESCs to be completely eliminated at 1 month post-transplantation.[38] Thus, questions regarding the exact character and intensity of immune responses

towards allogeneic hESCs and their derivatives remain. Solutions that reduce or eliminate the potential immunological response to transplanted allogeneic hESCs are urgently needed. Possible strategies to minimize rejection of hESC transplants have been extensively reviewed elsewhere.[39, 40] Examples of these strategies include: (1) forming HLA isotyped hESC-line banks; (2) creating a universal donor cell by genetic modification; (3) inducing tolerance by hematopoietic chimerism; or (4) generating isogeneic hESC lines by somatic nuclear transfer. To optimize these techniques in the future, it is crucial to develop sensitive and reliable imaging methods for monitoring the viability of transplanted cells *in vivo*.

Molecular imaging

To date, most studies on stem cell therapy have relied on conventional reporter genes such as GFP[41] and β-galactosidase (lacZ) to monitor cell survival and differentiation. However, these reporter genes cannot be used to reliably track *in vivo* characteristics of transplanted cells due to poor tissue penetration and the need for extrinsic excitation light, which produces an
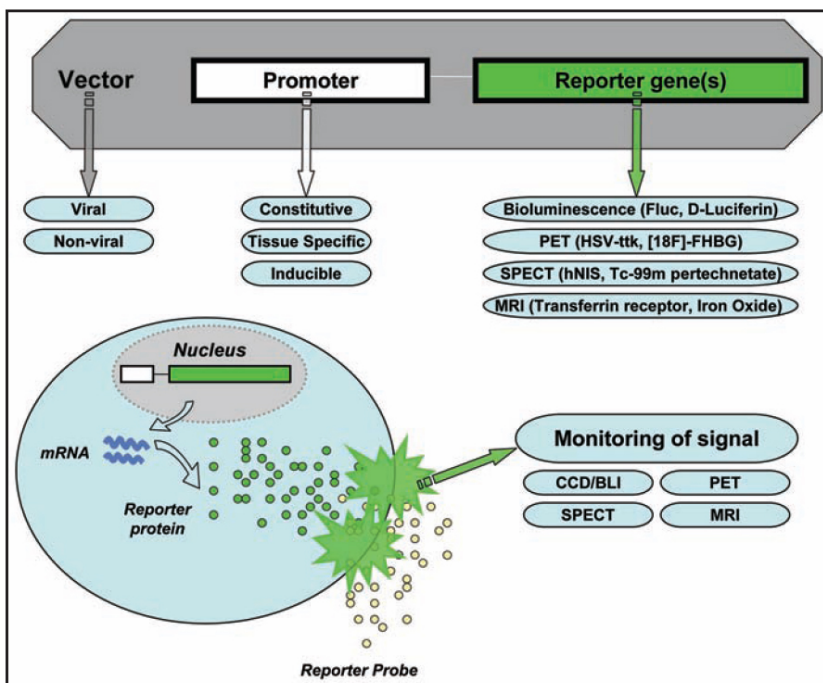
Figure 1: *Schematic overview of molecular imaging.* Outline of a vector containing a DNA reporter construct with the reporter gene(s) driven by a promoter of choice. Transcription and translation lead to production of mRNA and reporter protein, respectively. After administration of a reporter probe systemically, the reporter probe will be catalyzed by specific cells that have the reporter proteins. This amplification process can be detected by a sensitive imaging device. Examples of reporter genes and their specific reporter probes are listed per imaging modality. Abbreviations: Fluc, Firefly luciferase; PET, positron emission tomography; HSV-ttk, herpes simplex virus truncated thymidine kinase; [^{18}F]-FHBG, 9-(4-[^{18}F]-fluoro-3hydroxymethylbutyl) guanine; SPECT, single photon emission computed tomography; hNIS, human sodium/iodide symporter; MRI, magnetic resonance imaging; CCD, charged coupled device; BLI, bioluminescence imaging.

unacceptable amount of background signal. Instead, GFP-labeled cells are typically identified histologically, which provides only a single snapshot representation rather than a complete picture of cell survival over time. To solve these shortcomings, our group has been developing reporter gene-based molecular imaging techniques.[42]

Molecular imaging can be broadly defined as the *in vivo* characterization of cellular and molecular processes.[43] The backbone of reporter gene-based molecular imaging technique is the design of a suitable reporter construct. This construct carries a reporter gene linked to a promoter/enhancer, which can be inducible, constitutive, or tissue specific. The construct can be introduced into the target tissue by molecular biology techniques using either viral or non-viral techniques. Transcription of DNA and translation of mRNA lead to the production of reporter protein. After administration of a reporter probe, the reporter protein reacts with the reporter probe, giving rise to signals that are detectable by a charged-coupled device (CCD) camera, positron emission tomography (PET), single photon emission computed tomography (SPECT), or magnetic resonance imaging (MRI) (**Figure 1**). For thorough review, please refer to other relevant articles.[43, 44]

Imaging ESC Transplantation, Tumorigenicity, and Immunogenicity

A major advantage of reporter gene imaging is the incorporation of the reporter construct into the cellular DNA. This ensures that the reporter gene will only be expressed by living cells and will be passed on equally to the cell's progeny. Thus, this imaging modality can provide significant insight into cell viability and proliferation. As discussed earlier, monitoring cell viability is a critical requirement to assess immunogenicity, as a provoked immune reaction can kill transplanted cells. Monitoring cell proliferation is another important feature, considering the tumorigenic potential of undifferentiated hESCs. Moreover, the ability to image the whole-body will allow us to track cell migration in other organs. This is a major advantage when compared to tissue biopsies using GFP-labeled cells.

In addition, multiple reporter genes can also be introduced into the same cell for multimodality imaging. Recently, our group has tested the efficacy of mESC with a self-inactivating lentiviral vector carrying triple-fusion (TF) construct containing firefly luciferase (Fluc), monomeric red fluorescent protein (mRFP), and herpes simplex virus truncated thymidine kinase (HSV-ttk).[45] The mRFP in the construct facilitates the imaging of single cells by fluorescence microscopy and allows for the isolation of a stable clone population by fluorescence activated cell sorter (FACS). The Fluc can be used to perform high throughput bioluminescence imaging (BLI) for assessment of cell survival, proliferation and migration at relatively low costs. Finally, the HSV-ttk allows for deep-tissue PET imaging of gene expression in small animals[45, 46] as well as in patients.[47, 48] After transplantation into the hearts of athymic nude rats, mESCs could be successfully followed for 4 weeks using BLI and PET imaging. Between week 2 and 4, both BLI and PET reporter gene signals increased rapidly, indicating teratoma formation. This was confirmed by histological analysis.[45]

Because of the risk of teratoma formation, it would be ideal to have an *in vivo* imaging modality in combination with a fail-safe suicide-gene mechanism. Using the antiviral drug ganciclovir, which is toxic against cells expressing HSV-ttk, Cao and colleagues were able to ablate teratoma formation and follow this progress non-invasively.[49] This study reveals the excellent potential of reporter gene imaging for future use with hESC transplantation. In fact, preliminary studies in our lab suggest that as low as 100 undifferentiated hESCs (H9 line) can cause teratoma formation after subcutaneous injection (**Figure 2**). Whether lower cell numbers (e.g. 1, 10, 50), other graft sites (e.g. intramuscular, intravenous), or different cell lines (e.g., federally and non-federally approved) have similar kinetics of teratoma formation will need to be determined carefully in the future.

Finally, a very critical question with regard to reporter genes is whether they will affect ESC differentiation and hamper efforts for clinical applications. A previous study from our lab has shown that the TF reporter genes affect <2% of total genes of mESC using transcriptional
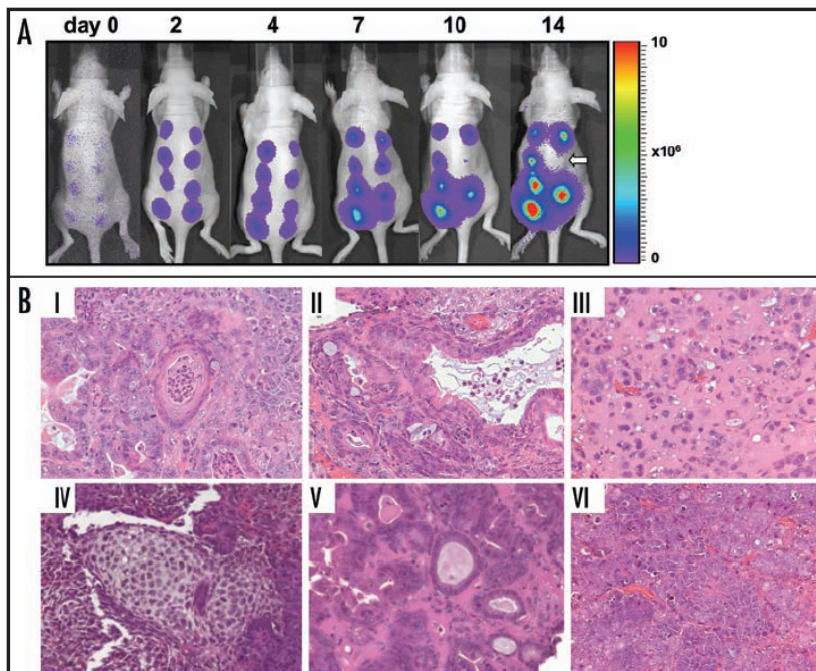
Figure 2: *In vivo bioluminescence imaging of teratoma formation after transplantation of 100 hESCs.* **(A)** Bioluminescence image showing longitudinal follow up after transplantation of 100 hESCs stably expressing a double fusion reporter gene (Fluc-GFP). Faint imaging signals were seen as early as 2 hrs after transplant, which became progressively stronger over 2 weeks. Histology at 8 weeks confirmed teratoma formation. Note one of the hESC transplanted sites did not successfully engraft (arrow) as there were no detectable signals by 2 weeks. **(B)** Histology from a representative explanted teratoma showing hESCs that have differentiated into Histology from a representative explanted teratoma showing hESCs that have differentiated into derivates from different germ layers. (I) squamous cell differentiation with keratin pearl; (II) respiratory epithelium with ciliated columnar and mucin producing goblet cells; (III) osteoid (non-mineralized bone) formation; (IV) cartilage formation; (V) gland cells; and (VI) rosette consistent with neuroectodermal differentiation (400x magnification).

profiling analysis.[50] A more recent follow up study using proteomic analysis show that there were no significant differences between control mESCs versus mESCs with reporter genes.[51] Importantly, reporter probes such as D-Luciferin (for Fluc) and [^{18}F]-FHBG (for HSV-ttk) had no adverse effects on mESC viability and proliferation as well.[45] Ongoing studies are evaluating the effects of reporter gene expression and reporter probes on various hESC cell lines.

CONCLUSION

Clearly, the capacity of hESCs to differentiate into almost all human cell types highlights their promising role in regenerative therapies for the treatment of heart disease, Parkinson's disease, leukemia, diabetes, and other degenerative disorders. But the pluripotency of hESCs may also pose major risks such as teratoma formation. Likewise, hESCs might not be immunoprivileged and could trigger host immune responses, leading to decreased cell survival or acute rejection. These are issues that can become significant barriers to future clinical application of hESC-based therapies. To meet these challenges, researchers must gain a better understanding of the *in vivo* behavior of transplanted hESCs. This review outlines the burgeoning application of molecular imaging to track transplanted hESCs *in vivo*. Continuing research merging molecular imaging and hESC biology will likely lead to significant advances in the future, both scientifically and medically.

REFERENCES

1. Kleinsmith LJ, Pierce GB, Jr. Multipotentiality Of Single Embryonal Carcinoma Cells. *Cancer Res.* Oct 1964;24:1544-1551.
2. Thomson JA, Itskovitz-Eldor J, Shapiro SS, Waknitz MA, Swiergiel JJ, Marshall VS, Jones JM. Embryonic stem cell lines derived from human blastocysts. *Science.* Nov 6 1998;282(5391):1145-1147.
3. Evans MJ, Kaufman MH. Establishment in culture of pluripotential cells from mouse embryos. *Nature.* Jul 9 1981;292(5819):154-156.
4. Martin GR. Isolation of a pluripotent cell line from early mouse embryos cultured in medium conditioned by teratocarcinoma stem cells. *Proc Natl Acad Sci U S A.* Dec 1981;78(12):7634-7638.
5. NIH. National Institutes of Health - Human Embryonic Stem Cell Registry.
6. Klimanskaya I, Chung Y, Becker S, Lu SJ, Lanza R. Human embryonic stem cell lines derived from single blastomeres. *Nature.* Aug 23 2006.
7. Amit M, Carpenter MK, Inokuma MS, Chiu CP, Harris CP, Waknitz MA, Itskovitz-Eldor J, Thomson JA. Clonally derived human embryonic stem cell lines maintain pluripotency and proliferative potential for prolonged periods of culture. *Dev Biol.* Nov 15 2000;227(2):271-278.
8. Xu C, Inokuma MS, Denham J, Golds K, Kundu P, Gold JD, Carpenter MK. Feeder-free growth of undifferentiated human embryonic stem cells. *Nat Biotechnol.* Oct 2001;19(10):971-974.
9. Amit M, Margulets V, Segev H, Shariki K, Laevsky I, Coleman R, Itskovitz-Eldor J. Human feeder layers for human embryonic stem cells. *Biol Reprod.* Jun 2003;68(6):2150-2156.
10. Richards M, Fong CY, Chan WK, Wong PC, Bongso A. Human feeders support prolonged undifferentiated growth of human inner cell masses and embryonic stem cells. *Nat Biotechnol.* Sep 2002;20(9):933-936.
11. Lee JB, Lee JE, Park JH, Kim SJ, Kim MK, Roh SI, Yoon HS. Establishment and maintenance of human embryonic stem cell lines on human feeder cells derived from uterine endometrium under serum-free condition. *Biol Reprod.* Jan 2005;72(1):42-49.
12. Hoffman LM, Carpenter MK. Characterization and culture of human embryonic stem cells. *Nat Biotechnol.* Jun 2005;23(6):699-708.
13. Wei H, Juhasz O, Li J, Tarasova YS, Boheler KR. Embryonic stem cells and cardiomyocyte differentiation: phenotypic and molecular analyses. *J Cell Mol Med.* Oct-Dec 2005;9(4):804-817.
14. Doetschman TC, Eistetter H, Katz M, Schmidt W, Kemler R. The in vitro development of blastocyst-derived embryonic stem cell lines: formation of visceral yolk sac, blood islands and myocardium. *J Embryol Exp Morphol.* Jun 1985;87:27-45.
15. Schuldiner M, Yanuka O, Itskovitz-Eldor J, Melton DA, Benvenisty N. Effects of eight growth factors on the differentiation of cells derived from human embryonic stem cells. *Proc Natl Acad Sci U S A.* Oct 10 2000;97(21):11307-11312.
16. Kehat I, Kenyagin-Karsenti D, Snir M, Segev H, Amit M, Gepstein A, Livne E, Binah O, Itskovitz-Eldor J, Gepstein L. Human embryonic stem cells can differentiate into myocytes with structural and functional properties of cardiomyocytes. *J Clin Invest.* Aug 2001;108(3):407-414.
17. Passier R, Oostwaard DW, Snapper J, Kloots J, Hassink RJ, Kuijk E, Roelen B, de la Riviere AB, Mummery C. Increased cardiomyocyte differentiation from human embryonic stem cells in serum-free cultures. *Stem Cells.* Jun-Jul 2005;23(6):772-780.
18. Xu C, Police S, Rao N, Carpenter MK. Characterization and enrichment of cardiomyocytes derived from human embryonic stem cells. *Circ Res.* Sep 20 2002;91(6):501-508.

Chapter 4

19. Yao S, Chen S, Clark J, Hao E, Beattie GM, Hayek A, Ding S. Long-term self-renewal and directed differentiation of human embryonic stem cells in chemically defined conditions. *Proc Natl Acad Sci U S A.* May 2 2006;103(18):6907-6912.

20. Reubinoff BE, Itsykson P, Turetsky T, Pera MF, Reinhartz E, Itzik A, Ben-Hur T. Neural progenitors from human embryonic stem cells. *Nat Biotechnol.* Dec 2001;19(12):1134-1140.

21. Schuldiner M, Eiges R, Eden A, Yanuka O, Itskovitz-Eldor J, Goldstein RS, Benvenisty N. Induced neuronal differentiation of human embryonic stem cells. *Brain Res.* Sep 21 2001;913(2):201-205.

22. Zhang SC, Wernig M, Duncan ID, Brustle O, Thomson JA. In vitro differentiation of transplantable neural precursors from human embryonic stem cells. *Nat Biotechnol.* Dec 2001;19(12):1129-1133.

23. Schulz TC, Palmarini GM, Noggle SA, Weiler DA, Mitalipova MM, Condie BG. Directed neuronal differentiation of human embryonic stem cells. *BMC Neurosci.* Oct 22 2003;4:27.

24. Muotri AR, Nakashima K, Toni N, Sandler VM, Gage FH. Development of functional human embryonic stem cell-derived neurons in mouse brain. *Proc Natl Acad Sci U S A.* Dec 20 2005;102(51):18644-18648.

25. Assady S, Maor G, Amit M, Itskovitz-Eldor J, Skorecki KL, Tzukerman M. Insulin production by human embryonic stem cells. *Diabetes.* Aug 2001;50(8):1691-1697.

26. Rajagopal J, Anderson WJ, Kume S, Martinez OI, Melton DA. Insulin staining of ES cell progeny from insulin uptake. *Science.* Jan 17 2003;299(5605):363.

27. Segev H, Fishman B, Ziskind A, Shulman M, Itskovitz-Eldor J. Differentiation of human embryonic stem cells into insulin-producing clusters. *Stem Cells.* 2004;22(3):265-274.

28. Reubinoff BE, Pera MF, Fong CY, Trounson A, Bongso A. Embryonic stem cell lines from human blastocysts: somatic differentiation in vitro. *Nat Biotechnol.* Apr 2000;18(4):399-404.

29. Cooke MJ, Stojkovic M, Przyborski SA. Growth of teratomas derived from human pluripotent stem cells is influenced by the graft site. *Stem Cells Dev.* Apr 2006;15(2):254-259.

30. Kehat I, Khimovich L, Caspi O, Gepstein A, Shofti R, Arbel G, Huber I, Satin J, Itskovitz-Eldor J, Gepstein L. Electromechanical integration of cardiomyocytes derived from human embryonic stem cells. *Nat Biotechnol.* Oct 2004;22(10):1282-1289.

31. Goldstein RS, Drukker M, Reubinoff BE, Benvenisty N. Integration and differentiation of human embryonic stem cells transplanted to the chick embryo. *Dev Dyn.* Sep 2002;225(1):80-86.

32. Janeway CA, Jr. The role of self-recognition in receptor repertoire development. Members of the Janeway Laboratory. *Immunol Res.* 1999;19(2-3):107-118.

33. Lechler RI, Lombardi G, Batchelor JR, Reinsmoen N, Bach FH. The molecular basis of alloreactivity. *Immunol Today.* Mar 1990;11(3):83-88.

34. Drukker M, Katz G, Urbach A, Schuldiner M, Markel G, Itskovitz-Eldor J, Reubinoff B, Mandelboim O, Benvenisty N. Characterization of the expression of MHC proteins in human embryonic stem cells. *Proc Natl Acad Sci U S A.* Jul 23 2002;99(15):9864-9869.

35. Draper JS, Pigott C, Thomson JA, Andrews PW. Surface antigens of human embryonic stem cells: changes upon differentiation in culture. *J Anat.* Mar 2002;200(Pt 3):249-258.

36. Swijnenburg RJ, Tanaka M, Vogel H, Baker J, Kofidis T, Gunawan F, Lebl DR, Caffarelli AD, de Bruin JL, Fedoseyeva EV, Robbins RC. Embryonic stem cell immunogenicity increases upon differentiation after transplantation into ischemic myocardium. *Circulation.* Aug 30 2005;112(9 Suppl):I166-172.

37. Li L, Baroja ML, Majumdar A, Chadwick K, Rouleau A, Gallacher L, Ferber I, Lebkowski J, Martin T, Madrenas J, Bhatia M. Human embryonic stem cells possess immune-privileged properties. *Stem Cells.* 2004;22(4):448-456.

38. Drukker M, Katchman H, Katz G, Even-Tov Friedman S, Shezen E, Hornstein E, Mandelboim O, Reisner Y, Benvenisty N. Human embryonic stem cells and their differentiated derivatives are less susceptible to immune rejection than adult cells. *Stem Cells*. Feb 2006;24(2):221-229.

39. Boyd AS, Higashi Y, Wood KJ. Transplanting stem cells: potential targets for immune attack. Modulating the immune response against embryonic stem cell transplantation. *Adv Drug Deliv Rev*. Dec 12 2005;57(13):1944-1969.

40. Drukker M. Immunogenicity of human embryonic stem cells: can we achieve tolerance? *Springer Semin Immunopathol*. Nov 2004;26(1-2):201-213.

41. Ro S. Magnifying stem cell lineages: the stop-EGFP mouse. *Cell Cycle*. Oct 2004;3(10):1246-1249.

42. Sheikh AY, Wu JC. Molecular imaging of cardiac stem cell transplantation. *Curr Cardiol Rep*. Mar 2006;8(2):147-154.

43. Blasberg RG, Tjuvajev JG. Molecular-genetic imaging: current and future perspectives. *J Clin Invest*. Jun 2003;111(11):1620-1629.

44. Wu JC, Tseng JR, Gambhir SS. Molecular imaging of cardiovascular gene products. *J Nucl Cardiol*. Jul-Aug 2004;11(4):491-505.

45. Cao F, Lin S, Xie X, Ray P, Patel M, Zhang X, Drukker M, Dylla SJ, Connolly AJ, Chen X, Weissman IL, Gambhir SS, Wu JC. In vivo visualization of embryonic stem cell survival, proliferation, and migration after cardiac delivery. *Circulation*. Feb 21 2006;113(7):1005-1014.

46. Wu JC, Chen IY, Sundaresan G, Min JJ, De A, Qiao JH, Fishbein MC, Gambhir SS. Molecular imaging of cardiac cell transplantation in living animals using optical bioluminescence and positron emission tomography. *Circulation*. Sep 16 2003;108(11):1302-1305.

47. Jacobs A, Voges J, Reszka R, Lercher M, Gossmann A, Kracht L, Kaestle C, Wagner R, Wienhard K, Heiss WD. Positron-emission tomography of vector-mediated gene expression in gene therapy for gliomas. *Lancet*. Sep 1 2001;358(9283):727-729.

48. Penuelas I, Mazzolini G, Boan JF, Sangro B, Marti-Climent J, Ruiz M, Ruiz J, Satyamurthy N, Qian C, Barrio JR, Phelps ME, Richter JA, Gambhir SS, Prieto J. Positron emission tomography imaging of adenoviral-mediated transgene expression in liver cancer patients. *Gastroenterology*. Jun 2005;128(7):1787-1795.

49. Cao F, Drukker M, Lin S, Sheikh A, Xie X, Li Z, Weissman I, Wu J. Molecular Imaging of Embryonic Stem Cell Misbehavior and Suicide Gene Ablation. *Cloning and Stem Cells - in press*.

50. Wu JC, Spin JM, Cao F, Lin S, Xie X, Gheysens O, Chen IY, Sheikh AY, Robbins RC, Tsalenko A, Gambhir SS, Quertermous T. Transcriptional profiling of reporter genes used for molecular imaging of embryonic stem cell transplantation. *Physiol Genomics*. Mar 13 2006;25(1):29-38.

51. Wu JC, Cao F, Dutta S, Xie X, Kim E, Chungfat N, Gambhir SS, Mathewson S, Connolly AJ, Brown M, Wang EW. Proteomic analysis of reporter genes for molecular imaging of transplanted embryonic stem cells (in press). *Proteomics*. 2006; ( ).

Chapter 4

CHAPTER 5

Clinical Hurdles for the Transplantation of Cardiomyocytes derived from Human Embryonic Stem Cells: Role of Molecular Imaging

Rutger-Jan Swijnenburg, Koen E.A. van der Bogt, Ahmad Y. Sheikh,
Feng Cao, and Joseph C. Wu

ABSTRACT

Over the past few years, human embryonic stem cells (hESCs) have gained popularity as a potentially ideal cell candidate for tissue regeneration. In particular, hESCs are capable of cardiac lineage-specific differentiation and confer improvement of cardiac function following transplantation into animal models. Although such data are encouraging, there remain significant hurdles before safe and successful translation of hESC-based treatment into clinical therapy, including the inability to assess cells following transplant. To this end, *molecular imaging* has proven a reliable methodology for tracking the long-term fate of transplanted cells. Imaging reporter genes introduced into the cells prior to transplantation enable non-invasive and longitudinal studies of cell viability, location, and behavior *in vivo*. Therefore, molecular imaging is expected to play an increasing role in characterizing the biology and physiology of hESC-derived cardiac cells in living subjects.

INTRODUCTION

Coronary artery disease remains the leading cause of death in the Western world [1]. As the human heart is not capable of regenerating the great numbers of cardiac cells that are lost after myocardial infarction, impaired cardiac function is the inevitable result of ischemic disease. Recently, three randomized clinical trails reported either clinically marginal [2,3] or no [4] significant benefit following adult bone marrow cell transplantation for patients suffering from acute and/or chronic ischemic heart disease. These reports add to a growing body of evidence that adult-derived stem cells have limited capacity to aid renewal and regeneration of damaged organs and structures. By contrast, hESCs show greater promise, as they are capable of self-renewal and differentiation. hESCs were first isolated by Thompson and colleagues in 1998 [5]. They are derived from the inner cell mass of the human blastocyst and can be kept in an undifferentiated, self-renewing state when cultured in the presence of inhibitory compounds, such as mouse embryonic fibroblast feeder layer cells. Compared to adult stem cells harvested from the bone marrow, hESCs have the advantage of being pluripotent, which provides them with the ability to differentiate into virtually all cells of the human body. For cardiac applications, hESCs have the ability to differentiate into cardiac cell lineages [6,7]. These hESC-derived cardiac cells have structural and functional properties of human cardiomyocytes and can integrate with host myocardium after transplantation into rats [8] and pigs [9]. However, in order to critically evaluate and optimize hESC-based therapy for the heart, new methodologies for assessing the viability, location, and behavior of transplanted cells are needed. This article aims to provide a concise overview of the major hurdles that need to be addressed before hESC-derived cardiac cell transplantation can become a clinical reality. This is followed by an outline of potential of molecular imaging tools that may help to overcome these challenges in the future.

HURDLES FOR CLINICAL TRANSLATION

Although substantial progress has been made in recent years towards improving culture conditions, differentiation strategies, and potential hESC-based cardiac regeneration, several unresolved issues exist between the laboratory and bedside that still need to be bridged (**Figure 1**). This article will cover some of the major areas of concern regarding hESC-derived cardiac cell transplantation, including: (1) optimization of *in vitro* differentiation into cardiac cells; (2) purification of cardiac cells to minimize post-transplant cellular misbehavior such as teratoma formation; (3) *in vivo* integration and function with host myocardium; and (4) evaluation of post-transplant immune rejection and cell death.
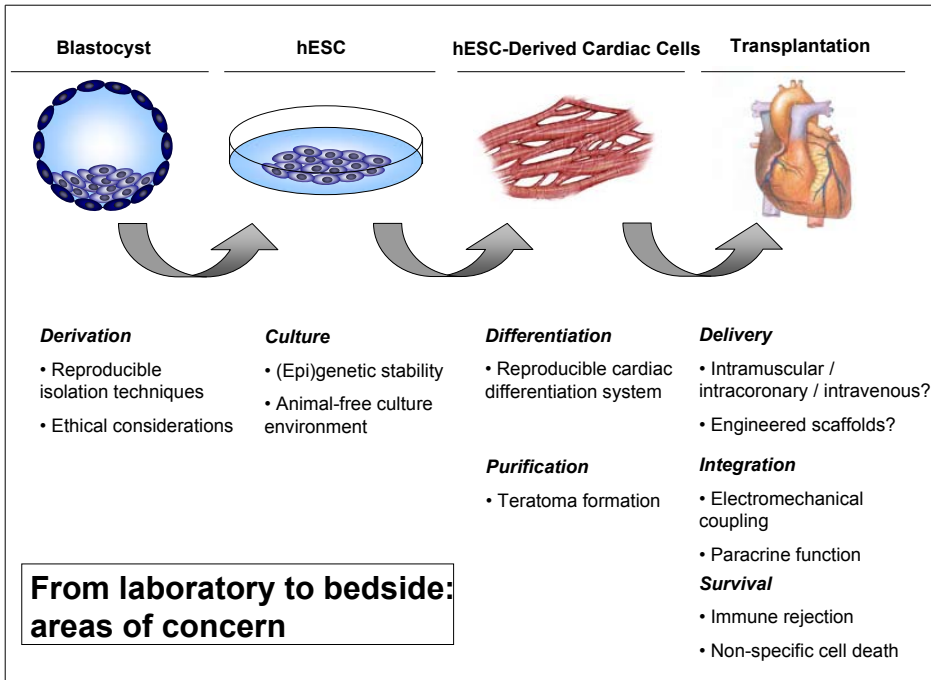
Figure 1. Human embryonic stem cells: from laboratory to bedside. Areas of concern in derivation, culture, differentiation, purification, delivery, integration, and survival are outlined.

In vitro differentiation to cardiomyocytes.

Following removal of the inhibitory feeder layer cells, hESCs can aggregate into clusters of cells known as embryoid bodies (EBs). Within these EBs, various signals are activated to promote differentiation of cells into all three germ layers, including mesoderm-derived cardiac cells **(Figure 2)**. Formation of cardiomyocytes usually starts 5 days after EB-formation, presenting as a beating area within the EB. Moreover, the hESC-derived cardiac cells within these beating areas actually resemble the structural and functional properties of early stage human cardiomyocytes [6]. Unfortunately, the rate of spontaneous differentiation of hESCs into cardiac cells is low. Typically ~8% of the EBs grown in suspension undergo differentiation into beating clusters, and ~30% of the cells contained in these clusters are actual cardiomyocytes [6]

Mouse ESCs (mESCs) were originally isolated in 1981 [10], and subsequent studies have focused on different strategies to induce cardiac-specific differentiation of mESCs *in vitro*. Retinoic acid was one of the first agents described that significantly increase the percentage of cardiomyocytes arising from ESCs [11]. Similar effects have been described for oxytocin [12], dynorphin B [13], nitric oxide [14], and ascorbic acid [15]. However, the efficacy of these compounds can be dose-dependent and bound to a specific time period in embryonic development [11]. Other groups have focused on the role of growth factors in mESC-derived cardiac cell differentiation, including transforming growth factor-β2 [16], basic fibroblast growth factor, and
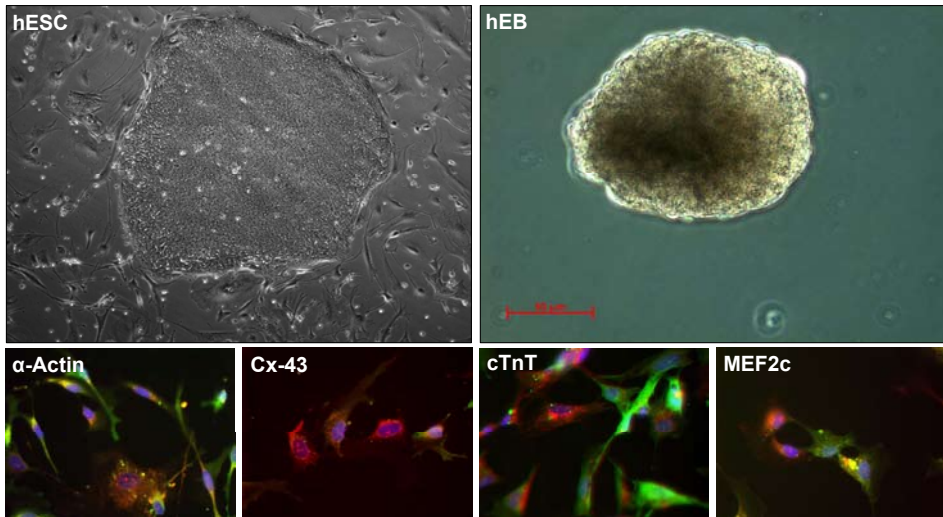
Figure 2. Undifferentiated hESCs (H9 cell line) grow indefinitely in culture on mouse embryonic fibroblast feeder layer cells (upper left panel). Following withdrawal of inhibitory feeder cells, hESCs can aggregate into EBs (upper right panel). Formation of cardiac cells usually starts 5 days after differentiation, initially presenting as a beating cluster within the EB. After isolation of EBs and further enrichment by Percoll gradient separation, these hESC-derived cardiac cells (lower panels) express cardiac lineage specific makers as shown by immunofluorescent staining of GFP-labeled cells with skeletal muscle alpha actin (α-Actin), connexin-43 (Cx-43), cardiac troponin T (cTnT), and Myosin Enhancer Factor 2c (MEF2c) (all in red; counterstaining with DAPI, blue).

bone-morphogenetic protein-2 [17]. Interestingly, findings from mESC studies *do not* appear to translate to hESC research. Thus far, only 5-aza-2'-deoxycytidine [7], combination of activin A and BMP-4 [18], and co-culture with murine END-2 visceral endoderm-like cells [19] have been shown to enhance cardiomyogenesis in hESC cultures.

Purification of hESC-derived cardiac cells.

Once ESCs are successfully induced to adopt cardiac fate, it becomes yet another challenge to isolate and further purify such subpopulations while avoiding contamination by undifferentiated, pluripotent ESCs. Following transplantation, undifferentiated ESCs could cause teratoma formation, which are complex tumors comprised of cellular or oganoid components reminiscent of normal derivatives from the three germ layers [20]. This indicates the need to achieve a highly, if not completely, pure population of cardiomyocytes prior to transplantation. Currently, selection methods for ESC-derived cardiac cells include Percoll density gradient-based isolation, which can enrich up to ~70% pure cardiac cell population for hESC [7] and ~90% for mESC [21]. An alternative strategy for cardiac cell purification combines genetic engineering and molecular biology techniques. Klug *et al.* utilized a fusion gene consisting of an alpha-cardiac myosin heavy chain (α-MHC) promoter that drives expression of aminoglycoside phosphotransferase, which is an enzyme that confers resistance to the antibiotic geneticin (G418). Once the transgenic mESCs differentiate into cardiac cells, activation of the cardiac specific α-MHC promoter

leads to expression of aminoglycoside phosphotransferase and allows these cells to survive against treatment with G418. The resultant surviving cells represent 99% pure cardiomyocyte population [22]. Similarly, Muller *et al.* reported transfection of mESCs with a fusion gene of of myosin light chain-2v (MLC-2v) linked to enhanced green fluorescent protein (eGFP). In this case, mESC-derived cardiac cells expressed eGFP that enabled fluorescent-activated cell sorting (FACS) and collection of cardiomyocyte population (97% pure) [23].

In vivo integration and function of ESC-derived cardiac cells.

Data from rodent models evaluating the fate of mESC transplantation into the heart have demonstrated mixed results. Early reports by Min *et al.* evaluating transplantation of mESC-derived beating cells into immunocompetent rat myocardium showed long-term (up to 32 weeks) cell survival, improvement of cardiac function, and improved angiogenesis in the infarct zone [24, 25]. Most notably, no adverse sequelae such as graft rejection, arrythmogenesis, or teratoma formation were observed. By contrast, two more recent studies demonstrated that mESCs transplanted into hearts of both immunocompetent mice [20] and athymic nude rats [26] formed teratomas by as early as 3 to 4 weeks following transplantation. At present, there are few published studies testing the efficacy of hESC-derived cardiac cell transplantation for cardiac repair. Kehat *et al.* showed promising results by injecting hESC-derived cardiac cells into swine heart with complete atrioventricular block [9]. They demonstrated electromechanical and structural coupling of the transplanted cells with the host myocardium. Xue *et al.* also showed functional integration and active pacing of hESC-derived cardiac cells following transfer into healthy myocardium of guinea pigs [27]. Furthermore, Laflamme *et al*. demonstrated that hESC-derived cardiac cells transplanted into athymic rat hearts successfully engrafted, proliferated, and expressed several cardiomyocyte markers [8]. Notably, none of these studies reported cellular misbehavior or teratoma formation. It is also not clear what percentage of these transplanted cells actually survived after transplantation.

Immune rejection of allogeneic hESC transplantation.

Several factors threaten hESC-derived cardiac cell survival following delivery into a new host, which, if properly modulated, might prevent the drastic post-transplant death of donor cells presently observed. One such major factor is cellular rejection based on immunological incompatibility. Theoretically, hESCs represent an immune-privileged cell population, since embryos consisting of 50% foreign material derived from the father are not rejected by the maternal host [28]. However, the understanding the immunogenicity of hESCs and their derivatives remains a challenge.

It has been shown that mESCs do not express major histocompatibility complex (MHC) antigens, the major system of alloantigens responsible for cell incompatibility [29]. Furthermore, mESCs can inhibit T-lymphocyte proliferation *in vitro* and establish multi-lineage mixed chimerism *in vivo* [30]. However, when allogeneic undifferentiated mESCs were transplanted into

a murine model of myocardial infarction, our group found progressive intra-graft infiltration of inflammatory cells mediating both adaptive (T cells, B cells, and dendritic cells) and innate (macrophages and granulocytes) immunity, leading to rejection of the mESC allograft [20]. In contrast to mESCs, hESCs express low levels of MHC-I antigens [31, 32]. Drukker *et al.* observed that MHC-I expression increased two to four-fold when cells were induced to spontaneously differentiate to EBs [31], and eight to ten-fold when cells differentiated into teratomas. In contrast, Draper *et al.* reported MHC-I downregulation upon hESC differentiation towards EB [32]. Thus, questions regarding the character and intensity of immune responses towards allogeneic hESC-derived cardiac cells still remain. Solutions that reduce or eliminate the potential immunological response are needed, including: (1) forming MHC isotyped hESC-line banks; (2) creating a universal donor cell by genetic modification; (3) inducing tolerance by hematopoietic chimerism; (4) generating isogeneic hESC lines by somatic nuclear transfer; (5) and/or using immunosuppressive medication. Details of these strategies to minimize rejection of hESC-derived transplants have been extensively reviewed by others [33, 34].

IMAGING HESC-DERIVED CARDIAC CELLS

Non-invasive cell tracking.

As outlined earlier, hESC-derived cardiac cell transplantation is potentially feasible, but there are several aspects that require improvement. For clinical translation to occur, it is essential that tools be developed for longitudinal tracking and evaluation of transplanted cell viability and behavior. Traditionally, cell therapy studies have relied upon conventional reporter genes such as GFP and β-galactosidase (LacZ) to monitor cell survival and differentiation. However, visualizing GFP and LacZ cells requires postmortem tissue analysis, which provides only a single snapshot representation of cell fate, not a complete picture over time. Moreover, sampling error inherent in *ex vivo* analysis requires large numbers of animals be sacrificed to develop a realistic picture of longitudinal survival kinetics.

Another technique for measuring the efficacy of cell therapy is to assess secondary endpoints. Cardiac contractility can be monitored by conventional methodologies such as echocardiography or magnetic resonance imaging (MRI). Cardiac perfusion can be assessed using positron emission tomography (PET) or single-photon emission computed tomography (SPECT). However, these data cannot be correlated to the biological state of the cells, as the cells themselves can neither be visualized nor assayed in the living subject. Aiming to provide insight into the location and survival of transplanted cells, recent studies have reported labeling mESCs with magnetic iron particles and following them by MRI [35]. Although these iron particles are robust and facilitate repeated imaging over time, they do not reliably provide insight into cell *proliferation* and *viability*, due to the disparate passing of the particles from parent to daughter cells and the ability of non-specific immune cells (e.g., macrophages) to engulf particles, respectively.

Chapter 5

Molecular imaging: direct vs. indirect approach.

Ideally, a non-invasive method for *in vivo* tracking of hESC-derived cardiac cells should be capable of providing insight into the following processes: (1) localization and migration of the cells, (2) cell survival and proliferation kinetics, and (3) cell differentiation or de-differentiation patterns. Molecular imaging of reporter genes offers potential promise in meeting these goals. Molecular imaging can be broadly defined as the visualization of molecular and cellular processes in the living subject. For *in vivo* molecular imaging to work, two basic elements are required: a molecular probe that detects a quantifiable signal based on the presence of gene, RNA, or protein, and a method to monitor these probes *in vivo* [36]. In general, molecular imaging can be divided into two categories: (a) *direct* imaging of probe-target interaction or (b) *indirect* imaging based on reporter gene and reporter probe.

The most commonly used *direct* cardiac imaging modality utilizes ^{18}F-fluorodeoxyglucose ([^{18}F]-FDG), a glucose analog which can cross intact membranes into living cells and is phosphorylated by the endogenous enzyme, hexokinase, trapping the probe inside the cell. The phosphorylated [^{18}F] will undergo positron annihilation to give off two 511 keV photon signals that can be detected by PET, providing a measurement of cell or tissue viability [37]. This approach has recently been shown feasible for imaging clinical cardiac cell therapy. Hofmann *et al.* labeled autologous bone marrow cells with [^{18}F]-FDG from nine patients suffering from acute myocardial infarction [38]. The [^{18}F]-FDG labeled cells were injected into either the infarct-related coronary artery or the antecubital vein five to ten days following coronary stenting. PET imaging was performed 50 to 75 minutes after the procedure and successfully detected the transplanted cell population in all patients, with higher signals in the intra-coronary group. Although PET is a valuable tool to monitor the location of cells shortly after transplant, the short half-life of the [^{18}F]-FDG radiotracer (~110 minutes) does not permit long-term follow-up of cell survival and/or migration. Furthermore, [^{18}F]-FDG is not passed on to daughter cells during cell division and therefore does not provide insight into cell proliferation.

The concept behind *indirect* molecular imaging is an expansion upon basic reporter gene technology whereby a promoter or enhancer region of interest is linked to the imaging reporter gene. The nature of the promoter can be inducible, constitutive, or tissue specific. The construct can be introduced into the target cell using either viral or non-viral techniques. Once incorporated, the reporter gene produces the reporter protein which then interacts with the introduced reporter probe, producing an analytic signal that can be detected by the detector system. Depending on the reporter gene used, available imaging modalities include PET, SPECT, MRI or a charged-coupled device (CCD) camera [39]. The two most widely used reporter gene imaging systems are firefly luciferase (Fluc)-based optical bioluminescence imaging and herpes simplex virus thymidine kinase (HSV-tk)-based PET imaging. For bioluminescence imaging, the Fluc reporter protein catalyzes the D-Luciferin reporter probe to produce low-energy photons (2-3 eV) that can be captured by an ultra-sensitive CCD

camera. The reporter probe can be administered before every imaging session, allowing for multiple imaging acquisitions over time. For PET imaging, the HSV-tk reporter protein phosphorylates radiolabeled thymidine analogue 9-(4-[18F]fluoro-3-(hydroxymethylbutyl) guanine ([18F]-FHBG) reporter probe, which emits high-energy photons (511 keV) that can be detected by PET. The reporter gene technique has been used to assay survival and localization of transplanted rat embryonic cardiomyoblasts [40] and more recently of mESCs [26].

Reporter gene imaging of ESCs and ESC-derived cardiac cells.

Regarding transplantation of hESC-derived cardiac cell transplantation, reporter gene imaging can be used to monitor critical events. First, since the reporter gene can be integrated into the DNA of transplanted cells, its expression is limited to only living cells, and thus facilitates assessment of cell survival. Second, the reporter gene can be passed onto daughter cells, thus providing insight into cell proliferation. This is an important feature given the tumorigenic potential of undifferentiated ESCs discussed earlier. Third, it is possible to introduce several reporter genes into the same cell, facilitating a multi-modality imaging approach. Recently, Cao *et al.* tested the efficacy of mESC with a self-inactivating lentiviral vector carrying the triple-fusion (TF) construct that consists of firefly luciferase (Fluc), red fluorescence protein (mRFP), and herpes simplex virus truncated thymidine kinase (HSV-ttk) [26]. The mRFP facilitates imaging of single cells by fluorescence microscopy and allows for the isolation of a stable clone population by FACS. The Fluc allows for bioluminescence imaging for assessment of cell survival, proliferation, and migration in small animals. Finally, the HSV-ttk affords the ability to use PET imaging in small and large animals, as well as humans. Following transplantation into the hearts of athymic nude rats, mESC survival, migration, and proliferation was monitored for 4 weeks by bioluminescence and PET imaging. PET imaging, both with [18F]-FHBG to image cells and [18F]-FDG to image myocardial viability, proved to be a very sensitive tool to assess the tomographic location of mESC engraftment **(Figure 3)**. However, reporter gene signals increased rapidly within 4 weeks due to teratoma formation. Histologic samples obtained from both intra- and extra-cardiac sites revealed spontaneous differentiation of the mESC into all three germ layers. In a subsequent study, our group also demonstrated the ability of an anti-viral drug to selectively target teratomas expressing the HSV-ttk reporter gene [41]. Thus, in addition to its use for monitoring cell fate, the reporter gene also serves as an inducible suicide gene that facilitates selective cellular ablation. This could be an important tool in controlling cellular misbehavior and/or teratoma formation of transplanted hESC-derived cells.

Recently, our group has successfully transduced hESCs (H9 line) with a lentiviral vector containing a double fusion (DF) reporter gene that consists of Fluc and eGFP. Cardiac cells derived from hESCs using EB formation and Percoll gradient enrichment constitutively express Fluc and eGFP. Following transplantation into ischemic myocardium of severe combined immunodeficient (SCID) mice, these cells can be monitored by bioluminescence imaging for
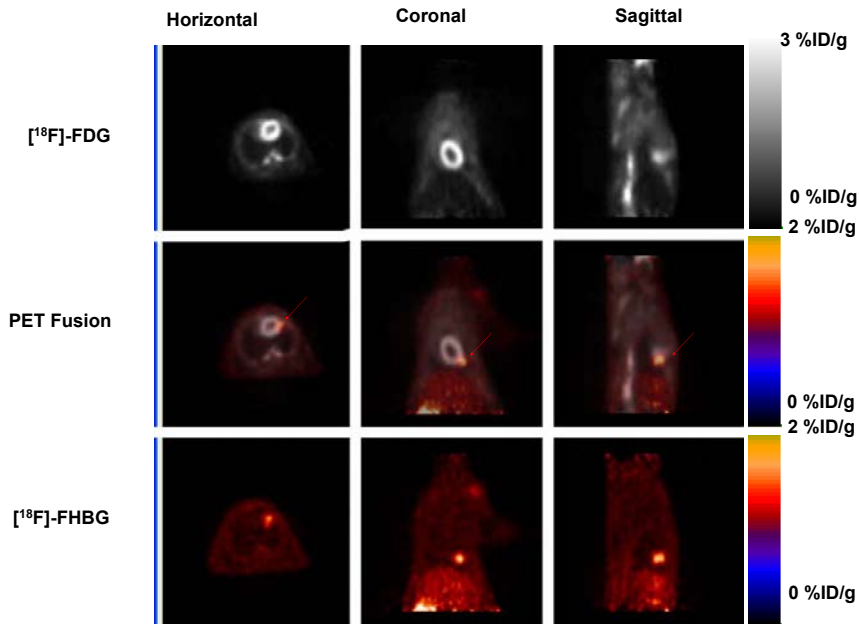
Figure 3. Positron emission tomography imaging of transplanted mESCs in the myocardium. Two weeks after mESC transplantation, nude rats underwent [18F]-FHBG reporter probe imaging (top row) followed by [18F]-FDG myocardial viability imaging (middle row). Fusion of [18F]-FHBG and [18F]-FDG images (bottom row) shows the exact anatomic location of transplanted mESC (arrow) at the anterolateral wall in horizontal, coronal, and sagittal views. (Reproduced with permission from Cao et al.[26])

>3 months (Cao *et al.,* unpublished data). By contrast, injection of undifferentiated hESCs caused teratoma formation during the same period (**Figure 4**). Taken together, these results highlight the valuable role of molecular imaging for following the developmental fate of transplanted hESCs and their derivates.

Finally, a critical question with regard to reporter genes is whether the might influence the biology and physiology of the stem cells. In the study by Cao *et al.,* the TF construct had no influence on mESC morphology, viability, proliferation, and differentiation capacity *in vitro* [26]. Likewise, both the bioluminescence (D-luciferin) and PET ([18F]-FHBG) reporter probes had no adverse effects on mESC behavior. In two recent studies, the TF reporter genes affected <2% of the total mESC genome using transcriptional profiling analysis [42] and caused no significant differences in protein expression quantified by proteomic analysis [43]. Ongoing studies are also evaluating the effects of reporter gene and reporter probe on hESCs as well.

CONCLUSION

The last several years have produced revolutionary advancements in exploring the capabilities of stem cells for treatment of cardiovascular disease. In particular, initial animal results
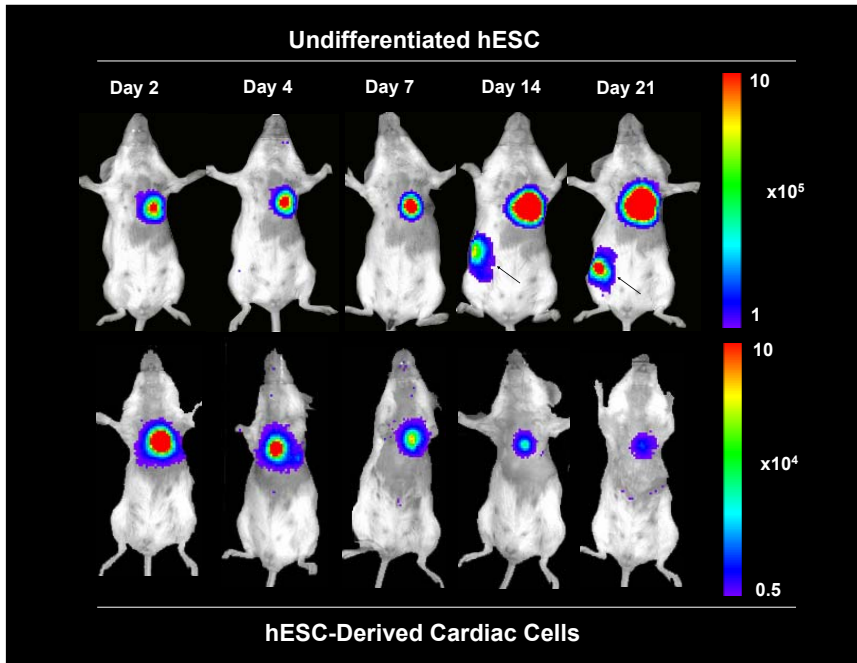
Figure 4. Comparison of undifferentiated hESCs versus hESC-derived cardiac cell survival and behavior *in vivo*. Both hESC (top row) and hESC-derived cardiac cells (bottom row) were transplanted into ischemic myocardium of SCID mice. Bioluminescence imaging during the first three weeks following transplantation reveals acute donor cell death followed by stable survival of hESC-derived cardiac cells. In contrast, undifferentiated hESCs proliferate uncontrollably in the heart as well as other seeded organs (arrows) to cause teratoma formation.

involving hESC-derived cardiac cells appear promising for improving cardiac function after ischemic injury. Nonetheless, we are still years away from safely translating these initial observations into therapy for humans. There are several issues within the field that require improvement, especially those related to *in vitro* differentiation and purification, as well as *in vivo* integration and survival of the transplanted cells. As the field of hESC-derived cell transplantation emerges, there will be an urgent need for reliable methodologies to track and assess behavior of the cells following transfer into the injured heart. Molecular imaging serves these needs and will likely play a prominent role in future hESC research.

ACKNOWLEDGEMENTS

REFERENCES

1. Thom T, Haase N, Rosamond W, Howard VJ, Rumsfeld J, Manolio T, Zheng ZJ, Flegal K, O'Donnell C, Kittner S, Lloyd-Jones D, Goff DC, Jr., Hong Y, Adams R, Friday G, Furie K, Gorelick P, Kissela B, Marler J, Meigs J, Roger V, Sidney S, Sorlie P, Steinberger J, Wasserthiel-Smoller S, Wilson M, Wolf P. Heart disease and stroke statistics--2006 update: a report from the American Heart Association Statistics Committee and Stroke Statistics Subcommittee. *Circulation*. Feb 14 2006;113(6):e85-151.

2. Assmus B, Honold J, Schachinger V, Britten MB, Fischer-Rasokat U, Lehmann R, Teupe C, Pistorius K, Martin H, Abolmaali ND, Tonn T, Dimmeler S, Zeiher AM. Transcoronary transplantation of progenitor cells after myocardial infarction. *The New England journal of medicine*. Sep 21 2006;355(12):1222-1232.

3. Schachinger V, Erbs S, Elsasser A, Haberbosch W, Hambrecht R, Holschermann H, Yu J, Corti R, Mathey DG, Hamm CW, Suselbeck T, Assmus B, Tonn T, Dimmeler S, Zeiher AM. Intracoronary bone marrow-derived progenitor cells in acute myocardial infarction. *The New England journal of medicine*. Sep 21 2006;355(12):1210-1221.

4. Lunde K, Solheim S, Aakhus S, Arnesen H, Abdelnoor M, Egeland T, Endresen K, Ilebekk A, Mangschau A, Fjeld JG, Smith HJ, Taraldsrud E, Grogaard HK, Bjornerheim R, Brekke M, Muller C, Hopp E, Ragnarsson A, Brinchmann JE, Forfang K. Intracoronary injection of mononuclear bone marrow cells in acute myocardial infarction. *The New England journal of medicine*. Sep 21 2006;355(12):1199-1209.

5. Thomson JA, Itskovitz-Eldor J, Shapiro SS, Waknitz MA, Swiergiel JJ, Marshall VS, Jones JM. Embryonic stem cell lines derived from human blastocysts. *Science*. Nov 6 1998;282(5391):1145-1147.

6. Kehat I, Kenyagin-Karsenti D, Snir M, Segev H, Amit M, Gepstein A, Livne E, Binah O, Itskovitz-Eldor J, Gepstein L. Human embryonic stem cells can differentiate into myocytes with structural and functional properties of cardiomyocytes. *J Clin Invest*. Aug 2001;108(3):407-414.

7. Xu C, Police S, Rao N, Carpenter MK. Characterization and enrichment of cardiomyocytes derived from human embryonic stem cells. *Circ Res*. Sep 20 2002;91(6):501-508.

8. Laflamme MA, Gold J, Xu C, Hassanipour M, Rosler E, Police S, Muskheli V, Murry CE. Formation of human myocardium in the rat heart from human embryonic stem cells. *Am J Pathol*. Sep 2005;167(3):663-671.

9. Kehat I, Khimovich L, Caspi O, Gepstein A, Shofti R, Arbel G, Huber I, Satin J, Itskovitz-Eldor J, Gepstein L. Electromechanical integration of cardiomyocytes derived from human embryonic stem cells. *Nat Biotechnol*. Oct 2004;22(10):1282-1289.

10. Evans MJ, Kaufman MH. Establishment in culture of pluripotential cells from mouse embryos. *Nature*. Jul 9 1981;292(5819):154-156.

11. Wobus AM, Kaomei G, Shan J, Wellner MC, Rohwedel J, Ji G, Fleischmann B, Katus HA, Hescheler J, Franz WM. Retinoic acid accelerates embryonic stem cell-derived cardiac differentiation and enhances development of ventricular cardiomyocytes. *J Mol Cell Cardiol*. Jun 1997;29(6):1525-1539.

12. Paquin J, Danalache BA, Jankowski M, McCann SM, Gutkowska J. Oxytocin induces differentiation of P19 embryonic stem cells to cardiomyocytes. *Proc Natl Acad Sci U S A*. Jul 9 2002;99(14):9550-9555.

13. Ventura C, Zinellu E, Maninchedda E, Maioli M. Dynorphin B is an agonist of nuclear opioid receptors coupling nuclear protein kinase C activation to the transcription of cardiogenic genes in GTR1 embryonic stem cells. *Circ Res*. Apr 4 2003;92(6):623-629.

14. Kanno S, Kim PK, Sallam K, Lei J, Billiar TR, Shears LL, 2nd. Nitric oxide facilitates cardiomyogenesis in mouse embryonic stem cells. *Proc Natl Acad Sci U S A.* Aug 17 2004;101(33):12277-12281.

15. Takahashi T, Lord B, Schulze PC, Fryer RM, Sarang SS, Gullans SR, Lee RT. Ascorbic acid enhances differentiation of embryonic stem cells into cardiac myocytes. *Circulation.* Apr 15 2003;107(14):1912-1916.

16. Behfar A, Zingman LV, Hodgson DM, Rauzier JM, Kane GC, Terzic A, Puceat M. Stem cell differentiation requires a paracrine pathway in the heart. *Faseb J.* Oct 2002;16(12):1558-1566.

17. Kawai T, Takahashi T, Esaki M, Ushikoshi H, Nagano S, Fujiwara H, Kosai K. Efficient cardiomyogenic differentiation of embryonic stem cell by fibroblast growth factor 2 and bone morphogenetic protein 2. *Circ J.* Jul 2004;68(7):691-702.

18. Yao S, Chen S, Clark J, Hao E, Beattie GM, Hayek A, Ding S. Long-term self-renewal and directed differentiation of human embryonic stem cells in chemically defined conditions. *Proc Natl Acad Sci U S A.* May 2 2006;103(18):6907-6912.

19. Mummery C, Ward-van Oostwaard D, Doevendans P, Spijker R, van den Brink S, Hassink R, van der Heyden M, Opthof T, Pera M, de la Riviere AB, Passier R, Tertoolen L. Differentiation of human embryonic stem cells to cardiomyocytes: role of coculture with visceral endoderm-like cells. *Circulation.* Jun 3 2003;107(21):2733-2740.

20. Cao YA, Bachmann MH, Beilhack A, Yang Y, Tanaka M, Swijnenburg RJ, Reeves R, Taylor-Edwards C, Schulz S, Doyle TC, Fathman CG, Robbins RC, Herzenberg LA, Negrin RS, Contag CH. Molecular imaging using labeled donor tissues reveals patterns of engraftment, rejection, and survival in transplantation. *Transplantation.* Jul 15 2005;80(1):134-139.

21. E LL, Zhao YS, Guo XM, Wang CY, Jiang H, Li J, Duan CM, Song Y. Enrichment of cardiomyocytes derived from mouse embryonic stem cells. *J Heart Lung Transplant.* Jun 2006;25(6):664-674.

22. Klug MG, Soonpaa MH, Koh GY, Field LJ. Genetically selected cardiomyocytes from differentiating embronic stem cells form stable intracardiac grafts. *J Clin Invest.* Jul 1 1996;98(1):216-224.

23. Muller M, Fleischmann BK, Selbert S, Ji GJ, Endl E, Middeler G, Muller OJ, Schlenke P, Frese S, Wobus AM, Hescheler J, Katus HA, Franz WM. Selection of ventricular-like cardiomyocytes from ES cells in vitro. *Faseb J.* Dec 2000;14(15):2540-2548.

24. Min JY, Yang Y, Converso KL, Liu L, Huang Q, Morgan JP, Xiao YF. Transplantation of embryonic stem cells improves cardiac function in postinfarcted rats. *J Appl Physiol.* Jan 2002;92(1):288-296.

25. Min JY, Yang Y, Sullivan MF, Ke Q, Converso KL, Chen Y, Morgan JP, Xiao YF. Long-term improvement of cardiac function in rats after infarction by transplantation of embryonic stem cells. *The Journal of thoracic and cardiovascular surgery.* Feb 2003;125(2):361-369.

26. Cao F, Lin S, Xie X, Ray P, Patel M, Zhang X, Drukker M, Dylla SJ, Connolly AJ, Chen X, Weissman IL, Gambhir SS, Wu JC. In vivo visualization of embryonic stem cell survival, proliferation, and migration after cardiac delivery. *Circulation.* Feb 21 2006;113(7):1005-1014.

27. Xue T, Cho HC, Akar FG, Tsang SY, Jones SP, Marban E, Tomaselli GF, Li RA. Functional integration of electrically active cardiac derivatives from genetically engineered human embryonic stem cells with quiescent recipient ventricular cardiomyocytes: insights into the development of cell-based pacemakers. *Circulation.* Jan 4 2005;111(1):11-20.

28. Li L, Baroja ML, Majumdar A, Chadwick K, Rouleau A, Gallacher L, Ferber I, Lebkowski J, Martin T, Madrenas J, Bhatia M. Human embryonic stem cells possess immune-privileged properties. *Stem Cells.* 2004;22(4):448-456.

29. Tian L, Catt JW, O'Neill C, King NJ. Expression of immunoglobulin superfamily cell adhesion molecules on murine embryonic stem cells. *Biology of reproduction.* Sep 1997;57(3):561-568.

30. Bonde S, Zavazava N. Immunogenicity and engraftment of mouse embryonic stem cells in allogeneic recipients. *Stem Cells.* Oct 2006;24(10):2192-2201.

31. Drukker M, Katz G, Urbach A, Schuldiner M, Markel G, Itskovitz-Eldor J, Reubinoff B, Mandelboim O, Benvenisty N. Characterization of the expression of MHC proteins in human embryonic stem cells. *Proc Natl Acad Sci U S A.* Jul 23 2002;99(15):9864-9869.

32. Draper JS, Pigott C, Thomson JA, Andrews PW. Surface antigens of human embryonic stem cells: changes upon differentiation in culture. *Journal of anatomy.* Mar 2002;200(Pt 3):249-258.

33. Drukker M. Immunogenicity of human embryonic stem cells: can we achieve tolerance? *Springer Semin Immunopathol.* Nov 2004;26(1-2):201-213.

34. Boyd AS, Higashi Y, Wood KJ. Transplanting stem cells: potential targets for immune attack. Modulating the immune response against embryonic stem cell transplantation. *Adv Drug Deliv Rev.* Dec 12 2005;57(13):1944-1969.

35. Arai T, Kofidis T, Bulte JW, de Bruin J, Venook RD, Berry GJ, McConnell MV, Quertermous T, Robbins RC, Yang PC. Dual in vivo magnetic resonance evaluation of magnetically labeled mouse embryonic stem cells and cardiac function at 1.5 t. *Magn Reson Med.* Jan 2006;55(1):203-209.

36. Blasberg RG, Tjuvajev JG. Molecular-genetic imaging: current and future perspectives. *J Clin Invest.* Jun 2003;111(11):1620-1629.

37. Schelbert HR. 18F-deoxyglucose and the assessment of myocardial viability. *Semin Nucl Med.* Jan 2002;32(1):60-69.

38. Hofmann M, Wollert KC, Meyer GP, Menke A, Arseniev L, Hertenstein B, Ganser A, Knapp WH, Drexler H. Monitoring of bone marrow cell homing into the infarcted human myocardium. *Circulation.* May 3 2005;111(17):2198-2202.

39. Wu JC, Tseng JR, Gambhir SS. Molecular imaging of cardiovascular gene products. *J Nucl Cardiol.* Jul-Aug 2004;11(4):491-505.

40. Wu JC, Chen IY, Sundaresan G, Min JJ, De A, Qiao JH, Fishbein MC, Gambhir SS. Molecular imaging of cardiac cell transplantation in living animals using optical bioluminescence and positron emission tomography. *Circulation.* Sep 16 2003;108(11):1302-1305.

41. Cao F, Drukker M, Lin S, Sheikh A, Xie X, Li Z, Weissman I, Wu J. Molecular imaging of embryonic stem cell misbehavior and suicide gene ablation. *Cloning and Stem Cells.* 2007 (in press).

42. Wu JC, Spin JM, Cao F, Lin S, Xie X, Gheysens O, Chen IY, Sheikh AY, Robbins RC, Tsalenko A, Gambhir SS, Quertermous T. Transcriptional profiling of reporter genes used for molecular imaging of embryonic stem cell transplantation. *Physiological genomics.* Mar 13 2006;25(1):29-38.

43. Wu JC, Cao F, Dutta S, Xie X, Kim E, Chungfat N, Gambhir S, Mathewson S, Connolly AJ, Brown M, Wang EW. Proteomic analysis of reporter genes for molecular imaging of transplanted embryonic stem cells. *Proteomics.* Nov 2 2006.

CHAPTER 6

Embryonic Stem Cell Immunogenicity Increases upon Differentiation After Transplantation into Ischemic Myocardium

Rutger-Jan Swijnenburg, Masashi Tanaka, Hannes Vogel, Jeanette Baker, Theo Kofidis, Feny Gunawan, Darren R. Lebl, Anthony D. Caffarelli, Jorg L. de Bruin, Eugenia V. Fedoseyeva, and Robert C. Robbins.

ABSTRACT

Background: We investigated whether differentiation of embryonic stem cells (ESCs) in ischemic myocardium enhances their immunogenicity, thereby increasing their chance for rejection.

Methods: In one series, 129/SvJ-derived mouse ESCs (ES-D3 line) were transplanted by direct myocardial injection (1×10^6 cells) into murine hearts of both allogeneic (BALB/c, n=20) and syngeneic (129/SvJ, n=12) recipients after LAD ligation. Hearts were procured at 1, 2, 4 and 8 weeks after ESC transplantation and analyzed by immunohistochemistry to assess immune cell infiltration (CD3, CD4, CD8, B220, CD11c, Mac-1, Gr-1) and ESC differentiation (H&E). In a second series (allogeneic n = 5, sham n = 3), ESC transplantation was performed similarly, however after 2 weeks, LAD-ligated and ESC-injected hearts were heterotopically transplanted into naive BALB/c recipients. After an additional 2 weeks, donor hearts were procured and analyzed by immunohistochemistry.

Results: In the first series, the size of all ESC grafts remained stable and there was no evidence of ESC differentiation 2 weeks post-transplantation; however, after 4 weeks both allogeneic and syngeneic ESC grafts showed the presence of teratoma. By 8 weeks, surviving ESCs could be detected in the syngeneic but not in the allogeneic group. Mild inflammatory cellular infiltrates were found in allogeneic recipients at 1 and 2 weeks post-transplantation, progressing into vigorous infiltration at 4 and 8 weeks. The second series demonstrated similar vigorous infiltration of immune cells as early as 2 weeks after heterotopic transplantation.

Conclusion: *In vivo* differentiated ESCs elicit an accelerated immune response as compared to undifferentiated ESCs. These data imply that clinical transplantation of allogeneic ESCs or ESC derivatives for treatment of cardiac failure might require immunosuppressive therapy.

INTRODUCTION

Stem cell transplantation has recently emerged as a novel approach for replacement of injured myocardium. The potential of both haematopoietic stem cells (HSCs), harvested from the adult bone marrow and embryonic stem cells (ESCs), harvested from the inner cell mass of embryos at the blastocyst stage, to develop into viable heart muscle cells in the damaged heart is now being explored. Despite early encouraging results with HSC transplantation[1], the ability of these cells to transdifferentiate into cardiomyocytes *in vivo* and to functionally repair ischemic myocardium has recently been seriously questioned[2,3]. Instead, previous studies have reported successful differentiation of ESCs into cardiomyocytes, both *in vitro* [4,5]and *in vivo*[6,7]. This prompted us to investigate the potential of ESCs as a source of cell transplantation for myocardial restoration.

Pluripotent ESCs are capable of spontaneous differentiation into cells of all three different germ layers[8]. Due to their early stage of development, ESCs are considered "immune privileged", i.e. unrecognizable by the recipient immune defences[9]. This assumption is bolstered by observations in neonatal tolerance. An embryo, consisting of 50% foreign material derived from the father, is usually not rejected by the maternal host. However, recent evidence suggests that even in their undifferentiated state, human ESCs express low levels of HLA class I antigen, that moderately increase as the cells differentiate[10,11]. In addition, rat embryonic stem cell-like cells (RESCs) also have been shown to express minimal, but detectable, levels of MHC class I molecules[12]. The presence of distinct MHC antigens, suggests that developing ESCs can be at risk for immune rejection when introduced *in vivo* across histocompatibility barriers[13]. However, no progressive studies analyzing the immune fate of ESCs during their development *in vivo* have been reported so far.

In this study, we tested the hypothesis that intramyocardially transplanted ESCs elicit an immune response that results in rejection of the transplanted cells. In addition, we investigated whether the state of cell differentiation affects their immunogenicity and the intensity of the recipient immune response.

METHODS

Animals.

Six- to ten-week-old female BALB/c (H-2d) and 129/SvJ (H-2b) mice (20-25 g) were purchased from The Jackson Laboratory (Bar Harbor, ME) and housed at no more than five per cage in our American Association for Accreditation of Laboratory Animal Care-approved facility with 12:12-h light-dark cycles and free access to standard rodent chow and water. All animal procedures were approved by the Animal Care and Use Committee of Stanford University.

Cell culture.

ES-D3 embryonic stem cells, a line developed from the 129/SvJ mouse strain, were kindly provided by Dr. I.L Weissman (Department of Pathology and Developmental Biology, Stanford University School of Medicine). Undifferentiated ES-D3 cells were maintained on gelatinized tissue culture dishes in Dulbecco modified Eagle medium (Specialty Media, Phillipsburg, NJ) supplemented with 15% fetal bovine serum (Hyclone, Logan, UT), 100µg/ml penicillin, 100 U/ml streptomycin, 1mM sodium pyruvate, 2mM L-glutamine, 1 x non essential amino acids, 0.1 mM 2-mercaptoethanol (all Gibco, Frankfurt, Germany) and 10^3 U/ml ESGRO™ (Chemicon, Temecula, CA). Cells were maintained at 37˚C in a humidified atmosphere of 5% CO_2. Monolayers were passaged by trypsinization at confluence of 70-80%. At the day of transplantation, ESC were harvested and aliquoted in culture medium.

Left coronary ligation and ESC transplantation.

Mice were premedicated with ketamine (100 mg/kg IP) and anesthetized with inhaled isoflurane (2-3%). Mice were intubated and ventilated with a mouse respirator (model 687, Harvard Apparatus, Inc., Holliston, MA) and anesthesia was maintained with inhaled isoflurane (1-2.5%). A left thoracotomy was performed in the 5th intercostal space, the left lung retracted and the pericardium opened. The left anterior descending (LAD) artery was permanently ligated with a 9-0 Ethilon suture just distal to the level of the left atrium. Infarction was visually confirmed by blanching of the antero-lateral region of the left ventricle along with dyskinesia. After five minutes, 1.0 x 10^6 ES cells were transplanted by injection into the injured myocardium (volume = 25 µL) of a series of allogeneic (BALB/c, n=20) and syngeneic (129/SvJ, n=12) recipients. Similar surgical procedure, with injection of cell free culture medium, was performed on sham control animals (BALB/c, n=8). A thoracostomy tube was placed and lungs were re-expanded using positive pressure at end expiration. The chest cavity was closed in layers with 5.0 Vicryl suture, and the animal was gradually weaned from the respirator. Once spontaneous respiration resumed, the endotracheal and thoracostomy tubes were removed, and the animal was placed in a temperature controlled chamber until they resumed full alertness and motility.

Heterotopic transplantation of LAD-ligated and ESC-injected hearts.

To study the immune response against in vivo matured ESC, a second series of animals (allogeneic n=5, sham controls n=3) underwent LAD ligation and ESC transplantation, however after 2 weeks, their hearts were explanted and heterotopically transplanted into the abdomen of naive syngeneic BALB/c recipients. Heterotopic cardiac transplantation was performed according to the method of Corry et al [14] with some modifications. Anaesthesia was induced and maintained as described above. Cardiac graft viability was assessed daily by abdominal palpitation.

Tissue collection, immunofluorenscent and histological analysis.

Subsets of allogeneic, syngeneic and sham operated animals from the first series were sacrificed at 1, 2, 4 and 8 weeks after ESC transplantation. Animals from the second series were sacrificed at 2 weeks after heterotopic heart transplantation. Hearts were perfused with cold saline and rapidly excised. They were fixed in 2% paraformaldehyde for 2 hours at room temperature and cryoprotected in 30% sucrose overnight at 4°C. Tissue was frozen in optimum cutting temperature compound (OCT compound, Sakura Finetek USA, Inc. Torrance, CA) and sectioned at 5 μm on a cryostat. To evaluate inflammatory cell infiltration, immunostaining was performed with a panel of hematolymphoid antibodies. Serial sections were blocked and incubated with hamster anti-CD3 (clone G4.18), rat anti-CD4 (H129.19), rat anti-CD8 (53-6.7), rat anti-CD45R/B220 (RA3-6B2), hamster anti-CD11c (HL3), rat anti-Mac-1 (M1/70) or rat anti-Gr-1 (RB6-8C5) antibody (BD Pharmingen, San Jose, CA) for 1 hour at room temperature. Primary antibodies were detected by incubation of the slides with goat anti-hamster Texas Red (Santa Cruz Biotechnology Inc., Santa Cruz, CA), goat anti-rat Alexa 488 or goat anti-rat Alexa 594 (Molecular Probes, Eugene, CA) for 45 minutes at room temperature. Sections were counterstained with 4,6-diamidino-2-phenylindole (DAPI, Molecular Probes) and analyzed with a Leica DMRB fluorescent microscope (Leica Microsystems, Frankfurt, Germany). Images were acquired with a SPOT RT Color camera and electronically merged with SPOT RT software (Diagnostic Instruments, Sterling Heights, MI). To detect differentiated structures within the ESC grafts and to evaluate morphological changes of the left ventricular wall, sections were stained with Hematoxylin and Eosin, Masson's trichrome and Mucin stain (all Sigma-Aldrich Corp., St. Louis, MO) according to established protocols and carefully analyzed by a blinded pathologist (H.V.).

Histological evaluation.

Shortly after immunofluorescent histology, sections were evaluated and graded a score for degree of inflammatory cell infiltration by three independent observers (R.J.S., M.T., F.G.). Scores related to the following descriptions: -, absent, no infiltration; +/-, trace, few infiltrating cells; +, mild, scattered infiltrate or focal accumulation; ++, moderate, modest infiltrate progressing into diffuse; +++, severe, intense and diffuse cell infiltration.

RESULTS

Transplantation of undifferentiated embryonic stem cells elicits progressive inflammatory graft infiltration.

Following successful LAD ligation and ESC injection, ESCs were detected in all transplanted animals at 1 week post-injection. (H&E staining, Figure 1) Masson's trichrome staining confirmed location of ESCs within the infarcted left ventricular wall. (Figure 2A) Immunofluorescent histological analysis demonstrated that allogeneic ES-D3 cell transplantation elicited

progressive graft infiltration of various types of immune cells, involved in both adaptive and innate types of immunity. As shown in figure 2B, immune cells strictly infiltrated the area of infarction and ESC transplantation. Table 1 summarizes the immunohistology data obtained over the 8-weeks time course.
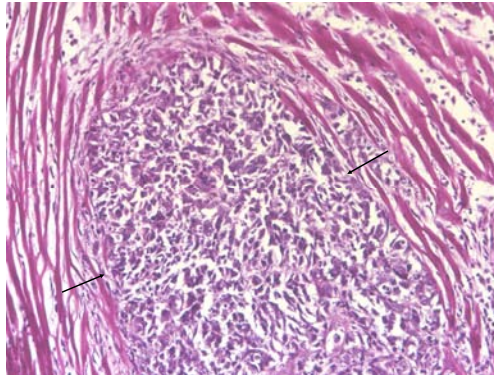

Figure 1. Intramyocardial engraftment of ESCs. H&E staining of the infarcted left ventricular wall revealed ESC grafts in all injected animals at 1 week post-transplantation. (arrows: borders of the ESC graft) *(Original magnification: 200x)*

Table 1. Cellular composition of graft infiltrates over time after intra-myocardial ESC injection. Cell surface markers of T lymphocytes (CD3), T helper cells (CD4), Cytotoxic T cells (CD8), B lymphocytes (B220), Dendritic cells (CD11c), Macrophages (Mac-1) and Granulocytes (Gr-1). Degree of infiltration: -, absent; +/-, trace; +, mild; ++, moderate; +++, severe.

	1wk*			2wks*			4wks*			8wks*			2wks post-htx†	
	Sham	Syn	Allo	Sham	Syn	Allo	Sham	Syn	Allo	Sham	Syn	Allo	Sham	Allo
CD3	+/-	+	+	+/-	+	++	+/-	+	+++	+/-	+	+++	+/-	+++
CD4	+/-	+	+	+/-	+	++	+/-	+	+++	+/-	+/-	+++	+/-	+++
CD8	+/-	+/-	+/-	+/-	+/-	++	+/-	+/-	+++	+/-	+/-	+++	+/-	++
B220	+/-	+	+	+/-	+	++	+/-	+	++	-	+/-	+	+/-	+++
CD11c	+/-	+/-	+/-	-	+/-	+	-	+	++	-	+/-	++	-	+
Mac-1	++	++	++	++	+++	+++	+	++	+++	+	++	+++	++	+++
Gr-1	+	+	+	+	+	++	+	+	+++	+	+	++	+	+++

*Time after LAD ligation and ESC injection
†Time after heterotopic heart transplantation (post-htx) of LAD-ligated and ESC-injected hearts

At 1 week post-injection, allogeneic ESC grafts displayed mild CD3+ T lymphocyte infiltration within the ESC allograft, which was composed predominantly of CD4+ T helper cells. At that time point, sparse CD4+ T cell clusters could be seen at the border of the graft area, whereas at weeks 4 and 8 after transplantation massive infiltration of both CD4+ and CD8+ T cells was observed throughout ESC graft including the inner area. (Figure 2C) Limited numbers of infiltrating T lymphocytes were present in syngeneic ESC grafts (Figure 2D) as well as in sham control hearts over the whole tested time period. These results show that
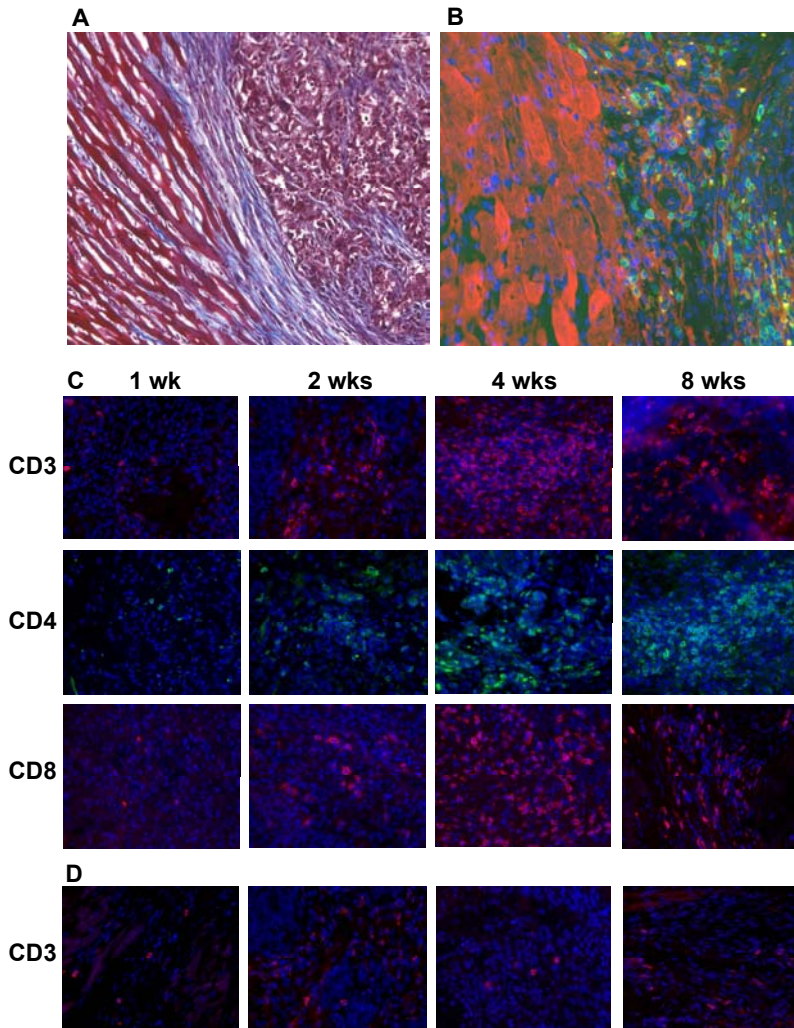
Figure 2. ESC graft infiltration of immune cells after allogeneic transplantation.

A. Masson's trichrome staining shows the ESC graft surrounded by infarcted (blue) and healthy myocardium (red). B. Immunofluorescent staining of a corresponding section shows infiltration of in this case CD4+ T cells (green) into the area of ESC transplantation. Note that the T cells are only found within the ESC graft. Healthy myocardium stains positive for the cardiomyocyte marker α-actinin (red). Counterstaining was performed with 4,6-diamidino-2-phenylindole (DAPI, blue) *(Original magnification: 200x)* C. Representative higher magnification images taken from the area of ESC transplantation (as shown in panel B) of progressive ESC graft infiltration of CD3+, CD4+ and CD8+ T cells over time. At 4 and 8 weeks after transplantation, severe graft infiltration of T lymphocytes was observed. D. In comparison, limited numbers of infiltrating T lymphocytes were present in syngeneic ESC grafts at all time points. *(Original magnification: 400x)*

over time, progressive T lymphocyte graft infiltration occurs following injection of allogeneic ESCs. Intensity of T cell infiltration depends on MHC incompatibility between donor ESCs and recipient. These data suggest that alloantigens presented by developing ESCs are recognized by allospecific host T cells.

Dendritic cell (DC) infiltration was absent in sham control hearts showing that, at least at the time points tested, the performed surgical procedures did not cause non antigen-specific DCs activation/migration. Also, no or minimal numbers of infiltrating DCs were found in syngeneic hosts demonstrating that MHC disparity is required for DC migration into the area of transplanted ESC grafts. Similar to alloreactive T cells, the numbers of graft infiltrating DCs increased progressively over time in full-mismatched hosts, and peaked at 4 and 8 weeks after ESC transplantation. On the overall, small numbers of ESC graft-infiltrating B cells were detected as compared to T cells.

Inflammatory cells mediating innate immunity, including macrophages and granulocytes, were also detected in the ESC graft area. Although more profound in the experimental (ESC injection) hearts, we found that macrophage and granulocyte cell infiltrates were also present in sham control hearts. This indicates that post-transplantation, innate response was not exclusively related to ESC antigens but could also be due to surgical trauma after transplantation (LAD ligation and/or medium injection procedures).

Embryonic stem cells differentiate into teratomas in ischemic myocardium.

In both allogeneic and syngeneic ESC grafts, tumor formation was observed. (Figure 3) From 1 to 4 weeks after transplantation, Masson's trichrome staining of infarcted left ventricular
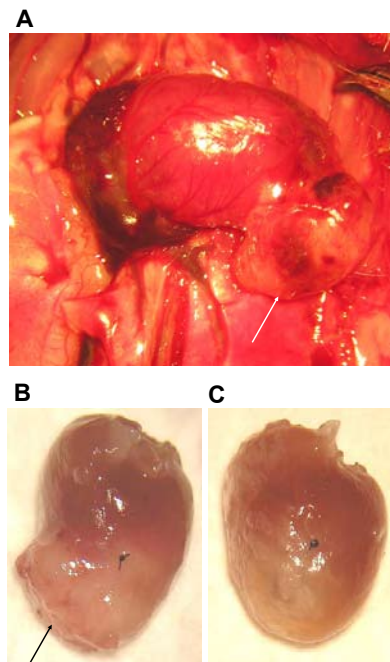

Figure 3. Transplantation of ESCs causes tumor formation. Tumors were found extending from the left ventricular wall after both syngeneic transplantation (A, white arrow), and allogeneic transplantation (B, black arrow). In sham operated hearts (C), as expected, no tumors were detected.
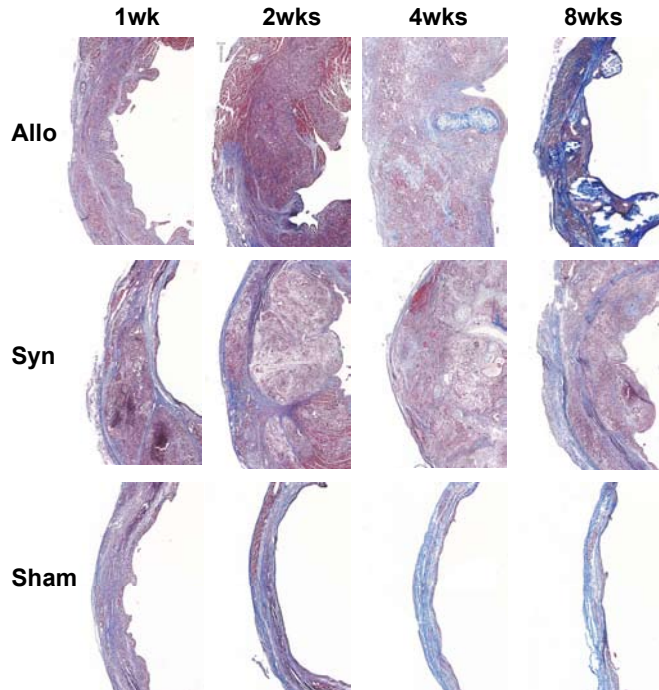
Figure 4. Morphological changes of left ventricular wall over time. Masson's trichrome staining of heart sections at different time points after allogeneic (allo) and syngeneic (syn) ESC transplantation revealed intramural tumors over time increasing in size. Note that at 8 weeks after allogeneic transplantation, the allogeneic ESC grafts had been destroyed as a result of the host inflammatory alloimmune response. The left ventricular walls of the sham control hearts are shown in the lower panels.

walls showed the intramural ESC grafts similarly increasing in size in both allogeneic and syngeneic hearts. (Figure 4) H&E staining revealed no evidence of ESC differentiation at 1 and 2 weeks post-transplantation. However, at 4 weeks, both in the allogeneic and syngeneic ESC grafts, differentiated structures originating from all three different germ layers could be observed. (Figure 5A-D) At this time point, tumors could be characterized as teratomas. At 8 weeks, apart from little intramural cartilage, no differentiated or undifferentiated ESCs were found in the allogeneic hearts, whereas in the syngeneic hearts both cell types were still present. (Figure 4) This finding suggested that at 8 weeks following transplantation the allogeneic ESC grafts had been destroyed as a result of the host inflammatory alloimmune response.

Embryonic stem cell immunogenicity increases upon differentiation.

In the present study, progressive host anti-ESC graft immunity associated with ESC differentiation. Thus, differentiated structures could be found within the ESC grafts at 4 weeks post-transplantation. At the same time, severe ESC graft infiltration of inflammatory cells was observed. Taken together, these findings suggest that once ESCs reach a more differentiated state, they can be more effectively recognized and rejected by the recipient immune system.
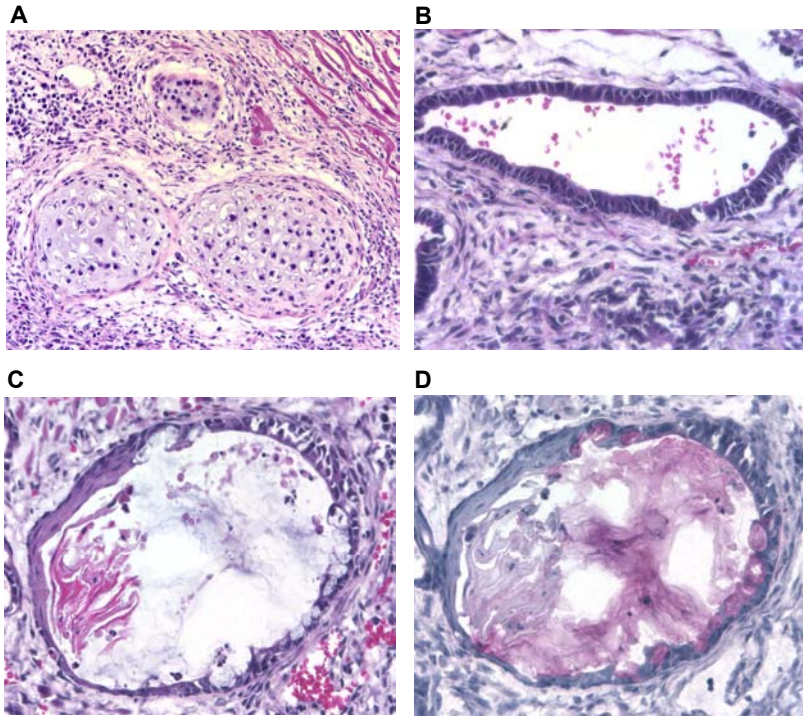
Figure 5. Intramyocardially transplanted undifferentiated ESCs differentiate into teratomas. Four weeks after ESC transplantation structures originating from all three different germ layers were found in both allogenic and syngenic recipient hearts. H&E staining shows formation of intramyocardial cartilage (A, mesodermal derivative, arrowheads, 200x), squamous epithelium (B, ectodermal derivative, 400x) and glandular epithelium (C, endodermal derivative, 400x). Secretion of mucus (pink) by the intramyocardial glands was confirmed by mucin staining (D, 400x).

To further investigate this hypothesis, we designed a model to study the immune response against *in vivo* matured ESCs. A group of BALB/c mice underwent similar procedure of myocardial infarction and allogeneic ESC transplantation. However, in this case, after 2 weeks, their hearts were explanted and heterotopically transplanted into naive syngeneic BALB/c recipients. Daily assessment of heterotopic cardiac grafts by abdominal palpation confirmed viability of the grafts throughout the study period. Interestingly, as early as 2 weeks after heterotopic transplantation of the isografts containing partly developed allogeneic ESC grafts, we found severe graft infiltration of various types of immune cells, including T and B-lymphocytes. (Figure 6 and Table 1, right column) Therefore, ESCs that have matured and differentiated *in vivo* for 2 weeks elicit more potent and immediate alloimmune response as compared to undifferentiated ESCs. These data indicate that the immunogenicity of ESC transplants increases upon *in vivo* differentiation.
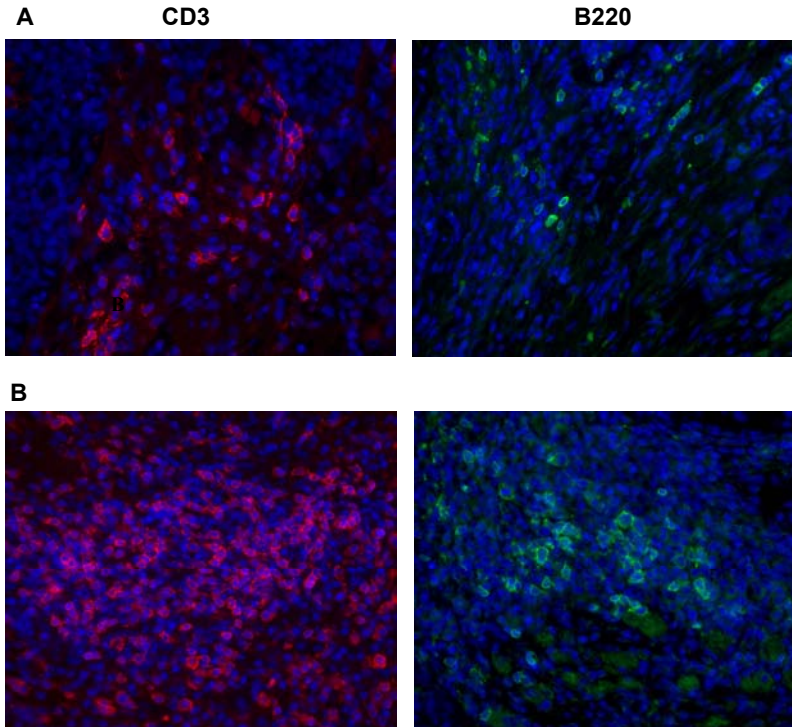
Figure 6. Graft infiltration of immune cells after transplantation of *in vivo* differentiated ESCs. Representative images of ESC graft infiltration of T- (red) and B-(green) lymphocytes at 2 weeks following undifferentiated ESC transplantation (A) versus 2 weeks following *in vivo* differentiated ESC transplantation through heterotopic transplantation of the LAD-ligated and ESC-injected hearts (B). *In vivo* differentiated ESCs elicited a vigorous and more immediate immune response as compared to undifferentiated ESCs. Counterstaining was performed with 4,6-diamidino-2-phenylindole (DAPI, blue) *(Original magnification: 400x)*

DISCUSSION

This study was designed to investigate whether ESCs elicit an immune response when transplanted into genetically identical or full MHC-mismatched ischemic myocardium. These data demonstrate, that there is progressive infiltration by various types of inflammatory cells within the ESC graft following transplantation across histocompatibility barriers. Severe cellulair invasion was observed 4 weeks after intra-myocardial injection, followed by disappearance of the ESC allografts between 4 and 8 weeks after transplantation, presumably due to a robust alloimmune response. When transplanted into a naive recipient after 2 weeks of in *vivo* maturation, ESCs triggered an accelerated infiltration of immune cells, indicating that the immune response towards developing ESCs in allotransplant settings increases over time.

In contrast to tissue allografts, ESC transplants are devoid of highly immunogenic mature dendritic cells, or any other type of professional antigen presenting cells. Thus, the transplanted cells do not express MHC class II molecules, required for effective priming of CD4^{+} alloreactive T cells through direct recognition[10,15]. Therefore, the direct pathway of alloresponse is likely to be dominated by MHC class I-reactive CD8^{+} T cells, whereas the indirect alloreactive pathway (presentation of processed allogeneic peptides by host APCs) would engage both CD4^{+} and CD8^{+} T cells[15]. In the present study, similar amounts of both CD8^{+} and CD4^{+} infiltrating T cells were detected within the ESC grafts. Similarly, the numbers of graft infiltrating DCs increased progressively over time. Co-localization of antigen presenting DCs and T lymphocytes within the ESC graft points at ongoing T cell-APC interaction, and suggest that both direct and indirect allorecognition were involved in immune reactions against allogeneic ESC antigens. Furthermore, ESC graft infiltration of B cells was observed following allogeneic ESC transplantation. CD4+ T cells primed by indirect allorecognition could provide contact-dependent help for B cells to produce alloantibody by a classical cognate T cell-B cell interaction. Alloantibody might mediate further graft damage by various mechanisms, including complement-dependent target-cell injury.[13]

ESC transplantation is being widely investigated as a potential novel approach to regenerate infarcted myocardium. However, a review of the current literature on transplantation of ESCs, revealed a surprising lack of concern for potential immunological conflict[13]. The issue of immune recognition by the host is often circumvented by syngeneic transplantation[16], immunosuppressive therapy[17], or transplantation into an immune privileged site[18]. Moreover, previous studies in xenogeneic transplant models provide no evidence for immune rejection of engrafted ESCs[6,7]. This may create an impression that the problem of immune rejection does not apply to ESC transplantation. The present study designed to address this question, does not support this notion. Thus, we detected potent progressive inflammatory ESC graft infiltration, indicating efficient recognition of ESC alloantigens by the host immune system.

One could argue, that ESC immunogenicity could be due to inflammation of the host heart tissue caused by LAD-associated ischemia injury. However, histological analysis following syngeneic ESC transplantation revealed no progressive infiltration, demonstrating that observed ESC immunogenicity *in vivo* could not be attributed to ischemia-induced inflammation of the recipient heart. In addition, it has been reported that transfection of ESCs with a genetic marker such as green fluorescent protein (GFP) could alter their immunogenicity.[19,20] Meanwhile, GFP transfection of ESCs is frequently used in quantitative analysis of ESC survival and differentiation. To exclude potential immune reactivity towards exogenous proteins, we used a non-manipulated ESC line.

It is known that undifferentiated ESCs may form teratomas when transplanted under the skin of immunodeficient SCID mice[8]. In addition, teratoma formation in the host retroperitoneum has been observed following ectopic transplantation of allogeneic ESC-derived cardiomyocytes[21]. On the other hand, it has been suggested that the infarcted heart pos-

sesses paracrine signaling pathways that are capable of directing *in vivo* differentiation of transplanted ESCs into functional cardiomyocytes[6]. In the present study, intramyocardial teratomas were observed in both allogeneic and syngeneic hearts at 4 weeks after ESC transplantation. Although, this study was not designed to evaluate cardiomyocyte differentiation parameters, detection of ESC derivatives originating from various germ layers demonstrates that, at least under current experimental conditions, the host environment could not guide differentiation of all transplanted cells into the cardiomyocyte lineage. Careful removal of undifferentiated elements from ESC derivatives prior to transplantation may possibly help to circumvent formation of intracardiac teratomas.

In conclusion, these data provide a clear demonstration of the induction of an alloimmune response against developing ESCs in an experimental animal model. Furthermore, it offers a novel experimental approach, in which immunogenicity of partly differentiated ESCs can be assessed following heterotopic transplantation of previously LAD-ligated and ESC-injected hearts into naïve syngeneic hosts. This model could provide further insight into the characterization of anti-ESC immunity in animal models. In the present study, immunogenicity of ESCs was analyzed by immunohistologic evaluation of graft infiltration by host immune cells. Intragraft migration and infiltration represents an important step in the sequence of immune reactions. It indicates that other systemic immune events, such as peripheral lymphocyte activation in the spleen and/or lymph nodes, cytokine release and production of circulating alloantibodies, likely are present in this model. Experiments evaluating these parameters are in progress in our laboratory.

In summary, we report that ESCs elicit alloimmune response after transplantation into MHC-mismatched ischemic myocardium. Upon *in vivo* differentiation, ESC immunogenicity increases, resulting in efficient recognition of ESC antigens by the host immune system, and alloimmune rejection. These results imply that clinical transplantation of ESCs or ESC derivatives harvested from allogeneic donors for treatment of cardiac failure might require immunosuppressive therapy.

Chapter 6

REFERENCES

1. Orlic D, Kajstura J, Chimenti S, Jakoniuk I, Anderson SM, Li B, Pickel J, McKay R, Nadal-Ginard B, Bodine DM, Leri A, Anversa P. Bone marrow cells regenerate infarcted myocardium. *Nature*. 2001;410:701-5.

2. Balsam LB, Wagers AJ, Christensen JL, Kofidis T, Weissman IL, Robbins RC. Haematopoietic stem cells adopt mature haematopoietic fates in ischaemic myocardium. *Nature*. 2004;428:668-73.

3. Murry CE, Soonpaa MH, Reinecke H, Nakajima H, Nakajima HO, Rubart M, Pasumarthi KB, Virag JI, Bartelmez SH, Poppa V, Bradford G, Dowell JD, Williams DA, Field LJ. Haematopoietic stem cells do not transdifferentiate into cardiac myocytes in myocardial infarcts. *Nature*. 2004;428:664-8.

4. Sachinidis A, Fleischmann BK, Kolossov E, Wartenberg M, Sauer H, Hescheler J. Cardiac specific differentiation of mouse embryonic stem cells. *Cardiovasc Res*. 2003;58:278-91.

5. Mummery C, Ward-van Oostwaard D, Doevendans P, Spijker R, van den Brink S, Hassink R, van der Heyden M, Opthof T, Pera M, de la Riviere AB, Passier R, Tertoolen L. Differentiation of human embryonic stem cells to cardiomyocytes: role of coculture with visceral endoderm-like cells. *Circulation*. 2003;107:2733-40.

6. Behfar A, Zingman LV, Hodgson DM, Rauzier JM, Kane GC, Terzic A, Puceat M. Stem cell differentiation requires a paracrine pathway in the heart. *Faseb J*. 2002;16:1558-66.

7. Min JY, Yang Y, Sullivan MF, Ke Q, Converso KL, Chen Y, Morgan JP, Xiao YF. Long-term improvement of cardiac function in rats after infarction by transplantation of embryonic stem cells. *J Thorac Cardiovasc Surg*. 2003;125:361-9.

8. Thomson JA, Itskovitz-Eldor J, Shapiro SS, Waknitz MA, Swiergiel JJ, Marshall VS, Jones JM. Embryonic stem cell lines derived from human blastocysts. *Science*. 1998;282:1145-7.

9. Fandrich F, Dresske B, Bader M, Schulze M. Embryonic stem cells share immune-privileged features relevant for tolerance induction. *J Mol Med*. 2002;80:343-50.

10. Drukker M, Katz G, Urbach A, Schuldiner M, Markel G, Itskovitz-Eldor J, Reubinoff B, Mandelboim O, Benvenisty N. Characterization of the expression of MHC proteins in human embryonic stem cells. *Proc Natl Acad Sci U S A*. 2002;99:9864-9.

11. Draper JS, Pigott C, Thomson JA, Andrews PW. Surface antigens of human embryonic stem cells: changes upon differentiation in culture. *J Anat*. 2002;200:249-58.

12. Fandrich F, Lin X, Chai GX, Schulze M, Ganten D, Bader M, Holle J, Huang DS, Parwaresch R, Zavazava N, Binas B. Preimplantation-stage stem cells induce long-term allogeneic graft acceptance without supplementary host conditioning. *Nat Med*. 2002;8:171-8.

13. Bradley JA, Bolton EM, Pedersen RA. Stem cell medicine encounters the immune system. *Nat Rev Immunol*. 2002;2:859-71.

14. Corry RJ, Winn HJ, Russell PS. Primarily vascularized allografts of hearts in mice. The role of H-2D, H-2K, and non-H-2 antigens in rejection. *Transplantation*. 1973;16:343-50.

15. Strom TB, Field LJ, Ruediger M. Allogeneic stem cells, clinical transplantation and the origins of regenerative medicine. *Curr Opin Immunol*. 2002;14:601-5.

16. Klug MG, Soonpaa MH, Koh GY, Field LJ. Genetically selected cardiomyocytes from differentiating embronic stem cells form stable intracardiac grafts. *J Clin Invest*. 1996;98:216-24.

17. Liu S, Qu Y, Stewart TJ, Howard MJ, Chakrabortty S, Holekamp TF, McDonald JW. Embryonic stem cells differentiate into oligodendrocytes and myelinate in culture and after spinal cord transplantation. *Proc Natl Acad Sci U S A*. 2000;97:6126-31.

18. Asano T, Ageyama N, Takeuchi K, Momoeda M, Kitano Y, Sasaki K, Ueda Y, Suzuki Y, Kondo Y, Torii R, Hasegawa M, Ookawara S, Harii K, Terao K, Ozawa K, Hanazono Y. Engraftment and tumor forma-

tion after allogeneic in utero transplantation of primate embryonic stem cells. *Transplantation*. 2003;76:1061-7.

19. Stripecke R, Carmen Villacres M, Skelton D, Satake N, Halene S, Kohn D. Immune response to green fluorescent protein: implications for gene therapy. *Gene Ther*. 1999;6:1305-12.

20. Rosenzweig M, Connole M, Glickman R, Yue SP, Noren B, DeMaria M, Johnson RP. Induction of cytotoxic T lymphocyte and antibody responses to enhanced green fluorescent protein following transplantation of transduced CD34(+) hematopoietic cells. *Blood*. 2001;97:1951-9.

21. Johkura K, Cui L, Suzuki A, Teng R, Kamiyoshi A, Okamura S, Kubota S, Zhao X, Asanuma K, Okouchi Y, Ogiwara N, Tagawa Y, Sasaki K. Survival and function of mouse embryonic stem cell-derived cardiomyocytes in ectopic transplants. *Cardiovasc Res*. 2003;58:435-43.

Chapter 6

CHAPTER 7

In Vivo Imaging of Embryonic Stem Cells Reveals Patterns of Survival and Immune Rejection Following Transplantation

Rutger-Jan Swijnenburg, Sonja Schrepfer, Feng Cao, Jeremy I. Pearl, Xiaoyan Xie, Andrew J. Connolly, Robert C. Robbins, Joseph C. Wu

ABSTRACT

Embryonic stem cell (ESC)-based transplantation is considered a promising novel therapy for a variety of diseases. This is bolstered by the suggested immune-privileged properties of ESCs. Here we used *in vivo* bioluminescent imaging (BLI) to non-invasively track the fate of transplanted murine ESCs (mESCs) stably transduced with a double fusion reporter gene consisting of firefly luciferase (Fluc) and enhanced green fluorescent protein (eGFP). Following syngeneic intramuscular transplantation of 1×10^6 mESCs, the cells survived and differentiated into teratomas. In contrast, allogeneic mESC transplants were infiltrated by a variety of inflammatory cells, leading to rejection within 28 days. Acceleration of rejection was observed when mESCs were allotransplanted following prior sensitization of the host. Finally, we demonstrate that mESC-derivatives were more rapidly rejected as compared to undifferentiated mESCs. These data show that mESCs do not retain immune-privileged properties *in vivo* and are subject to immunological rejection as assessed by novel molecular imaging approaches.

Embryonic stem cell (ESC)-based transplantation therapies have significant potential for treating a broad spectrum of human diseases through replacement or regeneration of lost or damaged tissues (*1*). ESCs are pluripotent and have the capacity to differentiate into multiple adult cell types *in vitro*, such as cardiomyocytes (*2*), pancreatic islet cells (*3*), and neurons (*4*). These ESC-derivatives have demonstrated therapeutic potential *in vivo (5)*. One potential benefit of ESC-based transplantation over adult cells is their suggested immune-privileged properties (*6*). Human (h) and murine (m) ESC have been shown to express low levels of major histocompatibility (MHC) antigens (*7, 8*). Previous studies have reported that both mESCs (*9*) and hESCs (*10*) are capable of inhibiting allogeneic T-cell proliferation *in vitro*. Furthermore, mESCs have been shown to evade immune recognition and survive in immunocompetent rats (*11*) and sheep (*12*) for many weeks after transplantation. Nevertheless, our group and others have found that mESCs transplanted into allogeneic mouse hearts can elicit local graft infiltration of inflammatory cells resulting in rejection (*13, 14*). Similarly, other reports have questioned the alleged immune-privilege of mESCs following xenotransplantation into immunocompetent baboons (*15*).

Clearly, the extent to which immunologic rejection of ESCs and/or ESC-derivatives occurs following allogeneic transplantation is a crucial question that has yet to be clarified. The results of aforementioned studies were primarily based on immunohistological evaluation, which provide only a "snapshot" representation rather than a comprehensive picture of cell survival over time (*16*). Such limited techniques may partly contribute to the conflicting observations of mESC survival in allogeneic or xenogeneic hosts. To address these limitations, we have previously validated *in vivo* bioluminescent imaging (BLI) to be a reliable technique for assessing engraftment and survival of mESCs following transplantation *in vivo (17)*. An important advantage in using BLI to track cell transplantation is that the expression of the firefly luciferase (Fluc) reporter gene, which is integrated into the DNA of the transplanted cells, is expressed only by living cells, making it a highly accurate tool for following cell graft rejection in the living subject (*18*). We have previously shown that transduction of mESCs with reporter genes that allow *in vivo* tracking does not alter cellular viability and their ability to differentiate into cells of all three germ layers (*19, 20*). To further delineate the novel field of ESC transplantation immunobiology, we used *in vivo* BLI to visualize patterns of survival and rejection of mESCs following transplantation across histocompatibility barriers.

To track the mESCs *in vivo* by BLI as well as *ex vivo* by immunohistochemistry, a double fusion (DF) reporter gene construct carrying Fluc and enhanced green fluorescent protein (eGFP) driven by a constitutive ubiquitin promoter (pUB) was transduced into undifferentiated mESCs (D3 cell line, derived from the 129/Sv mouse strain), using a self-inactivating (SIN) lentiviral vector (**Fig 1A**), as previously described (*20*). After transduction, mESCs robustly expressed Fluc (**Fig 1B**) and eGFP (**Fig 1C**). In agreement with previous reports (*9, 21*), flow cytometric analysis showed expression of pluripotency marker SSEA-1 and minimal expression of H-2k^b MHC class I or I-A^b MHC class II antigens on undifferentiated mESCs. By contrast,
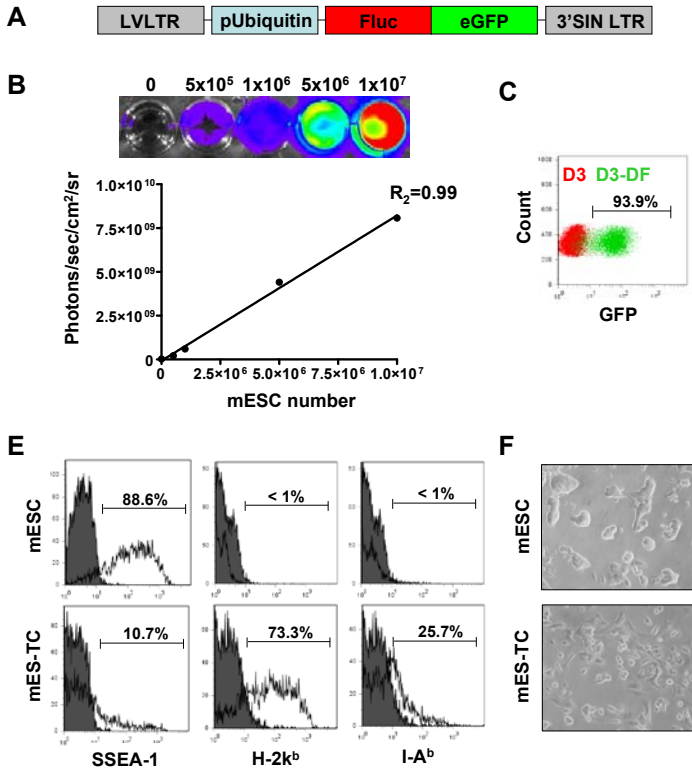
Figure 1. Characterization of the double fusion (DF) firefly luciferase (Fluc) and enhanced green fluorescent protein (eGFP) transduced D3 murine embryonic stem cells (mESCs). (a) Schema of the DF reporter gene containing Fluc and eGFP driven by an ubiquitin promoter. **(b)** Stably transduced mESCs show a robust correlation between cell number and reporter gene activity. BLI of a 24-well plate containing increasing numbers of mESCs are shown above the corresponding graph depicting correlation between cell number and Fluc activity. **(c)** Flow cytometric analysis of transduced mESCs (D3-DF) shows robust expression of eGFP following transduction with the DF reporter gene, as compared to non-transduced mESCs (D3). **(d)** Flow cytometric analysis of undifferentiated mESCs shows robust expression of pluripotency marker SSEA-1, but minimal expression of MHC-I (H-2k^b) or MHC-II (I-A^b) antigens. In contrast, cells isolated from a 6-week old teratoma derived from mESCs (mES-TCs) express low amounts of SSEA-1 but significant levels of MHC-I and MHC-II antigens. Filled histograms represent isotype control antibodies. **(e)** Phase-contrast images of undifferentiated mESCs and mES-TCs cultured *in vitro*.

mESC-derived teratoma cells (mES-TCs) isolated from 6-week-old surgically explanted teratomas by a 2-hour enzymatic digestion in Collagenase D (2 mg/mL in RPMI medium) clearly expressed both MHC-I and MHC-II antigens (**Fig 1D**). In culture, mES-TCs displayed a heterogeneous single cell morphology, as opposed to mESCs, which grow in tight clusters (**Fig 1E**).

Transduced mESCs (1x10^6) were transplanted by direct injection into the gastrocnemius muscle of syngeneic (129/Sv, H-2k^b, n=8) and allogeneic (BALB/c, H-2k^d, n=8) recipient mice after which BLI was performed weekly. The BLI protocol involved intra-peritoneal administration of the D-Luciferin reporter probe at a dose of 375 mg/kg body weight and imaging was performed using the Xenogen In Vivo Imaging System as previously described (*17*). Clearly,

impaired survival of mESCs in the allogeneic recipients was observed as compared to the syngeneic animals, reaching statistical significance at day 14 after transplantation (BLI signal: 129/Sv 9.00±0.57 vs. BALB/c 7.54±0.99 Log$^{[photons/sec]}$; *P*<0.01 by T-test). (**Fig 2A and 2B**). By 28 days, BLI signal in the allogeneic recipients had decreased to background levels, whereas signal in the syngeneic recipients continued to increase. These results suggest alloantigen specific rejection of the transplanted mESCs. At 28 days following transplantation, gastrocnemius muscles were surgically explanted. In syngeneic recipients, intramuscular tumors could be observed, whereas the shape of the allogeneic recipient muscles appeared normal (**Fig 2C**). Differentiated structures originating from all three germ layers could be demonstrated by H&E staining in the syngeneic muscles, indicating teratoma formation. Correlating with our findings using BLI, no teratoma formation and/or signs of surviving mESCs could be found in the allogeneic muscles (**Fig 2C**).

We next investigated the local immune response elicited by mESCs in a second group of allogeneic BALB/c and syngeneic 129/Sv mice (n=8 per group). At 10 days following transplantation, the muscles of these mice were explanted and investigated for graft infiltrating cells. Immunofluorescent staining of allogeneic muscle sections demonstrated massive infiltration of CD45$^+$ inflammatory cells surrounding the eGFP$^+$ mESC grafts (**Fig 2D**). Quantification and further characterization of graft infiltrating cells was carried out by enzymatic digestion (2 hours in 2mg/ml collagenase D in RPMI medium) of the explanted muscles followed by FACS analysis. Live cells were gated out from debris and further analyzed for expression of a panel of hematopoietic cell surface markers. Comparison of the syngeneic to the allogeneic mESC recipient muscles confirmed severe infiltration of various types of immune cells involved in both adaptive and innate types of immunity (**Fig 2E**). At this time-point, both the CD3$^+$ cells (total T-cell population) and CD8$^+$ cells (cytototoxic T-cells) were present at a significantly higher frequency in allogeneic versus syngeneic recipients (*P*<0.05 by T-test), suggesting a prominent role for T-cell mediated immunity in mESC rejection.

To investigate if mESCs could induce immunologic memory, we next performed infusion of 1x10^6 *non-transduced* D3 mESCs or 1x10^6 irradiated (3000 RAD) 129/Sv splenocytes (as control) into the tail vein of allogeneic BALB/c recipients (n=4 and 5 per group, respectively). Four weeks later, these same mice received intramuscular transplantation with the same number of transduced mESCs and cell survival was quantified using longitudinal BLI. Accelerated BLI signal loss was observed in both groups, with BLI signal reaching background levels as soon as post-transplant day 4 (control group) and 7 (mESC group) (**Fig 3A and 3B**). These findings confirm that a donor (129/Sv)-specific adaptive immune response is generated against transplanted mESCs.

Clinical ESC-based transplantation protocols will require differentiation of the donor cells into the desired cell type prior to transplantation, due to the risk of teratoma formation following transplantation of undifferentiated ESCs (*13*). Therefore, we thought it relevant to study survival of mESC-derivatives following allotransplantation. A group of BALB/c mice
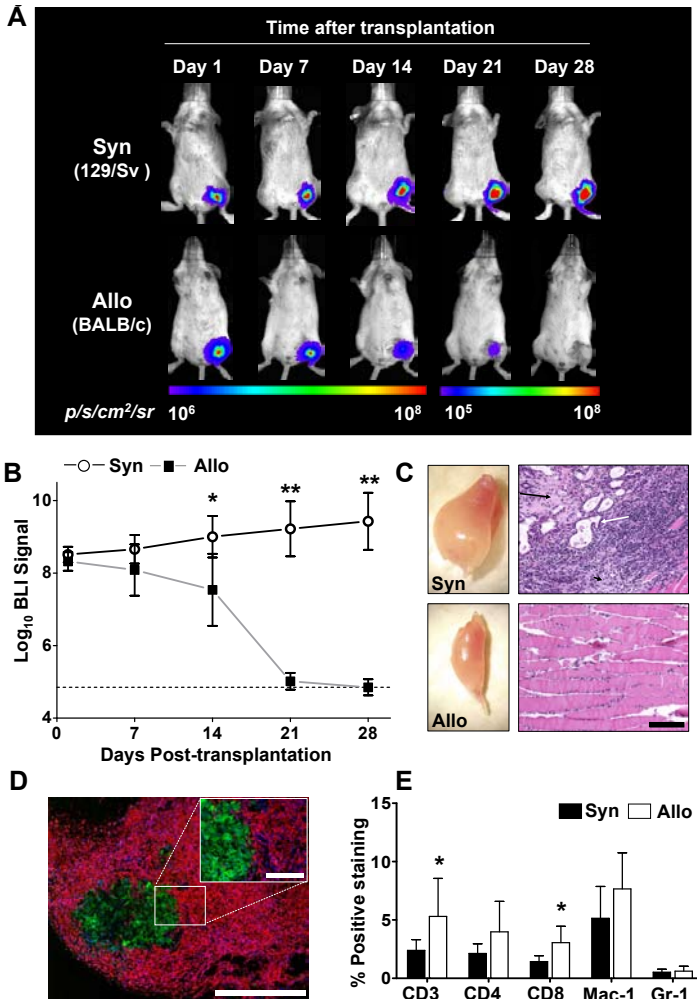
Figure 2. *In vivo* **bioluminescent imaging (BLI) of transplanted mESCs. (a)** Representative BLI images of animals following intramuscular (gastrocnemius muscle) transplantation of mESCs show a decrease in BLI signal in allogeneic animals (BALB/c), as opposed to syngeneic (129/Sv) mice, reaching background levels between post-transplant day 21 and 28. Color scale bar values are in photons/sec/cm^2/steridian (p/s/cm^2/sr). **(b)** Graphical representation of longitudinal BLI after mESC transplantation into syngeneic (129/Sv, n=8) and allogeneic (BALB/c, n=8) mouse strains. Note that in allogeneic recipients, BLI signals decreases to background levels over the course of 28 days, whereas BLI signals in the syngeneic recipients increases over time, suggesting mESC proliferation. Data-points represent mean ± s.d.; *$P<0.01$, **$P<0.001$ (by T-test). Dotted line = background BLI signal **(c)** *Ex vivo* images of harvested muscles (left panels) show intramuscular tumors in syngeneic, as opposed to allogeneic muscles. Corresponding H&E stained tissue sections (right panels) show presence of teratoma in syngeneic muscles, whereas no signs of teratoma formation are observed in allogeneic muscles. Black arrow: Osteoid differentiation (mesoderm); white arrow: glandular differentiation (endoderm); black arrow head: neural differentiation (ectoderm). Scale bars: 100μm. **(d)** Immunofluorescent staining of allogeneic transplants reveals severe infiltration of CD45$^+$ cells (red) surrounding eGFP$^+$ mESCs (green). Nuclear staining was performed with 4,6-diamidino-2-phenylindole (DAPI, blue). Scale bars: 100μm. **(e)** To quantify subpopulations of graft infiltrating inflammatory cells, flow cytometry analysis of enzymatically digested muscles was performed at day 10 following transplant. Graft infiltration of CD3$^+$ (T-cells), CD4$^+$ (T-helper cells), CD8$^+$ (cytotoxic T-cells), Mac-1$^+$Gr-1$^-$ (macrophages), and Mac-1$^+$Gr-1$^+$ (neutrophils) was observed. Note that CD3$^+$ and CD8$^+$ cells infiltrated the allogeneic grafts at a significantly higher rate than the syngeneic grafts (n=8 per group). Bars represent mean ± s.d.; *$P<0.05$ (by T-test).
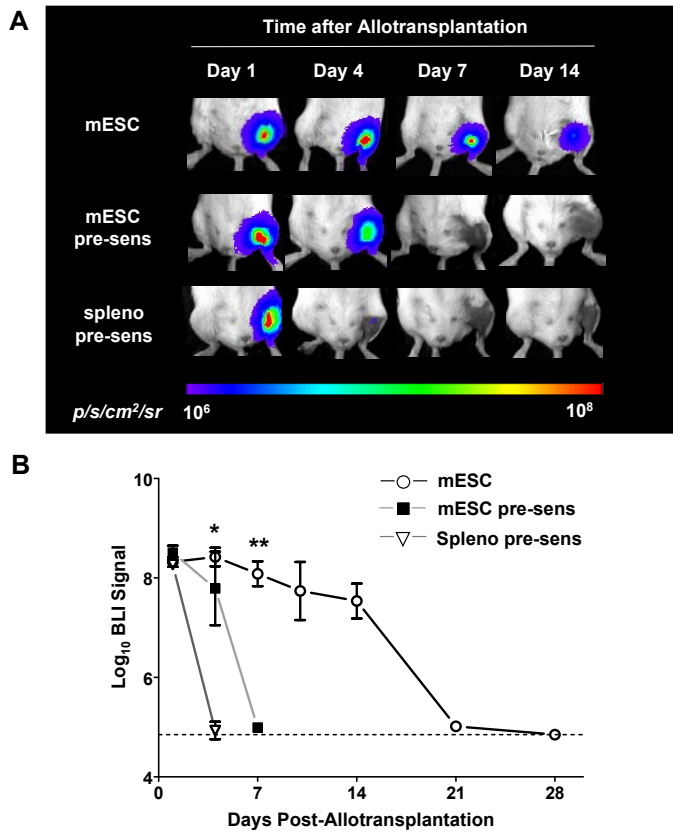
Figure 3. Accelerated rejection following pre-sensitization and/or pre-differentiation of donor mESCs. (a) Representative BLI images of animals following intramuscular allotransplantation of mESCs show an accelerated decrease in BLI signal in animals that were pre-sensitized with both non transduced mESCs (mESC pre-sens) or irradiated 129/Sv splenocytes (spleno pre-sens) as compared to naïve allogeneic mESC recipients. Color scale bar values are in p/s/cm²/sr. **(b)** Graphical representation of BLI of mESC survival in the three groups (n=4 to 8 per group). Data-points represent mean ± s.e.m.; *$P<0.001$ mESC vs. spleno pre-sens, ** $P<0.001$ mESC vs. mESC pre-sens (by ANOVA). Dotted line = background BLI signal.

(n=5) was injected with 1×10^6 mES-TCs and longitudinal BLI was performed. In comparison with undifferentiated mESCs, the BLI signal displayed a similar pattern up until 7 days following transplantation (**Fig 4A and 4B**). However, BLI signal in the mES-TC animals decreased substantially by day 10 (mESC 7.74±0.58 vs. mES-TC 5.46±0.17 Log[photons/sec]; $P<0.01$ by T-test) and reached background levels at day 14. These results show that differentiated mESCs have impaired survival capacity as compared to undifferentiated mESCs when transplanted over histocompatibility barriers.

In a recent report, higher numbers of transplanted undifferentiated mESCs (5×10^6 to 20×10^6) were shown capable of survival and formation of teratoma in allogeneic recipients (22). Similarly, in this study we found that when 10×10^6 mESCs were transplanted into allogeneic
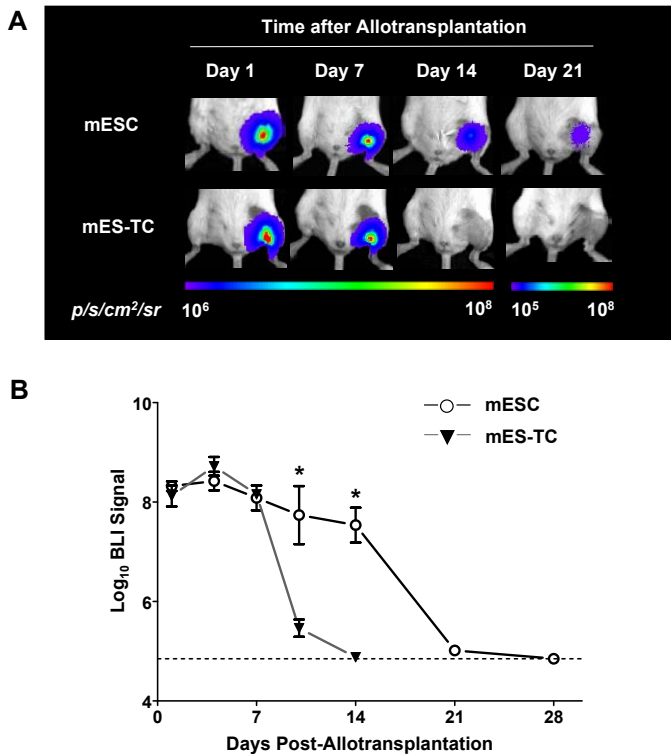
Figure 4. Impaired survival capacity of differentiated mESCs as compared to undifferentiated mESCs following allotransplantation.
(a) Representative BLI images of animals following intramuscular allotransplantation of mESCs or mES-TCs. Clearly, BLI signal in the mES-TC transplanted animals decreased more rapidly as compared to mESC-transplanted animals, reaching background levels at day 14. Color scale bar values are in p/s/cm²/sr. **(b)** Graphical representation of BLI of mESC survival in the two groups (n=5 to 8 per group). Data-points represent mean ± s.e.m.; *$P<0.01$ (by T-test). Dotted line = background BLI signal.

BALB/c recipient muscles, BLI signal could be followed out beyond 28 days following transplantation in 2 out of 10 animals (20%) and intramuscular teratomas could be observed in these two animals. However, when mESCs were allowed to differentiate for 14 days *in vitro* prior to transplantation, 10×10^6 cells were rejected by 10 out of 10 animals (100%) (data not shown).

Undifferentiated mESCs have been reported to possess immune-privileged properties, which has been attributed to low expression of MHC molecules (*21*), expression of perforin-deactivating Serpin-6 (*9*) and/or production of lymphocyte-inhibiting TGF-β (*22*) by the cells. However, our study clearly shows that transplantation of mESCs *in vivo* can result in donor-specific immune recognition and rejection, which leads to immunologic memory. Importantly, post-transplant cell death is accelerated when mESCs are allowed to differentiate prior to transplantation, a scenario likely to occur in clinical ESC-based transplantation settings in the future. Whether the latter phenomenon is truly a result of increased immunogenicity

of the cells, as suggested by their increased expression of MHC antigens (**Fig 1E**), or if other factors such as a decreased proliferation rate of differentiated cells play part in this process remains to be evaluated in detail. Nevertheless, the results of this study emphasize that immunologic rejection of ESCs or ESC-derivatives is likely to occur and the need exists for solutions that reduce or eliminate immunologic response following ESC-based transplantation (*23*). In order to develop and test such strategies, there will also be a need for reliable imaging technologies to track and assess behavior of the cells following transplantation. *In vivo* bioluminescent imaging serves these needs and has the potential to play a prominent role in future ESC-based transplantation research.

ACKNOWLEDGEMENTS

Chapter 7

REFERENCES

1. Wobus AM and KR Boheler. (2005). Embryonic stem cells: prospects for developmental biology and cell therapy. Physiological reviews 85:635-678.

2. Mummery C, D Ward-van Oostwaard, P Doevendans, R Spijker, S van den Brink, R Hassink, M van der Heyden, T Opthof, M Pera, AB de la Riviere, R Passier and L Tertoolen. (2003). Differentiation of human embryonic stem cells to cardiomyocytes: role of coculture with visceral endoderm-like cells. Circulation 107:2733-2740.

3. Segev H, B Fishman, A Ziskind, M Shulman and J Itskovitz-Eldor. (2004). Differentiation of human embryonic stem cells into insulin-producing clusters. Stem Cells 22:265-274.

4. Perrier AL, V Tabar, T Barberi, ME Rubio, J Bruses, N Topf, NL Harrison and L Studer. (2004). Derivation of midbrain dopamine neurons from human embryonic stem cells. Proceedings of the National Academy of Sciences of the United States of America 101:12543-12548.

5. Wu DC, AS Boyd and KJ Wood. (2007). Embryonic stem cell transplantation: potential applicability in cell replacement therapy and regenerative medicine. Front Biosci 12:4525-4535.

6. Fandrich F, B Dresske, M Bader and M Schulze. (2002). Embryonic stem cells share immune-privileged features relevant for tolerance induction. Journal of molecular medicine (Berlin, Germany) 80:343-350.

7. Drukker M, G Katz, A Urbach, M Schuldiner, G Markel, J Itskovitz-Eldor, B Reubinoff, O Mandelboim and N Benvenisty. (2002). Characterization of the expression of MHC proteins in human embryonic stem cells. Proceedings of the National Academy of Sciences of the United States of America 99:9864-9869.

8. Tian L, JW Catt, C O'Neill and NJ King. (1997). Expression of immunoglobulin superfamily cell adhesion molecules on murine embryonic stem cells. Biology of reproduction 57:561-568.

9. Abdullah Z, T Saric, H Kashkar, N Baschuk, B Yazdanpanah, BK Fleischmann, J Hescheler, M Kronke and O Utermohlen. (2007). Serpin-6 expression protects embryonic stem cells from lysis by antigen-specific CTL. J Immunol 178:3390-3399.

10. Li L, ML Baroja, A Majumdar, K Chadwick, A Rouleau, L Gallacher, I Ferber, J Lebkowski, T Martin, J Madrenas and M Bhatia. (2004). Human embryonic stem cells possess immune-privileged properties. Stem Cells 22:448-456.

11. Min JY, Y Yang, MF Sullivan, Q Ke, KL Converso, Y Chen, JP Morgan and YF Xiao. (2003). Long-term improvement of cardiac function in rats after infarction by transplantation of embryonic stem cells. The Journal of thoracic and cardiovascular surgery 125:361-369.

12. Menard C, AA Hagege, O Agbulut, M Barro, MC Morichetti, C Brasselet, A Bel, E Messas, A Bissery, P Bruneval, M Desnos, M Puceat and P Menasche. (2005). Transplantation of cardiac-committed mouse embryonic stem cells to infarcted sheep myocardium: a preclinical study. Lancet 366:1005-1012.

13. Swijnenburg RJ, M Tanaka, H Vogel, J Baker, T Kofidis, F Gunawan, DR Lebl, AD Caffarelli, JL de Bruin, EV Fedoseyeva and RC Robbins. (2005). Embryonic stem cell immunogenicity increases upon differentiation after transplantation into ischemic myocardium. Circulation 112:l166-172.

14. Nussbaum J, E Minami, MA Laflamme, JA Virag, CB Ware, A Masino, V Muskheli, L Pabon, H Reinecke and CE Murry. (2007). Transplantation of undifferentiated murine embryonic stem cells in the heart: teratoma formation and immune response. Faseb J 21:1345-1357.

15. Bonnevie L, A Bel, L Sabbah, N Al Attar, P Pradeau, B Weill, F Le Deist, V Bellamy, S Peyrard, C Menard, M Desnos, P Bruneval, P Binder, AA Hagege, M Puceat and P Menasche. (2007). Is xeno-transplantation of embryonic stem cells a realistic option? Transplantation 83:333-335.

16. van der Bogt KE, RJ Swijnenburg, F Cao and JC Wu. (2006). Molecular imaging of human embryonic stem cells: keeping an eye on differentiation, tumorigenicity and immunogenicity. Cell cycle (Georgetown, Tex 5:2748-2752.

17. Cao F, S Lin, X Xie, P Ray, M Patel, X Zhang, M Drukker, SJ Dylla, AJ Connolly, X Chen, IL Weissman, SS Gambhir and JC Wu. (2006). In vivo visualization of embryonic stem cell survival, proliferation, and migration after cardiac delivery. Circulation 113:1005-1014.

18. Cao YA, MH Bachmann, A Beilhack, Y Yang, M Tanaka, RJ Swijnenburg, R Reeves, C Taylor-Edwards, S Schulz, TC Doyle, CG Fathman, RC Robbins, LA Herzenberg, RS Negrin and CH Contag. (2005). Molecular imaging using labeled donor tissues reveals patterns of engraftment, rejection, and survival in transplantation. Transplantation 80:134-139.

19. Xie X, F Cao, AY Sheikh, Z Li, AJ Connolly, X Pei, RK Li, RC Robbins and JC Wu. (2007). Genetic modification of embryonic stem cells with VEGF enhances cell survival and improves cardiac function. Cloning and stem cells 9:549-563.

20. Cao F, KE van der Bogt, A Sadrzadeh, X Xie, AY Sheikh, H Wang, AJ Connolly, RC Robbins and JC Wu. (2007). Spatial and temporal kinetics of teratoma formation from murine embryonic stem cell transplantation. Stem cells and development 16:883-891.

21. Magliocca JF, IK Held and JS Odorico. (2006). Undifferentiated murine embryonic stem cells cannot induce portal tolerance but may possess immune privilege secondary to reduced major histocompatibility complex antigen expression. Stem cells and development 15:707-717.

22. Koch CA, P Geraldes and JL Platt. (2007). Immunosuppression By Embryonic Stem Cells. Stem Cells.

23. Drukker M. (2004). Immunogenicity of human embryonic stem cells: can we achieve tolerance? Springer seminars in immunopathology 26:201-213.

Chapter 7

CHAPTER 8

Immunosuppressive Therapy Mitigates Immunological Rejection of Human Embryonic Stem Cell Xenografts

Rutger-Jan Swijnenburg, Sonja Schrepfer, Johannes A. Govaert, Feng Cao,
Katie Ransohoff, Ahmad Y. Sheikh, Munif Haddad, Andrew J. Connolly, Mark M. Davis,
Robert C. Robbins, Joseph C. Wu

ABSTRACT

Given their self-renewing and pluripotent capabilities, human embryonic stem cells (hESCs) are well-poised as a cellular source for tissue regeneration therapy. However, the host immune response against transplanted hESCs is not well characterized. In fact, controversy remains as to whether hESCs have immune-privileged properties. To address this issue, we used *in vivo* bioluminescent imaging to track the fate of transplanted hESCs stably transduced with a double fusion reporter gene consisting of firefly luciferase (fLuc) and enhanced green fluorescent protein (eGFP). We show that post-transplant survival is significantly limited in immunocompetent as opposed to immunodeficient mice. Repeated transplantation of hESCs into immunocompetent hosts results in accelerated hESC death, suggesting an adaptive donor-specific immune response. Our data demonstrate that transplanted hESCs trigger robust cellular and humoral immune responses, resulting in intra-graft infiltration of inflammatory cells and subsequent hESC rejection. Moreover, we have found CD4+ T-cells to be an important modulator of hESC immune-mediated rejection. Finally, we show that immunosuppressive drug regimens can mitigate the anti-hESC immune response and that a regimen of combined tacrolimus (TAC) and sirolimus (SIR) therapy significantly prolongs survival of hESCs for up to 28 days. Taken together, these data suggest that hESCs are immunogenic, trigger both cellular and humoral-mediated pathways and, as a result, are rapidly rejected in xenogeneic hosts. This process can be mitigated by a combined immunosuppressive regimen as assessed by novel molecular imaging approaches.

INTRODUCTION

Human embryonic stem cells (hESCs) have generated great interest given their pluripotency and capacity to self-renew. Specifically, hESCs can be cultured indefinitely *in vitro*, and can differentiate into virtually any cell type in the adult body [1]. Given the limited potential for regeneration of most adult tissues following injury and the prevalence of numerous chronic diseases involving cell death and dysfunction, hESCs are an attractive source for tissue regeneration and repair therapies. Successful *in vitro* differentiation of hESCs into multiple somatic cell types has been reported, including cardiomyocytes [2], hematopoietic cells [3], neurons [4], pancreatic islet cells [5] and hepatocytes [6]. Furthermore, there is a growing number of reports showing the therapeutic benefit of hESC derivatives following transplantation into animal models of disease [7,8]. Although such data are encouraging, significant hurdles remain before hESC-based treatments can be safely and successfully translated into clinical therapy [9].

An important obstacle facing *in vivo* engraftment and function of hESCs is the potential immunologic barrier [10]. hESCs express low levels of Class I Human Leukocyte Antigen (HLA), which moderately increases as these cells differentiate [11]. The presence of distinct major histocompatibility complex (MHC) antigens suggests that hESCs may elicit an immune response and be at risk for immune rejection when introduced *in vivo* across histocompatibility barriers [10]. At the same time, hESCs theoretically represent an immune-privileged cell population, as embryos consisting of 50% foreign paternal material are usually not rejected by the maternal host. Recent reports have indeed shown that both mouse embryonic stem cells (mESCs) and hESCs seem to have the capability to evade immune recognition in allogeneic as well as in xenogeneic hosts. mESCs have been shown to survive in immunocompetent mice [12], as well as in rats [13] and sheep [14] for many weeks after transplantation. Similarly, rat ESC-like cells were demonstrated to permanently engraft in allogeneic recipients leading to allospecific down-regulation of the host immune response [15]. In addition, not only have hESCs been reported to inhibit allogeneic T-cell proliferation *in vitro*, but also to evade immune recognition in xenogeneic immunocompetent mice [16].

Nevertheless, our group and others have found that following transplantation into allogeneic murine hearts, mESCs triggered progressive immune cell infiltration and were subsequently rejected [17,18]. Others have concluded that hESC grafts are infiltrated by inflammatory cells [19] and do not form teratomas in immunocompetent mice [20], suggesting rejection. Clearly, questions of whether hESCs have immune-privileged properties and whether immunological rejection of transplanted hESCs and hESC derivatives is something that must be addressed remains to be clarified [21].

In this study, we used novel, non-invasive molecular imaging techniques to longitudinally track hESC fate following transplantation. We present evidence of an adaptive donor-specific xenogeneic immune response that is launched against hESCs shortly after transplantation into immunocompetent mice, resulting in rejection. We further delineate the role of T-

lymphocyte subsets in mediation of the murine anti-hESC immune response. Finally, we compared the efficacy of various combinations of clinically available immunosuppressive regimens for enhancing survival of transplanted hESCs *in vivo*.

RESULTS

Characterization of hESCs expressing a double fusion (DF) reporter gene.

To date, most studies on hESC therapy have relied on conventional reporter gene technology such as green fluorescent protein (GFP) [16] and β-galactosidase (LacZ) [22] to monitor cell survival and behavior following transplantation. These reporter genes are typically identified by immunohistochemical staining techniques, which provide only a "snapshot" representation rather than a comprehensive picture of cell survival over time [23]. Such limited techniques may, in part, contribute to the conflicting observations of hESC survival in xenogeneic hosts. Results from previous studies range from no signs of rejection [16] to complete rejection of hESCs [20] following transplantation into mice. To circumvent these issues, a double fusion (DF) reporter gene construct carrying firefly luciferase (fLuc) and enhanced green fluorescent
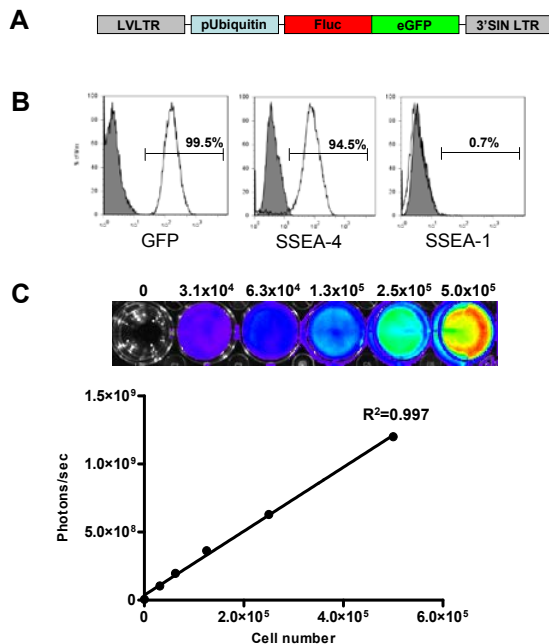

Figure 1. Characterization of the double fusion (DF) firefly luciferase (fLuc) and enhanced green fluorescent protein (eGFP) transduced hESCs. (a) Schema of the DF reporter gene containing fLuc and eGFP driven by a human ubiquitin promoter. **(b)** Flow cytometric analysis of H9[DF] hESCs shows robust expression of eGFP. Transduced hESCs are largely positive for SSEA-4, and negative for SSEA-1, confirming their pluripotent state. **(c)** Stably transduced hESCs show robust correlation between cell number and reporter gene activity. BLI of a 24-well plate containing increasing numbers of H9[DF] hESCs are shown above the corresponding graph depicting correlation between cell number and fLuc activity.

protein (eGFP) driven by a constitutive human ubiquitin promoter (pUB) was successfully transduced into undifferentiated hESCs (H9 line), using a self-inactivating (SIN) lentiviral vector (Fig 1A). This enabled us to track the hESCs *in vivo* by bioluminescent imaging (fLuc) as well as *ex vivo* by immunohistochemistry (eGFP). After 2 to 3 passages of feeder-free culture in mTersh culture medium, FACS analysis of H9^{DF} hESCs revealed robust expression of eGFP concomitant with expression of pluripotent hESC markers (SSEA-4$^+$ and SSEA-1$^-$) (Fig 1B). The cells exhibited a robust correlation between fLuc expression and hESC number (r^2=0.99, Fig 1C). *In vitro* analysis showed that H9^{DF} hESCs were able to proliferate and differentiate into cells of all three germ layers at a frequency similar to control H9 hESCs (data not shown).

The major system of alloantigens responsible for cell incompatibility is the major histocompatibility complex (MHC) [24]. In agreement with previous reports [11, 25], we found low expression levels of both MHC-I and β_2-microglobulin proteins and no expression of MHC-II on both H1 and H9 hESCs, as compared to a positive control (human lymphocytes). Importantly, these profiles were not altered by the introduction of our reporter genes (SI Fig. 6A). Also, lentiviral transduction did not result increased autocrine secretion of interferon (IFN)-γ, a cytokine known to induce MHC expression [11] (SI Fig 6B and C).

Monitoring of transplanted hESCs in immunocompetent and immunodeficient mice.

We investigated longitudinal hESC survival following intramuscular (gastrocnemius muscle) transplantation of 1x10^6 H9^{DF} hESCs into immunodeficient (NOD/SCID, n=5) versus two strains of immunocompetent mice (BALB/c and C57Bl/6a, n=5 per group) by *in vivo* bioluminescent imaging (BLI). hESC survival was significantly limited in immunocompetent animals as compared to NOD/SCID mice. (Day 5 BLI signal: NOD/SCID 7.37±0.3; BALB/c 5.91±0.47; C57BL/6a 6.1±0.19 Log$^{[photons/sec]}$; *P*<0.05 immunodeficient vs. immunocompetent). BLI signal completely disappeared in immunocompetent animals between 7 and 10 days post-transplant (Fig 2A and 2B). Repeated transplantation of H9^{DF} hESCs in the contralateral gastocnemius muscle at two weeks following primary injection resulted in accelerated hESC death in immunocompetent animals, with BLI signal reaching background levels by post-transplant day 3 (NOD/SCID 7.95±0.29; BALB/c 4.97±0.10; C57Bl/6a 4.97±0.19 Log$^{[photons/sec]}$; *P*<0.001 immunodeficient vs. immunocompetent), suggesting an adaptive, donor-specific immune response (Fig 2A and 2C). Post-transplant hESC death in immunocompetent mice was confirmed in a control experiment, in which 1x10^6 H1 hESC were transplanted into an additional group of BALB/c animals (n=5). Consistent with BLI data, histological evaluation of the graft site at 10 days following hESC injection revealed no evidence of hESC survival (SI Fig 7A). By contrast, H9^{DF} hESC survived well in NOD/SCID animals with progressively increasing BLI signal intensity starting at post-transplant day 10, suggesting hESC proliferation (Fig 2B). At 42 days following primary transplantation, intramuscular teratomas were found in transplanted NOD/SCID animals (SI Fig 7B), whereas neither teratomas nor persistent hESCs were seen in immunocompetent animals (data not shown).
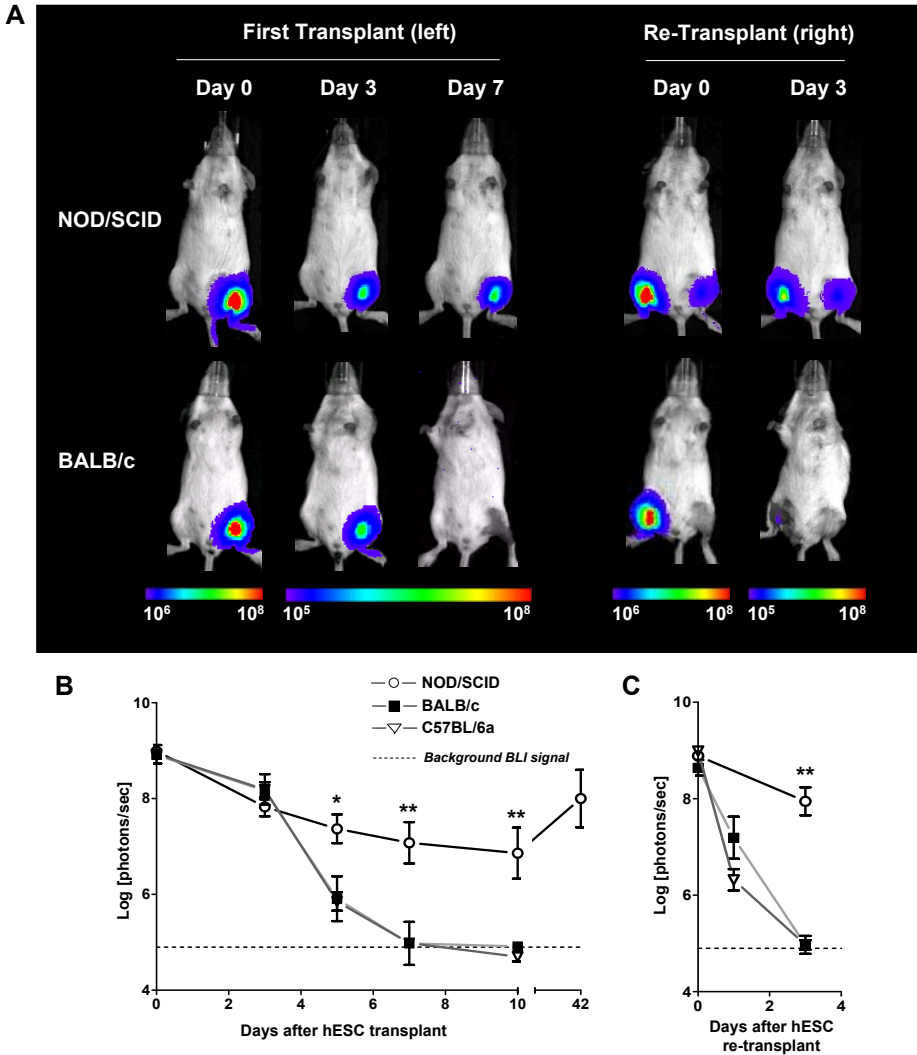
Figure 2. *In vivo* visualization of hESC survival. (a) Representative BLI images of H9^{DF} hESC transplanted animals show a rapid decrease in BLI signal in immunocompetent animals (BALB/c), as opposed to immunodeficient (NOD/SCID) mice, reaching background levels at post-transplant day 7. Accelerated BLI signal loss in BALB/c animals was seen following repeated hESC transplantation into the contralateral gastrocnemius muscle. Color scale bar values are in photons/s/cm^2/sr. Graphical representation of longitudinal BLI after **(b)** primary and **(c)** secondary hESC transplantation into immunodeficient (NOD/SCID, n=5) and two immunocompetent (BALB/c and C57Bl/6a, n=5 per group) mouse strains. Note that in NOD/SCID animals, starting at post-transplant day 10, BLI intensity increases progressively, suggesting hESC proliferation. *$P<0.05$, **$P<0.01$

To exclude the possibility that the adaptive immune reaction was launched against xeno-antigens produced by the reporter genes introduced into the cells, rather than against hESC xenoantigens, we next transplanted 1x10^6 non-transduced H9 hESCs into a second group of BALB/c mice (n=3), followed by re-transplantation of 1x10^6 H9^{DF} hESCs into the contralateral

leg at two weeks following primary injection. BLI following re-transplantation showed a similar loss of signal as compared to animals that were primarily stimulated with H9^{DF} hESCs (SI Fig. 8A and B), indicating that the adaptive immune response was in fact directed towards the hESCs.

In order to determine whether hESC differentiation would influence their capacity to escape immunological rejection, we next injected 1x10^6 H9^{DF} hESC-derivatives following spontaneous *in vitro* differentiation during 14 days prior to transplantation into BALB/c mice (n=5). Overall, our results did not show a significant difference in their survival compared to undifferentiated hESC (SI Fig 8C)

Transplantation of hESCs triggers severe graft infiltration by a variety of immune cells.

Five days following transplantation of either 1x10^6 H9^{DF} or H1 hESCs (n=6) or PBS (n=3) as a control, gastrocnemius muscles of BALB/c animals were analyzed for graft infiltrating cells. Histological analysis demonstrated severe intra-muscular infiltration of inflammatory cells (Fig 3A and B). Immunofluorescent staining showed that a large percentage of infiltrating cells stained positive for the T-lymphocyte surface marker CD3 (Fig 3C and D). Quantification and further characterization of graft infiltrating cells was carried out by enzymatic digestion of the explanted muscles followed by FACS analysis. Comparison of the control PBS to the hESC injected muscles confirmed that both H9^{DF} and H1 hESC transplantation elicited severe infiltration of various types of immune cells involved in both adaptive and innate types of immunity (Fig 3E). Interestingly, both CD3$^+$ T-cells (H9^{DF}: 4.5±0.3%; H1: 4.3±0.5% vs. PBS control: 0.5±0.1%, *P*<0.01) and B220$^+$ B-cells (H9^{DF}: 3.4±0.5%; H1: 4.9±0.7% vs. PBS control: 1.0±0.1%, *P*<0.01) were present at a high frequency, suggesting a prominent role for adaptive immunity in hESC rejection. Furthermore, CD4$^+$ T-cells, CD8$^+$ T-cells and Mac-1$^+$Gr-1$^+$ neutrophils, and Mac-1$^+$Gr-1$^-$ macrophages (the latter only in the H1 group) infiltrated into the hESC graft at a significantly higher frequency as compared to PBS controls (Fig 3E).

hESC transplantation triggers systemic cellular and humoral murine immune responses.

To investigate the cellular immune response, we next performed ELISPOT assays using splenocytes of both H9^{DF} and H1 hESC recipient animals. Cytokine release was abundant in these animals. At 5 days following transplantation, splenocytes from hESC recipients secreted significant amounts of both IFN-γ and Interleukin-4 (IL-4), compared to wild type animals (H9^{DF}: IFN-γ: 488±91, IL-4:529±57; H1: IFN-γ: 495±106, IL-4: 563±87 vs. WT group: IFN-γ: 0.5±0.3, IL-4: 8.5±2, *P*<0.001) (Fig 4A). IFN-γ is produced by T-helper (Th)-1 cells and induces cellular immune activity, whereas IL-4 produced by Th-2 cells activates humoral immune pathways. Thus, our data suggests the involvement of an antibody-mediated B-cell response. Indeed, FACS analysis showed a significantly higher presence of circulating xeno-reactive antibodies
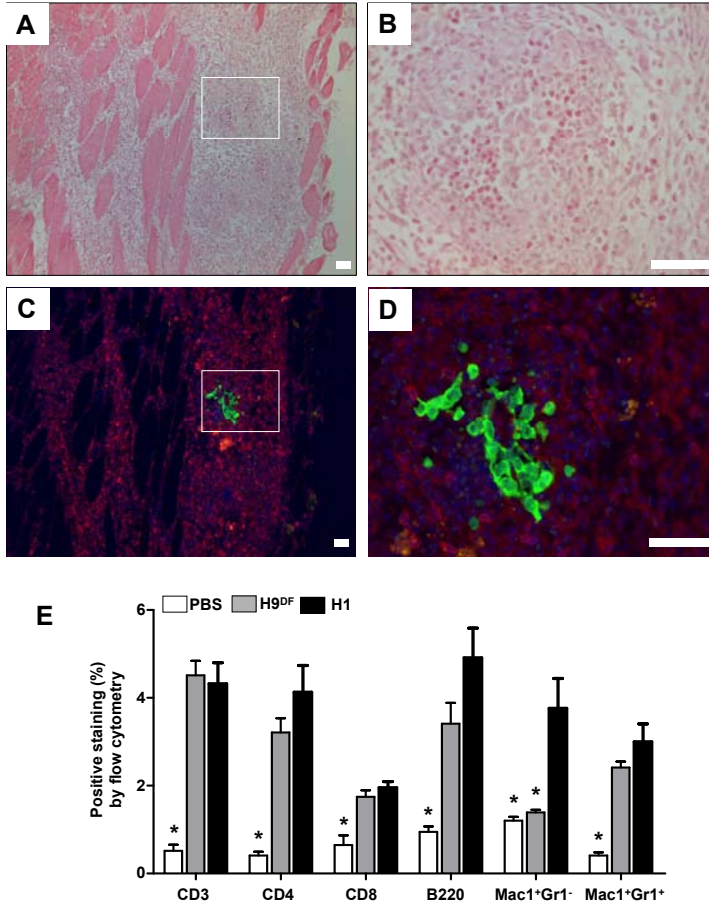
Figure 3. Robust inflammatory cell infiltration following intramuscular hESC transplantation. Histopathological evaluation by H&E staining of muscle sections of BALB/c animals, obtained at 5 days following H9^{DF} hESC transplantation, demonstrates robust intramuscular inflammatory cell infiltration at **(a)** low power and **(b)** high power view. **(c and d)** Immunofluorescent staining on corresponding sections reveals abundant presence of CD3$^+$ T-cells (red) surrounding eGFP$^+$ hESCs (green). Counterstaining was performed with 4,6-diamidino-2-phenylindole (DAPI, blue). Scale bars: 50µm. **(e)** FACS analysis of enzymatically digested muscles revealed intra- H9^{DF} and H1 hESC graft infiltration of CD3$^+$ T-cells, CD4$^+$ T-helper cells, CD8$^+$ Cytotoxic T-cells, B220$^+$ B-cells, and Mac-1$^+$Gr-1$^+$ neutrophils at significantly higher intensities, compared to PBS injections. Mac-1$^+$Gr-1$^+$ (macrophages) cells were had a significantly higher presence only in the H1 group. *P<0.05

in hESC recipient sera, as compared to wild type animals (mean fluorescent intensity (MFI): H9^{DF}: 7.0±1.2; H1: 6.8±1.5 vs. WT group: 3.8±0.6, P<0.05) (Fig 4B).

Prominent role for CD4$^+$ T-cells in mouse anti-hESC rejection.

The phylogenetic disparity between mice and humans may lead to a lower affinity of mouse T-cell receptors (TCR) for human MHC molecules [26]. Therefore, the indirect pathway of immune recognition, whereby the recipient's antigen presenting cells (APC) process and present xenoantigens to recipient CD4$^+$ T cells, plays a major role in discordant cellular xenorejection [26].
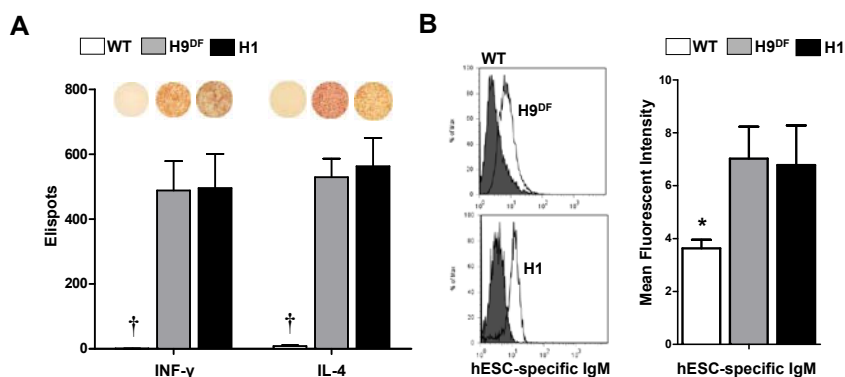
Figure 4. hESC transplantation triggers cellular and humoral murine immune responses. (a) ELISPOT assay revealed significantly higher production of both INF-γ and IL-4 by both H1 and H9^{DF} hESC recipient BALB/c splenocytes (n=6), compared to wild type (WT) animals (n=3). Representative images of ELISPOT wells are shown above the corresponding bars. †$P<0.001$ **(b)** Representative flow cytometry histograms (left panels) and graphical representation of hESC-specific xeno-reactive IgM antibodies detected at significantly higher rate in H1 and H9^{DF} hESC recipient BALB/c sera (n=6), as compared to WT animals (n=3). *$P<0.05$

For these reasons, combined with the fact that hESCs lack expression of MHC-II antigens (Fig 1D) necessary for direct xenograft recognition by recipient CD4$^+$ T cells, we hypothesized that *indirect* immune recognition by CD4$^+$ T cells could play an important role in mouse anti-hESC rejection. To further delineate the role of T-cell subsets in hESC rejection, we transplanted 1x10^6 H9^{DF} hESCs into T-cell deficient BALB/c Nude, CD4$^+$ T-cell knockout (CD4-KO), and CD8$^+$ T-cell knockout (CD8-KO) animals (n=4 or 5 per group) and followed cell survival by BLI. In agreement with prior data [20], hESCs survived in Nude mice over the 42 day study course (Fig 5 A and B), and were able to form teratomas. Interestingly, hESCs survived significantly longer in CD4-KO compared to CD8-KO animals (BLI signal at post-transplant day 5: CD4-KO: 6.5±0.6 vs. CD8-KO: 5.0±0.3 Log$^{[photons/sec]}$; $P<0.05$). However in both groups, hESC xenografts were eventually rejected (SI Fig 9 A and B).

Immunosuppressive therapy prolongs survival of hESCs following transplantation.

Since post-transplant hESC death appears largely due to T-cell mediated donor-specific immune response, we next investigated the efficacy of single and combined immunosuppressive drug regimens for preventing post-transplant hESC rejection. Clinically available immunosuppressants were chosen based on different mechanism of action: (1) calcineurin inhibitors (tacrolimus = TAC), (2) target of rapamycin (TOR) inhibitors (sirolimus = SIR), and

SI Table 1. Immunosuppressive treatment dosages and serum drug through levels. TAC = Tacrolimus, SIR = Sirolimus, MMF = mycophenolate mofetil (n=5 per group).

	Dosage (mg/kg/d)	Trough levels±SEM (ng/ml)	Target values (ng/ml)
TAC	4	11.4±3.6	10 – 15
SIR	3	11.6±3.8	10 – 15
MMF	30	3.8±1.2	3.5 – 5.5

Chapter 8

A Days after hESC transplant

B Days after hESC transplant
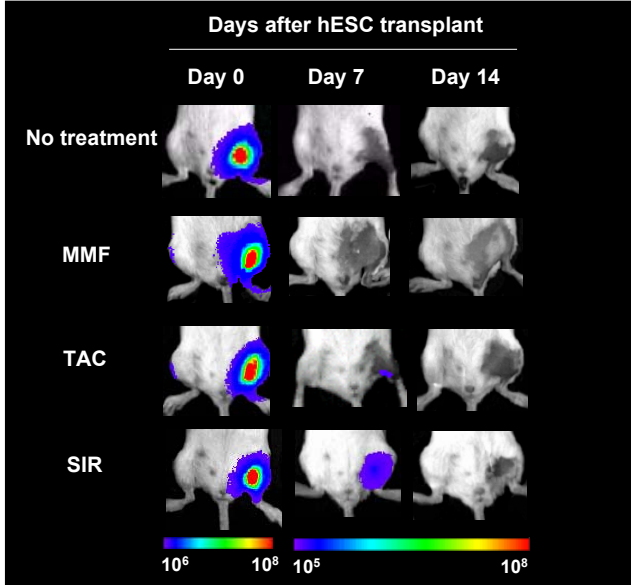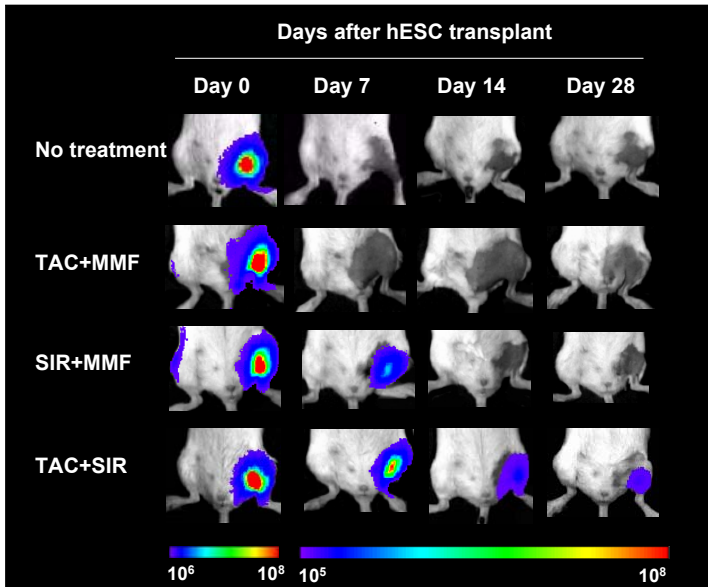
(3) anti-proliferatives (mycophenolate mofetil = MMF) [27]. A group of BALB/c mice (n=30) were randomized to receive daily TAC, SIR, MMF, TAC+MMF, SIR+MMF or TAC+SIR (n=5 per group) treatment following transplantation of 1×10^6 H9[DF] hESCs into the gastrocnemius muscle. The therapeutic dose range was confirmed by serum drug trough level measurements (SI Table 1).

As monotherapy, SIR extended hESC survival to the greatest degree. Significantly higher BLI signals from the SIR treated animals were seen up to 7 days after transplantation, as

C

D

E

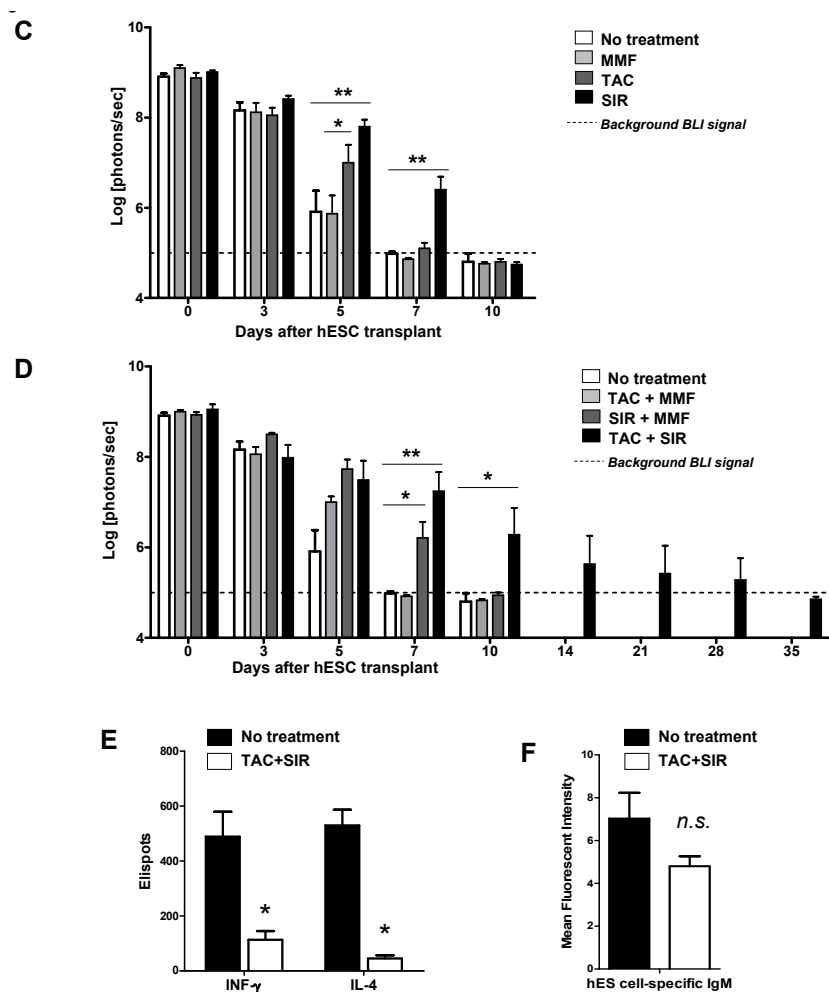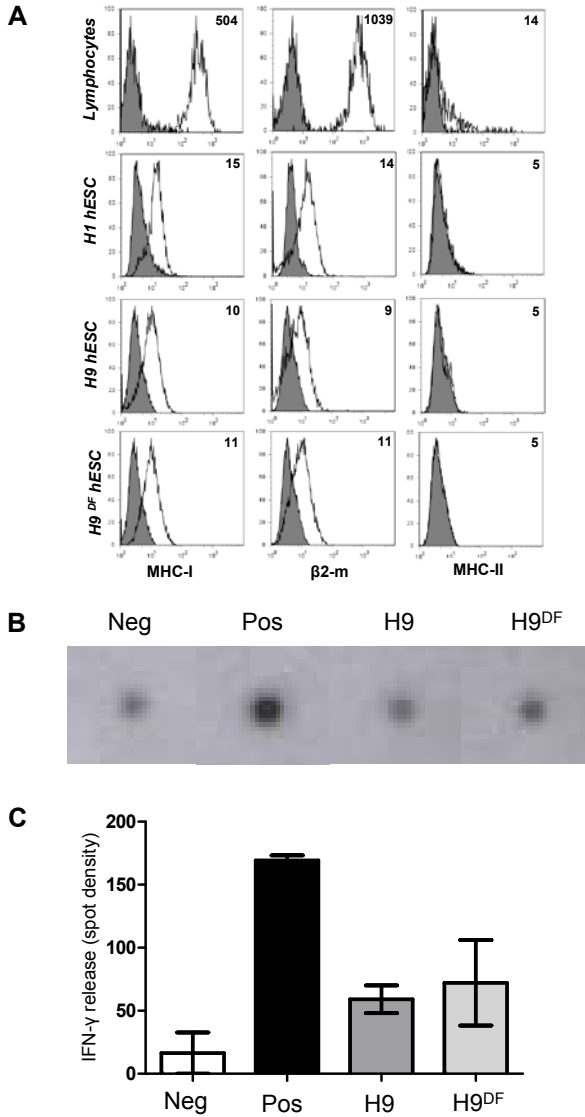**F**

Figure 5. Immunosuppressive drug treatment prolongs survival of transplanted hESCs and mitigates adaptive immune response. Representative BLI images of H9^{DF} hESCs transplanted mice receiving no treatment compared to those receiving **(a)** immunosuppressive monotherapy (MMF, TAC or SIR) or **(b)** combined therapy (TAC+MMF, SIR+MMF, TAC+SIR). Although SIR as monotherapy extended hESC survival significantly, TAC+SIR combination therapy proved to be optimal and extended survival of the cells up to post-transplant day 28. Color scale bar values are in photons/s/cm^2/sr. Graphical representation of **(c)** single or **(d)** combined drug treatment efficacy on post-transplant hESC survival (n=5 per group). *P<0.05, **P<0.01. Combined TAC+SIR treatment effectively suppressed **(e)** INF-γ and IL-4 production by hESC recipient splenocytes (**P<0.01) and **(f)** reduced production of donor-specific xeno-reactive antibodies (P=0.14; *n.s.* = not significant).

compared to the no treatment (NT) group (BLI signal at day 7: SIR: 6.4±0.29 vs. NT: 4.98±0.04 Log$^{[photons/sec]}$; P<0.05). However, the signal in all single drug treatment groups (TAC, SIR, MMF) had decreased to background levels by post-transplant day 10 (Fig 5A and C), emphasizing the strong anti-hESC immune response despite high dose immunosuppressive treatment. In our model, addition of MMF did not result in significant improvement of hESC survival over single TAC and/or SIR treatment (Fig 5B and D). Combined TAC+SIR treatment, however,

Chapter 8

A

Lymphocytes: MHC-I 504, β2-m 1039, MHC-II 14

H1 hESC: MHC-I 15, β2-m 14, MHC-II 5

H9 hESC: MHC-I 10, β2-m 9, MHC-II 5

H9^{DF} hESC: MHC-I 11, β2-m 11, MHC-II 5

MHC-I   β2-m   MHC-II

B

Neg   Pos   H9   H9^{DF}

C

IFN-γ release (spot density)

Neg   Pos   H9   H9^{DF}

SI Figure 6. Immunological characterization of H9^{DF} hESCs compared to non-transduced controls. (a) Compared to human lymphocytes as a positive control, both H1 and H9 hESCs as well as transduced H9^{DF} hESCs express low amounts of MHC-I and β2-microglobulin, and remain negative for MHC-II. Mean fluorescent intensity (MFI) is shown in the upper right corner of each panel. Results are representative of three independent experiments. **(b)** Representative images and **(c)** graphical representation of the cytokine antibody array show no difference in IFN-γ secretion by H9 or H9^{DF} hESC. (neg = negative control, hESC medium; pos = positive control, medium containing recombinant human IFN-γ at 25 ng/ml)

markedly improved survival of hESCs. BLI signals from the TAC+SIR treated animals were significantly higher starting at 7 days following transplantation and could be followed out to post-transplant day 28 (Fig 5B and D). Finally, the efficacy of combined TAC+SIR treatment
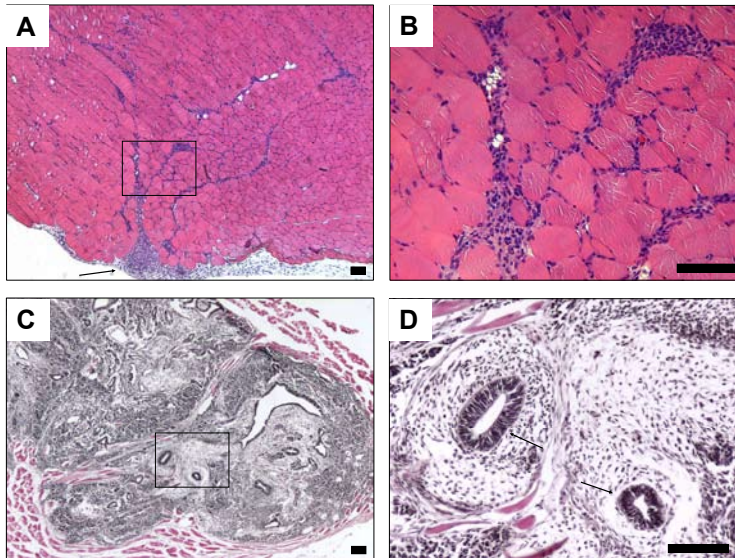
SI Figure 7. Histopathological evaluation of hESC survival. (a) Tissue sections of BALB/c recipient muscles show endomysial mixed inflammatory infiltrated, sometimes involving the perimysium and adjacent soft tissue, representing the injection track (black arrow). **(b)** On higher magnication, infiltrates consisting of mixed mononuclear and granulocyte infiltrates can be observed. No hESCs or cells with morphology that would suggest anything other then inflammatory could be detected. **(c)** Explanted muscles of NOD/SCID animals at 42 days after transplantation demonstrates formation of intramuscular hESC-derived teratomas, composed out of tissue representing the three germ layers. **(d)** On higher magnification endodermal derivatived glandular epithelium (black arrows) surrounded by mesodermal derived mesenchyme can be detected. Scale bars: 50μm.

for effective suppression of the recipient anti-hESC immune response was confirmed by *in vitro* analysis. ELISPOT assay showed a significant inhibition of effector cytokine production (TAC+SIR: INF-γ: 113±32; IL-4: 45±12 vs. NT: INF-γ: 488±91, IL-4: 529±57, *P*<0.01) (Fig 5E) and FACS analysis revealed a strong trend in reduction of circulating xeno-reactive antibodies (TAC+SIR: 4.8±0.5 vs. NT: 7.0±1.2, *P*=0.14) (Fig 5F).

DISCUSSION

The field of hESC-based therapy is advancing rapidly. Although federal regulations still restrict the generation of new hESC lines in the United States, regional funding institutions such as the California Institute of Regenerative Medicine foresee hESC-based therapies to go into phase I clinical trails within the next 10 years [28]. To accomplish such goals, several significant hurdles that preclude clinical translation of such therapy need to be overcome, of which hESC immunogenicity is a major concern [29].

This study was designed to characterize hESC immunogenicity in a human-to-mouse trans-plantation model, and to evaluate the efficacy of different immunosuppressive drug regimens

Chapter 8
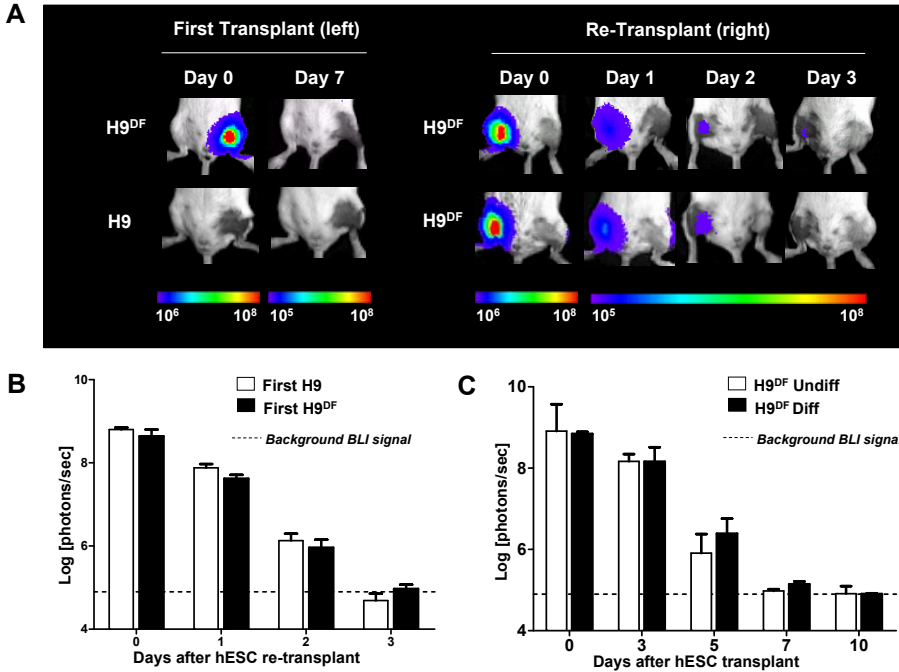
SI figure 8. Similar hESC death after re-transplantation following primary stimulation with either transduced hESCs or non-transduced hESCs. (a) Representative BLI images (color scale bar values are in photons/s/cm²/sr) and **(b)** graphical representation shows a similar trend in BLI signal loss in the 3 days following secondary transplantation of H9DF hESCs in BALB/c animals, after primary stimulation with either non-transduced H9 hESCs (n=3) or transduced hESCs (n=6) two weeks earlier. **(c)** Graphical representation of BLI signals comparing survival of undifferentiated H9DF hESC (H9DF undiff) versus 14 day differentiated H9DF hESC (H9DF diff) following transplantation. No significant difference in cell survival was found.

to improve transplanted hESC survival. Specifically, we have demonstrated that: (1) molecular imaging can be used to quantify hESC survival and non-invasively follow donor cell fate; (2) hESCs can trigger potent cellular and humoral immune responses following transplantation into immunocompetent mice, resulting in intra-graft infiltration of a variety of inflammatory cells, leading to rejection; (3) CD4+ T-lymphocytes play an important role in mouse anti-hESC rejection; and (4) an immunosuppressive drug regimen consisting of tacrolimus (TAC) and sirolimus (SIR) significantly mitigates the host immune response to prolong hESC survival.

Specific studies evaluating immunogenicity of hESCs *in vivo* are few and have yielded mixed conclusions regarding hESC's potential to induce immune response and/or survive in xenogeneic hosts [16, 20, 21]. In these studies, results were based on histological techniques to evaluate hESC survival and potential immunological rejection. Histological analysis is susceptible to sampling error, as each tissue section represents only one layer of the hESC graft and surrounding tissue at one time-point. To address these shortcomings, our group has been developing and validating reporter gene-based molecular imaging techniques. In particular, fLuc-based optical bioluminescent imaging has proven to be a reliable technique for assess-
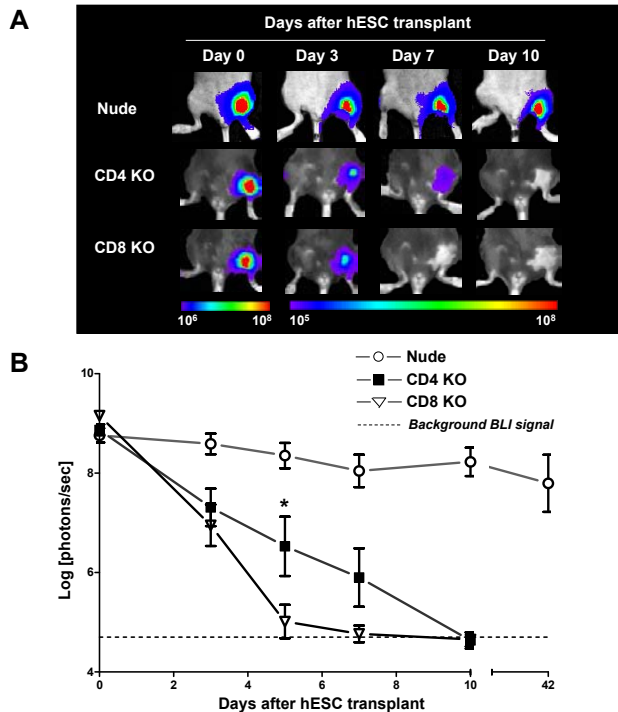
SI Figure 9. Role of T-cell subsets in mouse anti-hESC immune rejection. (a) Representative BLI images of H9[DF] hESCs transplanted into different immunodeficient mouse strains show survival of the donor cells in Nude mice up to 42 days following transplantation, suggesting an important role for T-cells in mouse anti-hESC rejection. Although hESCs are eventually rejected in both CD4 knockout (CD4-KO) and CD8 knockout (CD8-KO) mice, there is significantly longer survival of hESC in CD4-KO animals. Color scale bar values are in photons/s/cm²/sr. (b) Graphical representation of BLI of hESC survival in the three groups (n=4 or 5 per group). *$P < 0.05$

ing engraftment and survival of stem cells following transplantation *in vivo* [30]. An important advantage in using bioluminescent imaging to track cell transplantation is that the expression of the fLuc reporter gene, which is integrated into the DNA of the transplanted cells, is expressed only by living cells, making it a highly accurate tool for following cell graft rejection in the living subject [31]. Using this approach in this report, we have clearly showed impaired survival of hESCs in immunocompetent versus immunodeficient mice, a phenomenon which was even more pronounced after repeated transplantation of the hESCs.

Xenotransplantation of cells or organs is usually complicated by severe immunological responses [26]. Previous studies have addressed murine xenogeneic immune responses to adult human cells or tissues following transplantation. For example, human-to-mouse pancreatic islet transplants trigger progressive infiltration of lymphocytes leading to rejection within 5-6 days [32]. Human skin transplants are rejected by immunocompetent mice within 10 days, and a delay of rejection is seen when skin is transplanted onto mice lacking CD4+ T-cells, but not on those lacking CD8+ T cells [33]. A comparison of these data to the results of our study,

in which we show a similar time course of rejection of hESCs (7-10 days) that seems largely mediated by CD4+ T cells, suggests that hESCs are recognized by the murine immune system in a comparable way as adult human cells. This leads us to conclude that, in a discordant xenotransplant model, hESCs *do not* retain immune-privileged and/or immunosuppressive properties. During the first 10 days after transplantation, spontaneous non-immune related hESC death also occured in immunodeficient mice (Figure 2). In immunocompetent mice, spontaneous hESC death could have lead to activation of the adaptive immune system through the indirect pathway, in which intracellular antigens shed by hESC debris are phago-cytosed by host APCs and presented to CD4+ T lymphocytes. This would explain the major role of CD4+ cells that we found in our study.

Studies addressing the character and intensity of immune responses towards hESCs in a human allogeneic setting *in vivo* raises ethical considerations and thus are currently not feasible. However, the results of this study emphasize that solutions which can reduce or eliminate potential immune responses need to be evaluated. Strategies that could prevent hESC immune recognition include: (1) forming MHC isotyped hES cell-line banks; (2) creat-ing a universal donor cell by genetic modification; (3) inducing tolerance by hematopoietic chimerism; (4) generating isogeneic hESC lines by somatic nuclear transfer; (5) and/or using immunosuppressive medication [34, 35]. In the near future, successful clinical application of hESC-based transplantation will most likely rely on immunosuppressive therapy based in part on the experience learned from organ transplantation. Thus, the significance of evaluating the effects of immunosuppressive drugs upon hESC survival in our animal model is two-fold: (1) to investigate the efficacy of various compounds that may be used in conjunction with clinical hESC-based therapies in the future, and (2) to develop an immunosuppressive drug regimen that optimizes transplanted hESC survival in animal models. Our results show that, in a xenogeneic murine setting, a combined immunosuppressive drug regimen consisting of TAC and SIR optimally suppressed anti-hESC immune response and prolonged their survival to 28 days following transplantation. TAC and SIR are a potential combination for an im-munosuppressive strategy because of their different side mechanisms of action, side-effect profiles, and apparent synergism when used together[36]. TAC and SIR are structurally similar macrolide immunosuppressants. Both drugs bind to a common family of immunophilins called FK506 binding proteins (FKBPs). SIR binds to FKBP, thereby blocking signal transduc-tion by inhibiting two kinases late in the G_1 cell cycle progression. These kinases have been designated TOR-1 and -2, targets of Rapamycin. TAC exerts its effect through the inhibition of calcineurin, by the FK506/FKBP complex. Calcineurin plays a critical role in interleukin-2 promoter induction after T-cell activation[27]. Although this combination is used with caution in clinical transplantation because of potential adverse drug effects, we recommend apply-ing this treatment protocol to studies in pre-clinical animal models that address the biology and therapeutic efficacy of hESC-derivatives.

In summary, our data show that hESC xenografts are effectively recognized and rejected by the adaptive murine immune system following transplantation. We also show that standard immunosuppressive drugs have the potency to prolong survival of the transplanted cells but cannot completely prevent rejection. Finally, the integration of molecular imaging techniques for development and validation of different strategies to improve post-transplant survival of hESC-derivatives should accelerate progress in this field.

METHODS

Lentiviral production and generation of stable hESC line.

SIN lentivirus (LV) was prepared by transient transfection of 293T cells [37]. H9 hESCs (Wicell) were transduced with LV-pUB-fLuc-eGFP double fusion (DF) reporter gene at a multiplicity of infection (MOI) of 10. The infectivity was determined by eGFP expression as analyzed on FACScan (BD Bioscience, San Jose, CA). The eGFP positive cell populations (~20%) were isolated by fluorescence activated cell sorting (FACS) Vantage SE cell sorter (Becton Dickinson Immunocytometry Systems) followed by plating on the feeder layer cells for culturing.
Culture and transplantation of hESCs.

H1, H9 and H9^{DF} hESCs were initially maintained on top of murine embryonic fibroblasts feeder (MEF) layers as detailed in *SI Methods*. To prevent contamination of the transplanted hESC population with MEF, hESC colonies were separated from MEF by incubation with dispase (Invitrogen) and subcultured on feeder-free matrigel (hESC qualified, BD Biosciences) coated 6-well plates in mTeSR™1 maintenance medium (Stem Cell Technologies) for 2 to 5 passages. MHC expression on hESCs was evaluated by flow cytometry as detailed in *SI Methods*. Shortly prior to transplantation, hESCs were trypsinated, and resuspended in sterile PBS at 1×10^6 cells per 20μl. hESC viability was >95% as determined by flow cytometry using 7-amino-actinomycin D (7-AAD) cell viability solution (eBioscience). hESC transplantation was performed by direct injection into gastrocnemius muscles of recipient mice (using a 29.5 gauge insulin syringe.

Animal experiments.

All animal procedures were approved by the Animal Care and Use Committee of Stanford University. Mouse stains are detailed in *SI Methods*.

Optical bioluminescent imaging of hESC transplanted animals.

BLI was performed using the Xenogen In Vivo Imaging System as previously described [38]. Briefly, mice were anesthetized with isoflurane and D-luciferin was administered intraperitoneally at a dose of 375 mg/kg body weight. At the time of imaging, animals were placed in a light-tight chamber, and photons emitted from luciferase expressing hESCs transplanted into

Chapter 8

the animals were collected with integration times of 5 sec - 5 min, depending on the intensity of the bioluminescence emission. The same mice were scanned repetitively as per the study design. BLI signal was quantified in units of photons per second (Total flux) and presented as Log$^{[photons/sec]}$.

Quantification of graft infiltrating cells.

Intra-hESC graft infiltrating cells were measured by FACS analysis of enzymatically digested gastrocnemius muscles as detailed in *SI Methods*.

Quantification of cellular immune response.

During animal sacrifice on day 5, the spleens were harvested and splenocytes were isolated. Enzyme-linked immunosorbent spot (ELISPOT) assays using 1×10^5 γ-irradiated hESCs (1500 RAD) as stimulator cells and 1×10^6 recipient splenocytes as responder cells were performed according to the manufacturer's protocol (BD Bioscience) using IFN-γ and IL-4-coated plates. Spots were automatically enumerated using an ELISPOT plate reader (CTL) for scanning and analyzing.

Quantification of humoral immune response.

Donor-specific xenoreactive antibodies were detected by FACS analysis of target hESCs following incubation with recipient mouse serum as detailed in *SI Methods.*
Immunosuppressive therapy.
   Tacrolimus (TAC, 4 mg/kg/d; Sigma-Aldrich), sirolimus (SIR, 3 mg/kg/d; Rapamune oral solution; Sigma-Aldrich) and mycophenolat mofetil (MMF, 30 mg/kg/d; Roche) were administered once daily as detailed in *SI Methods*.

Statistical analysis.

Data are presented as mean ± SEM. Comparisons between groups were done by independent sample t-tests or analysis of variance (ANOVA) with LSD post hoc tests, where appropriate. Differences were considered significant for *P*-values<0.05. Statistical analysis was performed using SPSS statistical software for Windows (SPSS).

SI METHODS

Culture and transplantation of hESCs.

H1, H9 and H9^{DF} hESCs were initially maintained on top of murine embryonic fibroblasts feeder (MEF) layers seeded onto 0.1% gelatin coated plastic dishes and inactivated by γ-irradiation (6000 RAD). hESCs were maintained in hESC medium containing 80% Dulbecco's modified Eagle's medium/F12 (DMEM/F12, Invitrogen), 1 mM L-glutamine, 0.1 mM β-mercaptoethanol,

0.1 mM non-essential amino acids (Invitrogen), 20% Knockout Serum Replacement (Invitrogen) and 8 ng/ml human basic fibroblast growth factor (bFGF; Invitrogen) [39]. MEF were derived from CF-1 E12.5 embryos as previously described[1]. The hESC culture medium was changed daily and hESCs were passaged every 4-5 days. hESC differentiation was induced by embryoid body (EB) formation. hESC colonies were dispersed into cell aggregates using 1mg/ml Collagenase IV. These aggregates were then cultured in suspension in ultra-low attachment plates (Corning) in hESC differentiation medium, consisting of DMEM high glucose supplemented with 20% FBS (Hyclone), 1 mM L-glutamine, 0.1 mM β-mercaptoethanol and 0.1 mM non-essential amino acids for 7 days. Then, EBs were transferred to 10 cm culture dishes coated with 0.1% gelatin and cultured for an additional 7 days. hESC differentiation medium was changed every two days.

FACS analysis of hESC surface marker expression.

H1, H9 and H9^{DF} hESCs were trypsinated, washed and incubated with PE-conjugated mouse anti-human HLA-ABC (G46-2.6), β_2-microglobulin (Tü99), HLA-DR, DP, DQ (Tü39) or their respective isotype control antibodies (all BD Biosciences) in FACS buffer (PBS 2% FCS) for 45 min at 4°C. Cells were washed, incubated with 7-amino-actinomycin D (7-AAD) cell viability solution (eBiosciences), and analyzed on a FACSCalibur system (BD Biosciences). For analysis of pluripotency markers, a similar protocol was followed, using PE-conjugated anti-human SSEA-1 (MC-480) and purified anti-human SSEA-4 (MC-813-70) antibodies (R&D Systems). The latter followed by incubation with PE-conjugated anti-IgG secondary antibody (eBioscience) for 30 min at 4°C.

Quantification of IFN-γ secretion by hESC.

Cytokine Antibody Array (Raybiotech) were used to identify the H9 and H9^{DF} hESC secretion profiles of IFN-γ. Membranes were covered with 24-hour supernatant of H9 hESC, H9^{DF} hESC, medium alone as well as medium containing 25 ng/ml recombinant IFN-γ (Peprotech) as positive control. Membranes were developed according to the manufacturer's protocol. Integrated densities were calculated using National Institutes of Health imageJ 1.38. Values were normalized to the integrated positive control on each membrane.

Animal experiments.

Six- to ten-week-old female BALB/c (wild type), C57BL/6J-Tyr^{c-2J}/J (C57Bl/6 albino or C67Bl/6a), NOD.CB17-$Prkdc^{scid}$/J (NOD/SCID), B6.129S2-$Cd4^{tm1Mak}$/J (CD4 knockout), B6.129S2-$Cd8a^{tm1Mak}$/J (CD8 knockout) mice (The Jackson Laboratory), and BALB/c Nude (T-cell deficient, Charles River laboratories) mice were housed at no more than five per cage in our American Association for Accreditation of Laboratory Animal Care-approved facility with 12:12-h light-dark cycles and free access to standard rodent chow and water. All animal procedures were approved by the Animal Care and Use Committee of Stanford University.

Chapter 8

Tissue collection, immunofluorenscent and histological analysis .

Explanted muscles were fixed in 2% paraformaldehyde for 2 hours at room temperature and cryoprotected in 30% sucrose overnight at 4°C. Tissue was frozen in optimum cutting temperature compound (OCT compound, Sakura Finetek) and sectioned at 5 μm on a cryostat. Serial sections were blocked and incubated with hamster anti-CD3 (clone G4.18) (BD Biosciences) for 1 hour at room temperature, followed by goat anti-hamster Texas Red (Santa Cruz Biotechnology) Sections were counterstained with 4,6-diamidino-2-phenylindole (DAPI, Molecular Probes) and analyzed with a Leica DMRB fluorescent microscope (Leica Microsystems, Frankfurt, Germany). Hematoxylin and Eosin staining (Sigma) was performed according to established protocols. For histopathogical evaluation of hESC survival 6 sections of each explanted muscle were stained with H&E and carefully analyzed by a blinded pathologist (H.V.).

Quantification of graft infiltrating cells.

Gastrocnemius muscles were surgically explanted, minced and digested for 2 hours in Collagenase D (2 mg/mL; Worthington Biochemical) at room temperature in RPMI 1640 media (Sigma Chemical Co.) with 10% fetal calf serum (FCS; Life Technologies). Muscle cell suspensions were ran through a 70 μm cell strainer, washed in FACS buffer (PBS 2% FCS) and incubated with PE-conjugated CD3e (145-2C11), CD8a (53-6.7), Mac-1/CD11b (M1/70) and allophycocyanin (APC)-conjugated CD4 (GK1.5), B220 (RA3-6B2) and Gr-1 (RB6-8C5) antibodies (CD4 and CD8: eBiosciences, all others: BD Bioscience) for 45 min at 4°C. Cells were washed, incubated with 7-amino-actinomycin D (7-AAD) cell viability solution (eBiosciences), and analyzed on a FACSCalibur system (BD Biosciences).

Quantification of humoral immune response.

Sera from recipient mice were decomplemented by heating to 56°C for 30 minutes and subsequently diluted by 33% in PBS containing 3% fetal calf serum and 0.1% NaN_3. Equal amounts of sera and hESC (1×10^6 cells/ml) suspensions were incubated for 30 minutes at 4°C and washed with PBS through a calf-serum cushion. IgM xeno-reactive antibodies were stained by incubation of the cells with PE–conjugated goat antibodies specific for the Fc portion of mouse IgM (BD Bioscience) at 4°C for 45 minutes. Cells from all groups were washed twice with PBS containing 2% FCS and then analyzed on a FACSCalibur system (BD Biosciences). Fluorescence data were collected by use of logarithmic amplification and expressed as mean fluorescent intensity.

Immunosuppressive therapy protocol.

Adult female BALB/c mice (n=30) were randomized to receive Tacrolimus (TAC; Sigma-Aldrich), sirolimus (SIR; Rapamune oral solution; Sigma-Aldrich) and mycophenolat mofetil (MMF; Roche). All drugs were administered once daily by oral gavage, using the following doses

for TAC, SIR and MMF: 4 mg/kg/d, 3 mg/kg/d, and 30 mg/kg/d respectively to achieve drug serum levels comparable to clinical trough levels of 10-15 ng/ml for TAC and SIR and 3.5-5.5 ng/ml for MMF. Blood was drawn during animal sacrifice and 12 or 24-hour drug trough levels were quantified by high-performance liquid chromatography (HPLC) as described earlier [40].

ACKNOWLEDGEMENTS

Chapter 8

REFERENCES

1. Thomson JA, Itskovitz-Eldor J, Shapiro SS, Waknitz MA, Swiergiel JJ, Marshall VS, Jones JM. Embryonic stem cell lines derived from human blastocysts. *Science (New York, N.Y.* 1998;282:1145-1147.
2. Mummery C, Ward-van Oostwaard D, Doevendans P, Spijker R, van den Brink S, Hassink R, van der Heyden M, Opthof T, Pera M, de la Riviere AB, Passier R, Tertoolen L. Differentiation of human embryonic stem cells to cardiomyocytes: role of coculture with visceral endoderm-like cells. *Circulation.* 2003;107:2733-2740.
3. Chadwick K, Wang L, Li L, Menendez P, Murdoch B, Rouleau A, Bhatia M. Cytokines and BMP-4 promote hematopoietic differentiation of human embryonic stem cells. *Blood.* 2003;102:906-915.
4. Perrier AL, Tabar V, Barberi T, Rubio ME, Bruses J, Topf N, Harrison NL, Studer L. Derivation of midbrain dopamine neurons from human embryonic stem cells. *Proceedings of the National Academy of Sciences of the United States of America.* 2004;101:12543-12548.
5. Segev H, Fishman B, Ziskind A, Shulman M, Itskovitz-Eldor J. Differentiation of human embryonic stem cells into insulin-producing clusters. *Stem cells (Dayton, Ohio).* 2004;22:265-274.
6. Lavon N, Yanuka O, Benvenisty N. Differentiation and isolation of hepatic-like cells from human embryonic stem cells. *Differentiation; research in biological diversity.* 2004;72:230-238.
7. Ben-Hur T, Idelson M, Khaner H, Pera M, Reinhartz E, Itzik A, Reubinoff BE. Transplantation of human embryonic stem cell-derived neural progenitors improves behavioral deficit in Parkinsonian rats. *Stem cells (Dayton, Ohio).* 2004;22:1246-1255.
8. Laflamme MA, Chen KY, Naumova AV, Muskheli V, Fugate JA, Dupras SK, Reinecke H, Xu C, Hassanipour M, Police S, O'Sullivan C, Collins L, Chen Y, Minami E, Gill EA, Ueno S, Yuan C, Gold J, Murry CE. Cardiomyocytes derived from human embryonic stem cells in pro-survival factors enhance function of infarcted rat hearts. *Nature biotechnology.* 2007;25:1015-1024.
9. Swijnenburg RJ, van der Bogt KE, Sheikh AY, Cao F, Wu JC. Clinical hurdles for the transplantation of cardiomyocytes derived from human embryonic stem cells: role of molecular imaging. *Current opinion in biotechnology.* 2007;18:38-45.
10. Bradley JA, Bolton EM, Pedersen RA. Stem cell medicine encounters the immune system. *Nature reviews.* 2002;2:859-871.
11. Drukker M, Katz G, Urbach A, Schuldiner M, Markel G, Itskovitz-Eldor J, Reubinoff B, Mandelboim O, Benvenisty N. Characterization of the expression of MHC proteins in human embryonic stem cells. *Proceedings of the National Academy of Sciences of the United States of America.* 2002;99:9864-9869.
12. Koch CA, Geraldes P, Platt JL. Immunosuppression by embryonic stem cells. *Stem cells (Dayton, Ohio).* 2008;26:89-98.
13. Min JY, Yang Y, Sullivan MF, Ke Q, Converso KL, Chen Y, Morgan JP, Xiao YF. Long-term improvement of cardiac function in rats after infarction by transplantation of embryonic stem cells. *The Journal of thoracic and cardiovascular surgery.* 2003;125:361-369.
14. Menard C, Hagege AA, Agbulut O, Barro M, Morichetti MC, Brasselet C, Bel A, Messas E, Bissery A, Bruneval P, Desnos M, Puceat M, Menasche P. Transplantation of cardiac-committed mouse embryonic stem cells to infarcted sheep myocardium: a preclinical study. *Lancet.* 2005;366:1005-1012.
15. Fandrich F, Lin X, Chai GX, Schulze M, Ganten D, Bader M, Holle J, Huang DS, Parwaresch R, Zavazava N, Binas B. Preimplantation-stage stem cells induce long-term allogeneic graft acceptance without supplementary host conditioning. *Nature medicine.* 2002;8:171-178.

16. Li L, Baroja ML, Majumdar A, Chadwick K, Rouleau A, Gallacher L, Ferber I, Lebkowski J, Martin T, Madrenas J, Bhatia M. Human embryonic stem cells possess immune-privileged properties. *Stem cells (Dayton, Ohio)*. 2004;22:448-456.

17. Swijnenburg RJ, Tanaka M, Vogel H, Baker J, Kofidis T, Gunawan F, Lebl DR, Caffarelli AD, de Bruin JL, Fedoseyeva EV, Robbins RC. Embryonic stem cell immunogenicity increases upon differentiation after transplantation into ischemic myocardium. *Circulation*. 2005;112:I166-172.

18. Nussbaum J, Minami E, Laflamme MA, Virag JA, Ware CB, Masino A, Muskheli V, Pabon L, Reinecke H, Murry CE. Transplantation of undifferentiated murine embryonic stem cells in the heart: teratoma formation and immune response. *Faseb J*. 2007;21:1345-1357.

19. Grinnemo KH, Kumagai-Braesch M, Mansson-Broberg A, Skottman H, Hao X, Siddiqui A, Andersson A, Stromberg AM, Lahesmaa R, Hovatta O, Sylven C, Corbascio M, Dellgren G. Human embryonic stem cells are immunogenic in allogeneic and xenogeneic settings. *Reproductive biomedicine online*. 2006;13:712-724.

20. Drukker M, Katchman H, Katz G, Even-Tov Friedman S, Shezen E, Hornstein E, Mandelboim O, Reisner Y, Benvenisty N. Human embryonic stem cells and their differentiated derivatives are less susceptible to immune rejection than adult cells. *Stem cells (Dayton, Ohio)*. 2006;24:221-229.

21. Grinnemo KH, Sylven C, Hovatta O, Dellgren G, Corbascio M. Immunogenicity of human embryonic stem cells. *Cell Tissue Res*. 2007.

22. Caspi O, Huber I, Kehat I, Habib M, Arbel G, Gepstein A, Yankelson L, Aronson D, Beyar R, Gepstein L. Transplantation of human embryonic stem cell-derived cardiomyocytes improves myocardial performance in infarcted rat hearts. *Journal of the American College of Cardiology*. 2007;50:1884-1893.

23. van der Bogt KE, Swijnenburg RJ, Cao F, Wu JC. Molecular imaging of human embryonic stem cells: keeping an eye on differentiation, tumorigenicity and immunogenicity. *Cell cycle (Georgetown, Tex*. 2006;5:2748-2752.

24. Game DS, Lechler RI. Pathways of allorecognition: implications for transplantation tolerance. *Transplant immunology*. 2002;10:101-108.

25. Draper JS, Pigott C, Thomson JA, Andrews PW. Surface antigens of human embryonic stem cells: changes upon differentiation in culture. *Journal of anatomy*. 2002;200:249-258.

26. Auchincloss H, Jr., Sachs DH. Xenogeneic transplantation. *Annual review of immunology*. 1998;16:433-470.

27. Taylor AL, Watson CJ, Bradley JA. Immunosuppressive agents in solid organ transplantation: Mechanisms of action and therapeutic efficacy. *Critical reviews in oncology/hematology*. 2005;56:23-46.

28. Lomax GP, Hall ZW, Lo B. Responsible oversight of human stem cell research: the California Institute for Regenerative Medicine's medical and ethical standards. *PLoS medicine*. 2007;4:e114.

29. Grinnemo KH, Sylven C, Hovatta O, Dellgren G, Corbascio M. Immunogenicity of human embryonic stem cells. *Cell Tissue Res*. 2008;331:67-78.

30. Cao YA, Wagers AJ, Beilhack A, Dusich J, Bachmann MH, Negrin RS, Weissman IL, Contag CH. Shifting foci of hematopoiesis during reconstitution from single stem cells. *Proceedings of the National Academy of Sciences of the United States of America*. 2004;101:221-226.

31. Cao YA, Bachmann MH, Beilhack A, Yang Y, Tanaka M, Swijnenburg RJ, Reeves R, Taylor-Edwards C, Schulz S, Doyle TC, Fathman CG, Robbins RC, Herzenberg LA, Negrin RS, Contag CH. Molecular imaging using labeled donor tissues reveals patterns of engraftment, rejection, and survival in transplantation. *Transplantation*. 2005;80:134-139.

Chapter 8

32. Lenschow DJ, Zeng Y, Thistlethwaite JR, Montag A, Brady W, Gibson MG, Linsley PS, Bluestone JA. Long-term survival of xenogeneic pancreatic islet grafts induced by CTLA4lg. *Science (New York, N.Y.* 1992;257:789-792.

33. Uchida T, Tomita Y, Anzai K, Zhang QW, Yoshikawa M, Kishihara K, Nomoto K, Yasui H. Roles of CD4+ and CD8+ T cells in discordant skin xenograft rejection. *Transplantation.* 1999;68:1721-1727.

34. Drukker M. Immunogenicity of human embryonic stem cells: can we achieve tolerance? *Springer seminars in immunopathology.* 2004;26:201-213.

35. Boyd AS, Higashi Y, Wood KJ. Transplanting stem cells: potential targets for immune attack. Modulating the immune response against embryonic stem cell transplantation. *Advanced drug delivery reviews.* 2005;57:1944-1969.

36. Shapiro AM, Lakey JR, Ryan EA, Korbutt GS, Toth E, Warnock GL, Kneteman NM, Rajotte RV. Islet transplantation in seven patients with type 1 diabetes mellitus using a glucocorticoid-free immunosuppressive regimen. *The New England journal of medicine.* 2000;343:230-238.

37. De A, Lewis XZ, Gambhir SS. Noninvasive imaging of lentiviral-mediated reporter gene expression in living mice. *Mol Ther.* 2003;7:681-691.

38. Cao F, Lin S, Xie X, Ray P, Patel M, Zhang X, Drukker M, Dylla SJ, Connolly AJ, Chen X, Weissman IL, Gambhir SS, Wu JC. In vivo visualization of embryonic stem cell survival, proliferation, and migration after cardiac delivery. *Circulation.* 2006;113:1005-1014.

39. Amit M, Carpenter MK, Inokuma MS, Chiu CP, Harris CP, Waknitz MA, Itskovitz-Eldor J, Thomson JA. Clonally derived human embryonic stem cell lines maintain pluripotency and proliferative potential for prolonged periods of culture. *Dev Biol.* 2000;227:271-278.

40. Taylor PJ, Salm P, Lynch SV, Pillans PI. Simultaneous quantification of tacrolimus and sirolimus, in human blood, by high-performance liquid chromatography-tandem mass spectrometry. *Therapeutic drug monitoring.* 2000;22:608-612.

CHAPTER 9

Summary and Discussion

ESCs are showing promise to serve as a cellular source for tissue regeneration therapy. However, the host immune response against transplanted ESCs is not well characterized. In fact, controversy remains as to whether ESCs have immune-privileged properties. The aim of this thesis was to characterize the immunobiology of ESC transplantation with the help of non-invasive molecular imaging techniques. Specifically, this thesis presents evidence that: (1) molecular imaging can be used to quantify organ, BMC and ESC survival following transplantation and non-invasively follow donor graft fate; (2) mESCs and hESCs express MHC and co-signaling molecules that are upregulated upon differentiation; (3) mESCs and hESCs can trigger potent cellular and humoral immune responses following allogeneic and/or xenogeneic transplantation, resulting in intra-graft infiltration of a variety of inflammatory cells, leading to rejection; and (4) immunosuppressive drugs can significantly mitigate the host immune response to prolong hESC survival in immunocompetent mice.

IN VIVO BIOLUMINESCENCE IMAGING: A VALUABLE TOOL TO MONITOR TRANSPLANTATION REJECTION

In **Chapter 2**, molecular imaging was used to non-invasively follow cardiac allograft rejection. We have shown that BLI signal emitted from Fluc/GFP transgenic cardiac allografts decreases after 4 days in the course of acute rejection. In addition, the light intensity emitted from donor-derived passenger CD5$^+$ cells diminished within 1 day after allotransplantation. *In vivo* BLI of different promoter Fluc transgenic donor heart recipients allowed us not only to longitudinally quantify the kinetics of cardiac allograft viability, but also the location and distribution of donor-derived passenger CD5$^+$ cells. In a subsequent study, the value of non-invasive imaging was demonstrated in a different and upcoming field of research in cardiovascular medicine: BMC therapy for ischemic heart disease. By using *in vivo* BLI, the study in **Chapter 3** confirmed the therapeutic effect of BMC transplantation in the setting of acute MI. However, it also clearly showed that delivery of the cells in the time-window following the hostile acute inflammatory phase–7 days after MI–does not result in extended long-term survival of donor BMCs as compared to BMCs delivered acutely after MI. Again, molecular imaging allowed us to obtain these data longitudinally, without the necessity for animal sacrifice.

Clearly, *in vivo* BLI proved to be a valuable tool for monitoring graft survival and/or rejection following transplantation. These advantages are a result of the stable genetic integration of the Fluc reporter gene into the donor cells, which are also equally transferred to progeny cells. As long as the cells are viable, transcription and translation will lead to reporter protein, which can be detected by a CCD camera following administration of the D-luciferin reporter probe. However, because of the use of low-energy photons (2 to 3 eV), BLI is limited by photon attenuation and scattering within deep tissues. Therefore, the limitation of this technique is that it is not suitable for pre-clinical large animal or human studies. As explained in detail

Chapter 9

in **Chapter 4 and 5**, the *HSV-tk* reporter gene constructs have been applied to large animal[1] and human trials[2]. The basis behind this approach is injecting the subject with a radiolabeled thymidine analog (e.g., [18F]fluoro-3-hydroxymethylbutyl)guanine or [^{18}F]-FHBG) that can be detected by PET when it is phosphorylated by *HSV-tk* and subsequently trapped inside the cell. The *HSV-tk* allows emits high-energy photons (511 keV) and allows for deep-tissue PET imaging of gene expression. The development of multi-fusion reporter gene constructs enabling PET imaging and iron labeling for MRI, should lead to further application of molecular imaging in the clinical setting.

Immunogenicity of embryonic stem cells

The study described in **Chapter 6** was designed to investigate whether ESCs elicit an immune response when transplanted into genetically identical or full MHC-mismatched ischemic myocardium. The data demonstrate that there is progressive infiltration by various types of inflammatory cells within the ESC graft following transplantation across histocompatibility barriers. Severe cellular invasion was observed 4 weeks after intra-myocardial injection, followed by disappearance of the ESC allografts between 4 and 8 weeks after transplantation, presumably due to a robust alloimmune response. However, since non-labeled mESCs are used and the cells are transplanted into an infarcted area, questions regarding quantification of mESC survival and the potentially pro-inflammatory influence of the ischemic myocardium remained. These questions were addressed in **Chapter 7**, in which we describe the successful transfection of mESCs with a double fusion (DF) reporter gene carrying Fluc and eGFP. Transduced mESCs were transplanted by direct injection into the gastrocnemius muscle of syngeneic and allogeneic recipient mice after which *in vivo* BLI was performed weekly. By 28 days, BLI signal in the allogeneic recipients had decreased to background levels, whereas signal in the syngeneic recipients continued to increase. Moreover, ESC-derived teratomas could be detected in syngeneic, but not in allogeneic muscles. Further investigations showed that differentiated mESCs have a higher MHC-expression and impaired survival capacity as compared to undifferentiated mESCs when transplanted over histocompatibility barriers, suggesting increased immunogenicity.

Clinical ESC-based transplantation protocols will require the use of hESCs. Because of hESCs' potential to differentiate into teratomas, safety considerations prevent clinical research using hESC. Since both mESCs[3, 4] and hESCs[5] had been reported capable of escaping xenogeneic immune recognition, we thought it proper to test hESC immunogenicity in a mouse-to-human xenogeneic model, which resulted in the study described in **Chapter 8**. Similarly, a double fusion reporter gene construct carrying Fluc and eGFP driven by a constitutive human ubiquitin promoter (pUB) was successfully transduced into undifferentiated hESCs (H9 line), using a self-inactivating (SIN) lentiviral vector. Using *in vivo* BLI, we found that hESC survival was significantly limited in immunocompetent animals as compared to immunodeficient NOD/ SCID mice. Graft infiltration by host immune cells occurred within 5 days, and the BLI signal

disappeared completely within 10 days in immunocompetent hosts. Subsequent transplantation of additional hESCs 2 weeks after the original exposure led to accelerated rejection. In contrast, transplants into immunodeficient hosts expanded in number after only 10 days, and teratoma formation was evident at 42 days. Controls showed that the hESCs did not sensitize the hosts to the xenoantigens produced by the reporter genes; transplantation of unmanipulated hESCs elicited similar rejection of retransplanted transfected hESCs. Rejection was demonstrated to be mediated predominantly by CD4+ T cells, arguing for a predominantly indirect pathway of immune rejection.

In summary, by using a multimodality approach of cell surface marker analysis, in vivo mouse-to-mouse allogeneic and human-to-mouse xenogeneic ESC transplantation, this thesis unequivocally demonstrates the immunogenicity of ESC and their derivatives.

FUTURE PERSPECTIVES

How do we deal with the immunological challenges?

Before successful clinical application can be accomplished, immunological rejection of ESC following transplantation is something that must be overcome. Therefore, specific strategies to induce tolerance to an ESC-based transplant will be required. There are quite a few options available for the prevention of graft rejection.

Decades of experience in solid organ transplantation has learned that immunosuppressive medication can aid to long-term allograft acceptance by the recipient. In the context of ESC-derived transplants, it is possible to imagine that cocktails of immunosuppressive drugs could be used to control unwanted immune responses. In **Chapter 8**, we investigated the efficacy of single and combined immunosuppressive drug regimens for preventing post-transplant hESC rejection. Our results show that, in a xenogeneic murine setting, a combined immunosuppressive drug regimen consisting of high dose Tacrolimus and Sirolimus optimally suppressed anti-hESC immune response and prolonged their survival to 28 days following transplantation. These experiments confirm the efficacy of immunosuppressive drugs in the context of ESC transplantation. One can imagine that in an allogeneic clinical setting, in which a less robust immune response is expected, a less aggressive form or combination of immunosuppressive drugs could be successful.

It has been proposed that a hESC bank containing up to 150 hESC lines[9] would suffice to match the HLA haplotypes of most of the population. While the extent of genetic disparity in hESC or their derivatives that may be accommodated between donor and recipient is unclear, mouse models have shown that even single differences between donor ESC and recipient minor histocompatibility antigens may facilitate graft rejection[10]. Therefore, investigating strategies to induce donor graft tolerance becomes a crucial component for the clinical application and long-term survival of hESC-derived therapeutics.

Manipulating central tolerance such that the recipient immune system becomes "donor tolerant" would be ideal and circumvent the need for long-term, nonspecific immunosuppressive therapies[11]. Transplantation of hematopoietic stem cells derived from hESCs into the patient would create mixed hematopoietic chimerism, enabling subsequent therapeutic cells derived from the same hESC to escape rejection. In this process, donor APCs repopulate the thymus, contributing to negative selection of T-cells, allowing transplantation of hESC-derived cells from the same donor with limited risk of rejection.

Alternative strategies designed to produce patient-specific stem cells are being investigated to avoid immune tolerance issues. These approaches include production of patient-specific hESC lines by somatic cell nuclear transfer (SCNT) of a patient cell's nucleus into an enucleated oocyte. This process, referred to as therapeutic cloning, has allowed successful creation of ESC lines from sheep and mice, but has been proven difficult for the creation of hESC lines[12]. An infamous study by Hwang et al[13], published in *Science* in 2005, in which he claimed to have succesfully created hESCs lines by therapeutic cloning, was later editorially retracted after it was found to contain a large amount of fabricated data.

An interesting development has occurred recently in field of ESC research that could potentially circumvent immunological problems: the derivation of induced pluripotent stem (iPS) cells from human somatic cells. This study demonstrated reprogramming of adult fibroblasts[14]. A cocktail of four retrovirally encoded transcription factors—either Oct4, Sox2, c-*myc* and Klf-4 or Oct4, Sox2, Nanog, and Lin28— was used to reprogram human fibroblasts to cells that closely resemble hESCs. These iPS cells had gene-expression profiles and DNA-methylation patterns closely resembling hESCs, grew vigorously while expressing telomerase, maintained a normal karyotype, and formed teratomas after transplantation into immunocompromised mice. The ability to generate pluripotent cells from readily available fibroblasts offers the potential to generate patient-specific cells that would be recognized as "self" by the immune system, thus preventing rejection[15].

FINAL REMARKS

Ethical considerations of embryonic stem cell research

In a thesis on a subject that has been the topic of such furious political debate in the past several years; we feel that the ethical aspects of ESC research can not be left undiscussed.

ESC are isolated from the inner cell mass of a preimplantation embryo at the blastocyste stage around 5-8 days after conception, a procedure that destructs the remainder of the fertilized egg. As a consequence, two radically opposed groups have emerged in society: those who advocate absolute respect for human life beginning at conception, and those who do not[16]. In the USA, controversy on this subject resulted in contrasting political action. On August 9, 2001, former President George W. Bush, a strong opponent of ESC research, announced that

no new hESC lines would be made using government dollars. In contrast, in 2004, the California Institute of Regenerative Medicine (CIRM) was established, a granting agency charged with distributing $3 billion for stem cell research. Only very recently, President Obama lifted the ban on federal funding for hESC research allowing the field to move forward in the years to come.

At the core of this whole debate is how we define human life. The key question is whether it is permissible to prevent the death or severe suffering of a child or adult by using cells derived from fertilized eggs. But do adults and embryos have equal moral status or does this increase with advancing development? How else to explain our legal approach to abortion and our readiness to remove ectopic pregnancies? Moreover, human preimplantation embryos have only a limited potential to become humans. Most are lost before a menstrual period. Contraceptive methods that destroy embryos are used widely and there is general public approval of *in vitro* fertilization (IVF): only around 10% of transferred IVF embryos produce a baby, other generated embryos cannot be transferred and perish[17].

A frequent argument used by opponents of ESC research is that scientist should focus on the use of adult stem cells to treat human disease. However, as stated in the introduction of this thesis, there is increasing evidence that there are no pluripotent ASCs in the human body, meaning that these cells do not have the ability to transdifferentiate into other cell lineages then their own.[18] For example, in **Chapter 3**, we concluded that intramyocardially transplanted BMCs continue develop along the hematopoietic lineage and no new cardiomyocytes or endothelial cells were formed.

The development of iPS cells is exciting and could circumvent both ethical and immunological issues of ESC transplantation. There are, however, drawbacks to the clinical use of iPS cells. The first is the current need to use integrating retroviruses to deliver the reprogramming factors. These viruses may still face immune barriers. The second is that iPS cells are not an "off-the-shelf" product and would likely only be produced after the patient becomes ill, precluding their use in the acute phase of the disease[15].

CONCLUDING REMARKS

The field of hESC-based therapy has been advancing rapidly. The CIRM foresees hESC-based therapies to go into phase I clinical trails within the next 10 years[19]. To accomplish such goals, several significant hurdles that preclude clinical translation of such therapy need to be overcome. These include the development of animal product-free culture protocols, reproducible differentiation methods for specific cell types, purification of cell populations to be transplanted to preclude teratoma formation *in vivo*, and optimizing cell survival following transplantation. The results presented in thesis clearly indicate that the latter issue seems to be greatly influenced by the immunological response towards allogeneic ESC-derived cells.

Chapter 9

Clearly, more in depth research on the use of ESC to treat human disease is essential. How-ever, if one thinks about the enormous progress that has been made in the decade since Thompson's first successful creation of a human embryonic stem cell line in 1998[20], one can only imagine where this field of research leads us to in the years to come. Or to quote Christopher Scott, Executive Director of the Stem Cells in Society Program at Stanford University; *"It is difficult to find a biologist who will say that stem cells alone hold the key to solving our most intractable diseases. But it is safe to say that no single area of biomedicine holds such great promise for improving human health[21]"*

REFERENCES

1. Rodriguez-Porcel M, Brinton TJ, Chen IY, Gheysens O, Lyons J, Ikeno F, Willmann JK, Wu L, Wu JC, Yeung AC, Yock P, Gambhir SS. Reporter gene imaging following percutaneous delivery in swine moving toward clinical applications. *Journal of the American College of Cardiology.* 2008;51:595-597.

2. Jacobs A, Voges J, Reszka R, Lercher M, Gossmann A, Kracht L, Kaestle C, Wagner R, Wienhard K, Heiss WD. Positron-emission tomography of vector-mediated gene expression in gene therapy for gliomas. *Lancet.* 2001;358:727-729.

3. Min JY, Yang Y, Sullivan MF, Ke Q, Converso KL, Chen Y, Morgan JP, Xiao YF. Long-term improvement of cardiac function in rats after infarction by transplantation of embryonic stem cells. *The Journal of thoracic and cardiovascular surgery.* 2003;125:361-369.

4. Menard C, Hagege AA, Agbulut O, Barro M, Morichetti MC, Brasselet C, Bel A, Messas E, Bissery A, Bruneval P, Desnos M, Puceat M, Menasche P. Transplantation of cardiac-committed mouse embryonic stem cells to infarcted sheep myocardium: a preclinical study. *Lancet.* 2005;366:1005-1012.

5. Li L, Baroja ML, Majumdar A, Chadwick K, Rouleau A, Gallacher L, Ferber I, Lebkowski J, Martin T, Madrenas J, Bhatia M. Human embryonic stem cells possess immune-privileged properties. *Stem cells (Dayton, Ohio).* 2004;22:448-456.

6. Drukker M, Katz G, Urbach A, Schuldiner M, Markel G, Itskovitz-Eldor J, Reubinoff B, Mandelboim O, Benvenisty N. Characterization of the expression of MHC proteins in human embryonic stem cells. *Proceedings of the National Academy of Sciences of the United States of America.* 2002;99:9864-9869.

7. Draper JS, Pigott C, Thomson JA, Andrews PW. Surface antigens of human embryonic stem cells: changes upon differentiation in culture. *Journal of anatomy.* 2002;200:249-258.

8. Semnani RT, Nutman TB, Hochman P, Shaw S, van Seventer GA. Costimulation by purified intercellular adhesion molecule 1 and lymphocyte function-associated antigen 3 induces distinct proliferation, cytokine and cell surface antigen profiles in human "naive" and "memory" CD4+ T cells. *The Journal of experimental medicine.* 1994;180:2125-2135.

9. Taylor CJ, Bolton EM, Pocock S, Sharples LD, Pedersen RA, Bradley JA. Banking on human embryonic stem cells: estimating the number of donor cell lines needed for HLA matching. *Lancet.* 2005;366:2019-2025.

10. Robertson NJ, Brook FA, Gardner RL, Cobbold SP, Waldmann H, Fairchild PJ. Embryonic stem cell-derived tissues are immunogenic but their inherent immune privilege promotes the induction of tolerance. *Proceedings of the National Academy of Sciences of the United States of America.* 2007;104:20920-20925.

11. Chidgey AP, Boyd RL. Immune privilege for stem cells: not as simple as it looked. *Cell stem cell.* 2008;3:357-358.

12. Boyd AS, Higashi Y, Wood KJ. Transplanting stem cells: potential targets for immune attack. Modulating the immune response against embryonic stem cell transplantation. *Advanced drug delivery reviews.* 2005;57:1944-1969.

13. Hwang WS, Roh SI, Lee BC, Kang SK, Kwon DK, Kim S, Kim SJ, Park SW, Kwon HS, Lee CK, Lee JB, Kim JM, Ahn C, Paek SH, Chang SS, Koo JJ, Yoon HS, Hwang JH, Hwang YY, Park YS, Oh SK, Kim HS, Park JH, Moon SY, Schatten G. Patient-specific embryonic stem cells derived from human SCNT blastocysts. *Science (New York, N.Y.* 2005;308:1777-1783.

Chapter 9

14. Takahashi K, Tanabe K, Ohnuki M, Narita M, Ichisaka T, Tomoda K, Yamanaka S. Induction of pluripotent stem cells from adult human fibroblasts by defined factors. *Cell.* 2007;131:861-872.

15. Murry CE, Keller G. Differentiation of embryonic stem cells to clinically relevant populations: lessons from embryonic development. *Cell.* 2008;132:661-680.

16. Ruiz-Canela M. Embryonic stem cell research: the relevance of ethics in the progress of science. *Med Sci Monit.* 2002;8:SR21-26.

17. Winston R. Embryonic stem cell research. The case for. *Nature medicine.* 2001;7:396-397.

18. Wagers AJ, Weissman IL. Plasticity of adult stem cells. *Cell.* 2004;116:639-648.

19. Lomax GP, Hall ZW, Lo B. Responsible oversight of human stem cell research: the California Institute for Regenerative Medicine's medical and ethical standards. *PLoS medicine.* 2007;4:e114.

20. Thomson JA, Itskovitz-Eldor J, Shapiro SS, Waknitz MA, Swiergiel JJ, Marshall VS, Jones JM. Embryonic stem cell lines derived from human blastocysts. *Science (New York, N.Y.* 1998;282:1145-1147.

21. Scott CT. *Stem Cell Now*. New York: Penguin Group; 2006.

CHAPTER 10

Samenvatting

STAMCELLEN

Stamcellen hebben twee unieke eigenschappen. Allereerst zijn ze in staat zichzelf te vermenigvuldigen en zijn daardoor een onuitputbare bron van cellen te gebruiken voor celvervangende of weefselreparatie therapie. Ten tweede kunnen stamcellen zich ontwikkelen tot meer gespecialiseerde dochtercellen. Zij kunnen differentiëren tot zowel voorlopercellen als volledig gespecialiseerde cellen van het menselijk lichaam. Gezien deze eigenschappen wordt het gebruik van stamcellen als bron voor regeneratieve celtransplantatie therapie als veelbelovend beschouwd. Er zijn twee typen stamcellen, volwassen (adult) stamcellen (ASC) en embryonale stamcellen (ESC).

Volwassen stamcellen bevinden zich op vele plekken in het menselijk lichaam. Een volwassen stamcel is een nog niet gedifferentieerde of een niet-gespecialiseerde cel die na de geboorte voorkomt in een gedifferentieerd en gespecialiseerd weefsel van een organisme. Deze cellen zijn multipotent, hun differentiatie en proliferatiemogelijkheden zijn beperkt, omdat zij zich enkel tot cellen van één embryonale kiemlaag (endoderm, ectoderm of mesoderm) kunnen differentiëren. Ze zijn nodig in het lichaam om bepaalde cellen met een korte levensduur te verversen. Voorbeelden van ASC zijn de hematopoietische (bloedvormende) stamcellen, neurale stamcellen uit hersenweefsel en stamcellen in huid- en vetweefsel.

Embryonale stamcellen daarentegen worden gewonnen door het isoleren van een aantal cellen uit de binnenste celmassa van een blastocyst, ongeveer 4 to 5 dagen na bevruchting van de eicel. Deze cellen zijn pluripotent, dat willen zeggen dat zij zich kunnen ontwikkelen tot elke cel van het menselijk lichaam. Sinds ontwikkeling van de eerste humane ESC (hESC) lijn in 1998 zijn er in de literatuur onder andere hartspiercellen, levercellen, alvleescliercellen en neuronen beschreven die *in vitro* zijn gekweekt uit ESC. Transplantatie van deze cellen zou een regeneratieve therapie kunnen betekenen voor ziekten als het hartinfarct, leverziekten, diabetes mellitus en de ziekte van Parkinson. Alvorens regeneratieve celtherapie met ESC kan worden toegepast is zal een aantal hordes moeten worden genomen.

Een van de obstakels is de potentiele immunologische afweerreactie die teweeg wordt gebracht na het transplanteren van ESC. Uit de transplantatiegeneeskunde is bekend dat er een afstotingsreactie op gang wordt gebracht door het immuunsysteem als men organen of cellen transplanteert tussen twee genetisch niet-identieke individuen. Deze immuunreactie richt zich tegen Major Histocompatibility Complex (MHC) antigenen op het celmembraan, die door het immuunsysteem als 'niet eigen' worden herkend. Echter, een embryo, die voor 50% genetisch materiaal van de vader bezit, wordt over het algemeen niet afgestoten door de moeder. Bovendien zijn er uit de vroege ESC literatuur studies bekend waarin langdurige overleving van ESC wordt beschreven na allogene (tussen genetisch niet-identieke individuen) transplantatie en zelfs xenogene (interspecies) transplantatie.

Het onderzoek in dit proefschrift richt zich op de vraag in hoeverre embryonale stamcellen na transplantatie een afweerreactie van het immuunsysteem opwekken. Hierbij wordt

gebruik gemaakt van molecular imaging om de getransplanteerde ESC in beeld te brengen en overleving van de cellen non-invasief te kunnen volgen.

IN VIVO BIOLUMINESCENT IMAGING: EEN GEVOELIGE METHODE OM GETRANSPLANTEERDE CELLEN IN BEELD TE BRENGEN

Het eerste deel van dit proefschrift bestaat uit een introductie op het gebruik van een nieuwe vorm van molecular imaging: 'in vivo bioluminescent imaging (BLI)', voor het in beeld brengen van getransplanteerde cellen en/of organen. BLI kan cellen in beeld brengen die getransfecteerd zijn met het enzym 'firefly luciferase (Fluc)'. Cellen die Fluc tot expressie brengen produceren na interactie met de lichtproducerende stof luciferine, een vorm van biologisch licht (bioluminiscentie, zoals de vuurvlieg) dat kan worden opgevangen door ultra-sensitieve 'charged coupled device (CCD)' camera's. In **Hoofdstuk 2** wordt het gebruik van BLI bij experimentele harttransplantatie beschreven. Na heterotope transplantatie van harten van transgene Fluc donormuizen in allogene non-transgene ontvangers kan de acute afstoting van de organen non-invasief in beeld worden gebracht. In een volgend experiment worden harten getransplanteerd van transgene muizen waarin een CD5-promotor het Fluc gen aandrijft. Met behulp van BLI kunnen vervolgens CD5-positieve donor leukocyten in beeld worden gebracht, die vanuit het donorhart in de circulatie van de ontvanger worden opgenomen; zogenaamde 'passenger leukocytes', die een belangrijke rol spelen bij acute rejectie. Een volgende toepassing van BLI wordt beschreven in **Hoofdstuk 3**. In deze studie wordt gekeken naar het injecteren van autologe mononucleaire beenmergcellen in harten van muizen na hartinfarct. Deze experimentele therapie heeft zowel in basaal als klinisch onderzoek verbetering van de hartfunctie laten zien. In de eerste dagen na hartinfarct vindt er een heftige ontstekingsreactie plaats in het geïnfarceerde hartspierweefsel. Deze vijandige omgeving zou de overleving van getransplanteerde cellen in dit gebied negatief kunnen beïnvloeden. In deze studie wordt onderzocht wat de invloed is van timing van cel injectie na hartinfarct op overleving van de getransplanteerde cellen en verbetering van de hartfunctie. Mononucleaire beenmergcellen van Fluc transgene muizen werden direct of 7 dagen na hartinfarct geinjecteerd in harten van syngene (genetisch identieke) muizen. BLI liet geen verschil in overleving van de cellen zien; in beide groepen was het signaal na zes weken tot achtergrondwaarden gereduceerd. Ook verbetering van de hartfunctie verschilde niet significant. Daarbij viel op dat er geen nieuwe hart- en/of endotheelcellen werden gevormd uit de donorcellen; de getransplanteerde beenmergcellen behielden hun hematopoietische fenotype.

IMMUNOGENICITEIT VAN EMBRYONALE STAMCELLEN

In het tweede deel van het proefschrift wordt specifiek gekeken naar de immunogeniciteit van ESC en de waarde van molecular imaging bij het volgen van de overleving van deze cellen na transplantatie. **Hoofdstuk 4** geeft een inleiding op het potentieel van hESC in de regeneratieve geneeskunde. Het geeft een overzicht van gespecialiseerde cellen die tot nu toe uit ESC zijn gekweekt. Daarbij geeft het een beschrijving van molecular imaging en de waarde daarvan voor het non-invasief in beeld brengen van de hESC na transplantatie. In **Hoofdstuk 5** wordt vervolgens meer specifiek ingegaan op hartspiercellen die uit hESC kunnen worden gekweekt. Het belang van generatie van cardiomyocyten is groot; de hartspier bezit niet de capaciteit zich te regenereren na een hartinfarct, hetgeen in de loop van de tijd kan leiden tot hartfalen. In dit hoofdstuk wordt derhalve uitgelegd welke vooruitgang er is geboekt in het kweken van cardiomyocyten en er wordt een overzicht gegeven van de hordes die nog genomen moeten worden om transplantatie van uit hESC gekweekte cardiomyocyten in de kliniek te kunnen toepassen. Om dit laatste mogelijk te kunnen maken, zou molecular imaging een belangrijke rol kunnen spelen.

  Hoofdstuk 6 is, voor zover bekend in de literatuur, de eerste studie waarin wordt gekeken naar de immunogeniciteit van ESC. In een muis-myocardinfarct-model wordt de mate van infiltratie van immuuncellen in de hartspier onderzocht na allogene transplantatie van ESC van muizen (mESC). In vergelijking met syngene controle muizen, vindt robuuste infiltratie van immuuncellen plaats, hetgeen leidt tot afstoting van de cellen. Een tweede bevinding is dat er in de syngene groep, waarbij de cellen niet worden afgestoten, intramyocardiale teratomen worden gevormd. Deze tumorvorming laat zien dat ongedifferentieerde ESC na transplantatie in hartspierweefsel zich niet per definitie ontwikkelen tot cardiomyocyten, maar zich ontwikkelen tot cellen van alle embryologische kiemlagen.

  In de voorgaande studie, wordt overleving van getransplanteerde cellen geanalyseerd door middel van histologische technieken, hetgeen vereist dat de muizen moeten worden geofferd om deze informatie te vergaren. Om dit laatste te voorkomen, en bovendien de tijd van overleving tot in groter detail te kwantificeren wordt in **Hoofdstuk 7** molecular imaging van ESC toegepast. mESC worden succesvol getransfecteerd met een reporter gen, bestaande uit onder meer Fluc. Vervolgens kunnen de cellen na transplantatie met behulp van BLI worden gevisualiseerd. Na allogene transplantatie in de kuitspier van muizen worden de cellen in een tijdsbestek van ongeveer 28 dagen afgestoten. Intramusculaire teratomen worden wederom aangetroffen na syngene, maar niet na allogene ESC transplantatie. Verdere analyse laat zien dat gedifferentieerde ESC een sterkere expressie van MHC antigenen hebben in vergelijking met ongedifferentieerde moedercellen. Ook worden gedifferentieerde ESC sneller afgestoten. Dit suggereert dat de immunogeniciteit van ESC versterkt wordt naarmate de cellen differentiëren. Vervolgens wordt in **Hoofdstuk 8** de stap gemaakt naar het analyseren van transplantatieimmunologie van hESC. Ook nu worden de cellen getransfecteerd met het

Chapter 10

Fluc reporter gen. Deze studie laat zien dat de overleving van hESC significant beperkt is na intramusculaire transplantatie in xenogene immunocompetente muizen in vergelijking met immunodeficiente muizen. Herhaalde transplantatie van hESC in de contralaterale kuitspier van dezelfde muis leidt tot versnelde afstoting, hetgeen bewijzend is voor een adaptieve immuunreactie tegen hESC. Naast een lokale immuuncelinfiltratie in de kuitspier wordt ook aangetoond dat deze afstotingsreactie zowel een systemische cellulaire (door T-cellen) als een humorale (door B-cellen) component heeft. Tot slot wordt met behulp van BLI gekeken naar de meest potente combinatie van immunosuppressieve medicatie om de afstoting van hESC na xenotransplantatie te vertragen. **Hoofdstuk 9** bestaat uit een samenvatting en discussie van de studies in dit proefschrift en wordt een aantal mogelijke oplossingen en ontwikkelingen beschreven dat zou kunnen bijdragen aan onderdrukking of voorkoming van afstoting van ESC na transplantatie.

CONCLUSIES

BLI lijkt een betrouwbare en accurate techniek voor het non-invasief en longitudinaal in beeld brengen van getransplanteerde ESC. Deze ESC brengen MHC antigenen tot expressie. Deze expressie wordt versterkt naarmate de cel differentieert. Bovendien blijkt dat ESC worden herkend en afgestoten door het adaptieve allogene en xenogene immuunsysteem na transplantatie. Het gebruik van immunosuppressiva kan deze afstotingsreactie onderdrukken, hetgeen leidt tot een significant langere overleving van de cellen, doch niet tot het voorkomen van afstoting.

Voordat regeneratieve ESC therapie veilig en succesvol zal kunnen worden toegepast in de kliniek, zal de immunogeniciteit en afstoting van de cellen na transplantatie moeten worden overwonnen. Bij de ontwikkeling van strategieën ter voorkoming van afstoting van ESC zal molecular imaging een belangrijke rol kunnen spelen.

**List of publications
Curriculum Vitae
Acknowledgements**

LIST OF PUBLICATIONS

1. Van der Bogt KE, Sheik AY, Schrepfer S, Hoyt G, Cao F, Ransohoff K, **Swijnenburg RJ**, Pearl JI, Lee A, Fischbein M, Contag CH, Robbins RC, Wu JC. Comparison of different adult stem cell types for treatment of myocardial ischemia. Circulation. 2008;118[14 suppl]:S121-9

2. **Swijnenburg RJ**, Schrepfer S, Govaert JA, Cao F, Ransohoff K, Sheikh AY, Haddad M, Connolly AJ, Davis MM, Robbins RC, Wu JC. Immunosuppressive therapy mitigates immunological rejection of human embryonic stem cell xenographs. Proc Na*t Acad Sci USA. 2008;*105(35):12991-6

3. **Swijnenburg RJ,** Schrepfer S, Cao F, Pearl JI, Xie X, Connolly AJ, Robbins RC, Wu JC. In vivo imaging of embryonic stem cells reveals patterns of survival and immunological rejection following transplantation. *Stem Cells Dev. 2008* Dec;17(6):1023-9.

4. **Swijnenburg RJ**, Sheikh AY, Robbins RC. Comment on "Transplantation of undiffer-entiated murine embryonic stem cells in the heart: teratoma formation and immune response". *FASEB J. 2007* May;21(7):1290

5. **Swijnenburg RJ**, Van der Bogt KE, Sheikh AY, Cao F, Wu JC. Clinical hurdles for transplan-tation of cardiomyocytes derived from human embryonic stem cells: Role of molecular imaging. *Curr Opin Biotechnol. 2007* Feb;18(1):38-45

6. Van der Bogt KE, **Swijnenburg RJ**, Cao F, Wu JC. Molecular Imaging of Human Embryonic Stem Cells: Keeping an Eye on Differentiation, Tumorigenicity and Immunogenicity. *Cell Cycle 2006* Dec;5(23):2748-52.

7. Kofidis T, Lebl DR, **Swijnenburg RJ**, Greeve JM, Klima U, Robbins RC. Allopurinol/uricase and ibuprofen enhance engraftment of cardiomyocyte-enriched human embryonic stem cells and improve cardiac function following myocardial injury. *Eur J Cardiothorac Surg*. 2006 Jan;29(1):50-5.

8. **Swijnenburg RJ**, Tanaka M, Vogel H, Baker J, Kofidis T, Gunwan F, Lebl DR, Caffarelli AD, de Bruin JL, Fedoseyeva EV and Robbins RC. Embryonic Stem Cell Immunogenicity Increases upon Differentiation Following Transplantation into Ischemic Myocardium. *Circulation* 2005;112[suppl I]:I-166-I-172

9. Tanaka M, **Swijnenburg RJ**, Gunawan F, Cao YA, de Bruin JL, Kofidis T, Fedoseyeva EV, Contag CH and Robbins RC. *In Vivo* Visualization of Cardiac Allograft Rejection

and Trafficking Passenger Leucocytes Using Bioluminescence Imaging. *Circulation* 2005;112[suppl I]:I-105-I-110

10. Coa YA, Bachmann MH, Beilhack A, Yang Y, Tanaka M, **Swijnenburg RJ**, Reeves R, Taylor-Edwards C, Schulz S, Doyle TC, Fathman CG, Robbins RC, Herzenberg LA, Negrin RS, Contag CH. Molecular Imaging Using Labeled Donor Tissues Reveals Patterns of Engraftment, Rejection, and Survival in Transplantation. *Transplantation* 2005;80(1):134-139

11. Kofidis T, de Bruin JL, Hoyt EG, Ho Y, Tanaka M, Yamane T, Lebl DR, **Swijnenburg RJ**, Chang CP, Quertermous T and Robbins RC. Myocardial Restoration with Embryonic Stem Cell Bioartificial Tissue Transplantation. *J Heart Lung Transplant* 2005;24(6):737-44

12. Kofidis T, de Bruin JL, Yamane T, Tanaka M, Lebl DR, **Swijnenburg RJ,** Weissman IL and Robbins RC. Stimulation of Paracrine Pathways with Growth Factors Enhances Embryonic Stem cell Engraftment and Host Specific Differentiation in the Heart Following Ischemic Myocardial Injury. *Circulation* 2005;111(19):2486-93

13. Kofidis T, de Bruin JL, Yamane T, Balsam LB, Lebl DR, **Swijnenburg RJ**, Tanaka M, Weissman IL, Robbins RC. Insulin-like growth factor promotes engraftment, differentiation, and functional improvement after transfer of embryonic stem cells for myocardial restoration. *Stem Cells* 2004;22(7):1239-45

14. **Swijnenburg RJ**, Lange CP, Salm LP. Non-invasieve visualisatie van coronairarteriele stenosen; ontwikkeling van Coronary Magnetic Resonance Angiography. *Ned Tijdschr Geneesk Studenten Ed* 2003; March:7(1)

CURRICULUM VITAE

The author of this thesis was born on June 28, 1978 in Amersfoort, The Netherlands. In Amersfoort, he grew up and graduated from The Meridiaan College (VWO) in 1996. The following year he started Medical School at Leiden University in 1997. During the years in University, he worked as an allocation coordinator for the Eurotransplant International Foundation. As part of his studies, he performed a research fellowship in the transplantation laboratory of the Leiden University Medical Center, supervised by Prof.dr. O.T. Terpstra. In 2003, he moved to California, United States of America, to work as visiting researcher in Dr. R.C. Robbins' Cardiothoracic Transplantation Laboratory at Stanford University. The research projects described in this thesis were initiated at that time. For his work, he received the Hippocrates Foundation Research Award in 2005. He returned to The Netherlands and graduated from Medical School in June of 2006, where after he returned to Stanford to continue his research as a post-doctoral research fellow at the department of Cardiothoracic Surgery, supervised by Prof.dr. J.F. Hamming, Dr. R.C. Robbins and Dr. J.C. Wu. He presented his work at several international meetings, including American Heart Association's Scientific Sessions in 2004 and 2008. His work was awarded fellowships by the European Society for Organ Transplantation, the Fulbright Foundation and the Professor Michaël-van Vloten Foundation. Currently, he is a surgical resident at the Leiden University Medical Center under the supervision of Prof. dr. J.F. Hamming.

ACKNOWLEDGEMENTS

There are many people who have substantially contributed to the completion of this thesis. A few I would like to mention in particular:

All my colleagues in the Robbins lab, the Wu lab and others spread out over the Stanford campus for their help, criticism and for a great time in California.

Grant, my big friend, who's thirty-some years of small animal surgery have directly led to many breakthroughs in cardiothoracic transplantation.

My buddies Koen and Johannes for putting long lab hours into this project.

Those of you that in a time of financial crisis still dared to donate some…

My dear parents, who have always supported me in every step of the way.

Charlotte, whose passion and unceasing support can be found in every character of this thesis. When my mice were quarantined due to an infection and all my cells died for an unknown reason, she made me go back to the lab the next day.

Julia, who I thank for breaking the water after most of the work was done. Sorry that your first book had to be such a complex one.

Rutger-Jan Swijnenburg
March 2009